Targeting the Vascular and Immunosuppressive Networks in Glioblastoma

---

Dissertation

zur

Erlangung der naturwissenschaftlichen Doktorwürde
(Dr. sc. nat.)

vorgelegt der

Mathematisch-naturwissenschaftlichen Fakultät

der

Universität Zürich

von

Davide Mangani

aus

Italien

Promotionskommission

Prof. Dr. Michael Weller (Vorsitz und Leitung der Dissertation)
Prof. Dr. Burkhard Becher
Prof. Dr. Jörg-Christian Tonn
PD Dr. Patrick Roth
Dr. Hannah Schneider

Zürich, 2017

Acknowledgments

I would like to express my gratitude to Professor Michael Weller. I thank you for encouraging my research, being there in the moment of need and for allowing me to successfully complete my PhD. Likewise, I would like to thank my two supervisors Dr. Patrick Roth and Dr. Hannah Schneider for the support given throughout my PhD and for the goals achieved together. I would also like to thank my thesis committee members, Professor Burkhard Becher and Professor Jörg Tonn for giving me essential advices to perform and complete my projects and PhD.

I shall not forget my two previous mentors. Prof. Antonio Giordano whom introduced me to the lab life by giving me the opportunity to join his lab at Temple University. The experience acquired during my summer internships was crucial to foster my love for Science; I will be forever grateful for the opportunity you gave me, and for being always there whenever I need help or advice. Prof. Gerolama Condorelli guided me throughout my BSc and MSc. She is a special person and has been an outstanding support helping me to successfully complete my studies.

A special thank goes to all lab members that shared with me all or part of the journey. In particular, I shall mention the “Mediterranean colony” made of Alexandros Papachristodoulou, Eleanna Papa and Elisa Ventura. With you, I shared the entire journey and you three made it enjoyable.

A special mention goes to all my invaluable friends whom were always there for me in the moments of need.

A special thanks to all my family. My grandparents that always supported me and are longing every time for my short periods back home. My uncle Alfredo deserves a special place, as I would not be the person I am without is invaluable encouragement and backing.

The biggest heartfelt thank goes to the most important person of my life, my mother Giovanna. You have been a tremendous support. I will never thank you enough for the love you gave me and for teaching me the inner elements with which emotions are built of.

I want to dedicate this thesis to my father Luigi. I miss you, and wherever you are, I hope you can receive this message of love and nostalgia.

Lastly, I want to thank my city, “*Terra Mia*”, Naples to which I will be forever bond. I am proud of being Neapolitan and I will never forget from where I come from.

I. Table of contents

II. List of abbreviations

ABC	ATP binding cassette
ALK	activin receptor-like kinase
AMH	anti-Müllerian hormone
ANG	angiopoietin
APC	antigen presenting cell
ARF	alternative reading frame
Arg	Arginase I
ATG	autophagy-related
ATRX	α-thalassemia/mental retardation syndrome X-linked
B20	B20-4.1.1
BBB	blood brain barrier
Bcl-xL	B cell lymphoma-extra large
BMP	bone morphogenetic proteins
CA	carbonic anhydrase
CAR	chimeric antigen receptor
CCL	C-C motif chemokine ligand
CCR	C-C motif chemokine receptor
CDK	cyclin-dependent kinase
CDKN	cyclin-dependent kinase inhibitor
CNS	central nervous system
CSF-1R	colony stimulating factor-1 receptor
CTLA	cytotoxic T lymphocyte antigen 4
CXCL	C-X-C motif chemokine ligand
CXCR	C-X-C motif chemokine receptor
DAB	3,3′-diaminobenzidine
DAPI	4’,6-diamidino-2-phenylindole
DC	dendritic cell
DDR	DNA damage response
DMEM	dulbecco’s modified eagle medium
DSS	distal slice site
EGFR	epidermal growth factor receptor
EGFRvIII	epidermal growth factor receptor variant III
ELISA	enzyme-linked immunosorbent assay
ERK	extracellular signal–regulated kinase
E:T	effector to target ratio
FACS	fluorescence-activated cell sorting
FCS	fetal calf serum
FGF	fibroblast growth factor
FoxP3	forkhead box P3
GDF	growth and differentiation factor
GITR	glucocorticoid-induced tumor necrosis factor receptor
GSC	glioma stem cells
GsT	glioblastoma-derived T cell suppressor factor
HHT	hemorrhagic teleangiectasia

HIF-1α	hypoxia-inducible factor-1α
HPRT	hypoxanthine phosphoribosyltransferase
HRP	horseradish peroxidase
IDH	isocitrate dehydrogenase
IFN	interferon
IFP	interstitial fluid pressure
IL	interleukin
IRF	IFN regulatory factor-1
iTreg	induced Treg
LLT	lectin-like transcript
LY	LY2157299
MAPK	mitogen-activated protein kinase
MC	monolayer culture
MDM	mouse double minute
MDSC	myeloid-derived suppressor cells
MFI	median fluorescence intensity
MGMT	O^6-methyl guanine methyl transferase
MHC	major histocompatibility complex
MMP	matrix metalloproteinase
MRI	magnetic resonance imaging
MTOR	mechanistic target of rapamycin
MVD	microvessel density
NBT	normal brain tissue
NF-1	neurofibromatosis type 1
NF-κB	nuclear factor kappa B
NK	natural killer cell
NO	nitric oxide
NOD-SCID	non-obese diabetic, severe combined immunodeficient
NSC	neuronal stem cell
nTreg	natural Treg
p38	p38 mitogen-activated protein kinase
PD	programmed cell death (protein)
PDCD	programmed cell death (gene)
PDGFR	platelet-derived growth factor receptor
PD-L	PD ligand
PDX	patient-derived xenograft
PGE	prostaglandin E
PI3K	phosphoinositide 3-kinase
PI3KCA	PI3K subunit alpha
PKCβ	protein kinase Cβ
PlGF	placental growth factor
PSS	proximal splice site
PTEN	phosphotensin homolog
RB	retinoblastoma
RGMb	repulsive guidance molecule b
ROI	region of interest
RTF	regeneration and tolerance factor

RTK	receptor tyrosine kinase
RT-PCR	real-time polymerase chain reaction
SD	standard deviation
SDF	stromal-derived factor
SEM	standard error of the mean
SHP	SH2-domain containing tyrosine phosphatase
STRING	Search Tool for the Retrieval of Interacting Genes/Proteins
sVEGFR	soluble VEGFR
TAK	TGF-β-activated kinase
TCR	T cell receptor
TERT	telomerase reverse transcriptase
TGF	transforming growth factor
TGFβR	TGF-β receptor
Th	T helper cell
TMZ	temozolomide
TRAF	tumor necrosis factor receptor-associated factor
Treg	regulatory T cells
VCAM	vascular cell adhesion molecule
VEGF	vascular endothelial growth factor
VEGFR	VEGF receptor
VPF	vascular permeability factor
WHO	World Health Organization
ZEB	zinc finger e-box binding homeobox
ZO	zonula occludens

III. Index of figures

IV. Index of tables

1. Summary

Glioblastoma remains a fatal neoplasm regardless of recent advances in understanding the signalling pathways that fuel this devastating disease. Sustained angiogenesis and marked immunosuppression are major features of glioblastoma, and approaches targeting these pathways have been regarded as promising. The transforming growth factor (TGF)-β and vascular endothelial growth factor (VEGF) pathways drive key overlapping functions in glioblastoma biology, such as angiogenesis, immunosuppression, stem cell maintenance and invasion. In part I of the thesis, we investigated whether TGF-β pathway can act as an escape pathway during anti-angiogenic therapy, substituting for VEGF activity. We found that TGF-β is an up-stream regulator of VEGF whereas VEGF pathway activity does not alter TGF-β pathway *in vitro*. *In vivo*, single agent activity was observed for the VEGF antibody B20-4.1.1 (B20) in three, and for the TGF-β receptor I antagonist LY2157299 (LY) in two of four models. Reduction of tumor volume and blood vessel density, but not induction of hypoxia, correlated with benefit from B20. Reduction of SMAD2 phosphorylation by LY2157299 was seen in all models, but did not predict survival. Resistance to B20 was associated with gene expression pathways attributed a role in anti-angiogenic therapy escape whereas resistance to LY2157299 was associated with different immune response gene signatures in SMA-497 and GL-261 gliomas. The combination of B20 with LY2157299 was ineffective against SMA-497, but provided prolongation of survival in GL-261, associated with early suppression of pSMAD2 in tumor and host immune cells, prolonged suppression of angiogenesis, and delayed accumulation of tumor-infiltrating microglia/macrophages. These findings highlight the complex heterogeneity of glioblastoma, and suggest that dual targeting of the TGF-β and VEGF pathways may provide a valuable option in subsets of glioblastoma.

TGF-β also plays a crucial role in glioblastoma-mediated immunosuppression. Several studies have demonstrated how TGF-β signalling dampens T cell-mediated effector functions, which results in immune escape of gliomas. Therefore, in the second project we aimed to investigate whether TGF-β inhibition can boost the efficacy of anti-PD1 antibodies in experimental glioma models as several studies have highlighted the need of targeting multiple pathways to achieve a durable therapeutic effect. Experiments with *in vitro* syngeneic co-culture models of glioma cells and T lymphocytes showed that dual targeting of the PD-1 and TGF-β pathways elicited T cell effector responses

linked with increased anti-tumor activity. These findings warrant further investigation of dual PD-1 and TGF-β blockade in experimental glioma models *in vivo* and these experiments are currently ongoing in our laboratory.

In summary, these findings highlight the complexity of glioblastoma and the need of targeting multiple pro-tumorigenic features to reach significant clinical improvements in the future.

2. Zusammenfassung

Trotz nennenswerter Fortschritte im Verständnis der zugrundeliegenden Signalwege, handelt es sich bei Glioblastomen um aggressive Hirntumoren, für die es bis heute keine Heilung gibt. Typische Eigenschaften dieses Tumors sind eine kontinuierliche Neubildung von Blutgefässen, die sogenannte Angiogenese, und eine erhebliche lokale Immunsuppression. Therapieansätze, die zum Ziel haben, die Signalwege dieser beiden Prozesse zu hemmen, gelten seit Langem als vielversprechend. In der Biologie des Glioblastoms spielen der “Transforming Growth Factor" (TGF)-β- und der “Vascular Endothelial Growth Factor" (VEGF)-Signalweg eine wichtige Rolle. Beide weisen überlappende Funktionen auf und sind in verschiedene biologische Prozesse involviert. Hierzu zählen Angiogenese, Immunsuppression, Erhaltung von Stammzelleigenschaften und Vorgänge der Zellinvasion.

Im ersten Teil der Arbeit wurde untersucht, ob der TGF-β-Signalweg während anti-angiogener Therapie gegen VEGF alternativ aktiviert wird und somit als eine Art Therapie-Fluchtweg dienen könnte. Wir haben durch *in vitro* Experimente herausgefunden, dass TGF-β in der Signalkaskade oberhalb von VEGF steht und die VEGF-Expression regulieren kann, wohingegen die Aktivität des TGF-β-Signalweges nicht durch VEGF beeinflusst wird. *In vivo* konnten wir für den gegen VEGF gerichteten Antikörper B20-4.1.1 (B20) eine Anti-Tumor-Aktivität in drei von vier, und für den TGF-β Rezeptor I-Antagonisten LY2157299, in zwei von vier syngenen Mausgliommodellen nachweisen. Dabei korrelierten die Reduktion des Tumorvolumens und die Blutgefässdichte mit der Sensitivität gegenüber B20, wohingegen in einigen Modellen Hypoxie unabhängig von der Behandlung induziert wurde. Die SMAD2-Phosphorylierung wurden in allen Modellen durch LY2157299 reduziert, war aber kein prognostischer Faktor für das Überleben der Mäuse. Anhand von Transkriptomanalysen konnten wir zeigen, dass eine Resistenz gegenüber B20 mit der Aktivierung eines anti-angiogenen Therapieresistenz-Genexpressionsmusters assoziiert ist. Dagegen war die Resistenz gegenüber LY2157299 mit unterschiedlichen Immunantwort-Gensignaturen in den SMA-497- und GL-261-Gliommodellen verbunden. Im SMA-497-Tumormodell war die Kombination von B20 mit LY2157299 ineffektiv, dagegen wirkte sie sich positiv auf das Überleben von GL-261 Tumor-tragenden Mäusen aus. Dieser Effekt war mit einer frühen Suppression der SMAD2-Phosphorylierung in Tumorzellen und Immunzellen, einer verlängerten Hemmung der

Angiogenese und einer verspäteten Anreicherung von Mikroglia/Makrophagen im Tumor assoziiert. Diese Ergebnisse unterstreichen die Heterogenität von Glioblastomen und deuten darauf hin, dass eine duale Hemmung des TGF-β- und VEGF-Signalwegs eine vielversprechende Option bei einigen Glioblastom-Subtypen sein könnte.

TGF-β spielt auch eine entscheidende Rolle im Rahmen der Gliom-vermittelten Immunsuppression. Im zweiten Teil der Arbeit wollten deswegen wir anhand von syngenen Mausgliommodellen herausfinden, ob die Wirksamkeit einer "Immun-Checkpoint"-Blockade durch die Hemmung von TGF-β verstärkt werden kann. Unsere eigenen Daten und die Ergebnisse frührer Studien deuten darauf hin, dass eine Hemmung mehrerer tumorspezifischer Signalwege essentiell ist, um einen anhaltenden immun-vermittelten Therapieerfolg zu erzielen.

Experimente mit *in vitro* Ko-Kulturen aus Gliomzellen und T-Lymphozyten haben gezeigt, dass die duale Blockierung des PD-1- und des TGF-β-Signalwegs, die Wirksamkeit der T-Effektorzellen erhöht, indem die anti-Tumoraktivität verstärkt wird. Diese Beobachtungen erfordern weitere Untersuchungen in experimentellen *in vivo* Mausgliommodellen, die aktuell in unserem Labor stattfinden.

Zusammenfassend deuten unsere Befunde darauf hin, dass in Glioblastomen eine komplexe Interaktion zwischen verschiedenen Signalwegen vorliegt. Basierend auf diesen Daten lassen sich möglicherweise kombinierte Therapieansätze entwickeln, die zu einer verbesserten Prognose der betroffenen Patienten führen können.

3. Introduction

3.1 Gliomas

3.1.1 Classification of gliomas and epidemiology

Gliomas are primary brain tumors that have been classified by the World Health Organization (WHO) into four prognostic grades based on histological features of malignancy. Grade I tumors, such as pilocytic astrocytomas, appear mainly in children and are characterized by slow growth, alteration in the mitogen-activated protein kinase (MAPK) pathway and favorable prognosis as they can often be removed by resection. Grade II and grade III tumors represent the most frequent gliomas in young adults and are distinguished by an infiltrative phenotype in the brain parenchyma and frequent mutation of the isocitrate dehydrogenase (IDH) 1 or 2 genes. They typically recur and may progress to higher grades of malignancy. Traditionally, these tumors were histologically classified as astrocytic, oligodendroglial or mixed oligo-astrocytic tumors, but recent advances in molecular profiling allowed for a classification into two subtypes. The first, the astrocytic type, is marked by mutations of the genome guardian *TP53*, along with frequent mutations of the *α-thalassemia/mental retardation syndrome X-linked* (*ATRX*) gene. The second, or oligodendroglial type, is characterized by co-deletion of chromosomal arms 1p/19q and linked with *telomerase reverse transcriptase* (*TERT*) promoter mutation. Grade IV tumors, referred as glioblastomas, are the most prominent and malignant primary brain tumors, which usually manifest after the fifth decade of life. These tumors are associated with a dismal prognosis, infiltrative phenotype, microvascular proliferation and extensive presence of pseudopalisading necrosis. They are referred as primary when arise *de novo* and secondary when progressed from lower grade tumors (Weller *et al.*, 2015; Louis *et al.*, 2016) (Figure 1). Importantly, the progress in the so-called omic-technologies, may lead to a new way to classify, and therefore treating, gliomas. This is particularly true for the diffusely infiltrative gliomas in adults, which can be subdivided in three major groups that differ in their pathogenesis and response to treatment: IDH-mutant, 1p/19q co-deleted tumors; IDH-mutant, 1p/19q non co-deleted tumors; and IDH wild-type tumors. Accordingly, the assessment of these molecular markers has been included into the new WHO classification (Weller *et al.*, 2015; Louis *et al.*, 2016).

Epidemiologically, the incidence of neuroepithelial tumors in the US has been 6.6 per 100'000 persons in the period of time between 2008 and 2012 (Ostrom *et al.*, 2015). Around half of the diagnosed tumors were classified as glioblastomas. The incidence rate in Northern Europe or United States is about double of the rate found in Japan, and the reasons for these regional differences are still unknown. The most important risk factor associated with glioblastoma is aging, but the underlying biological reasons are also not yet known (Weller *et al.*, 2015)

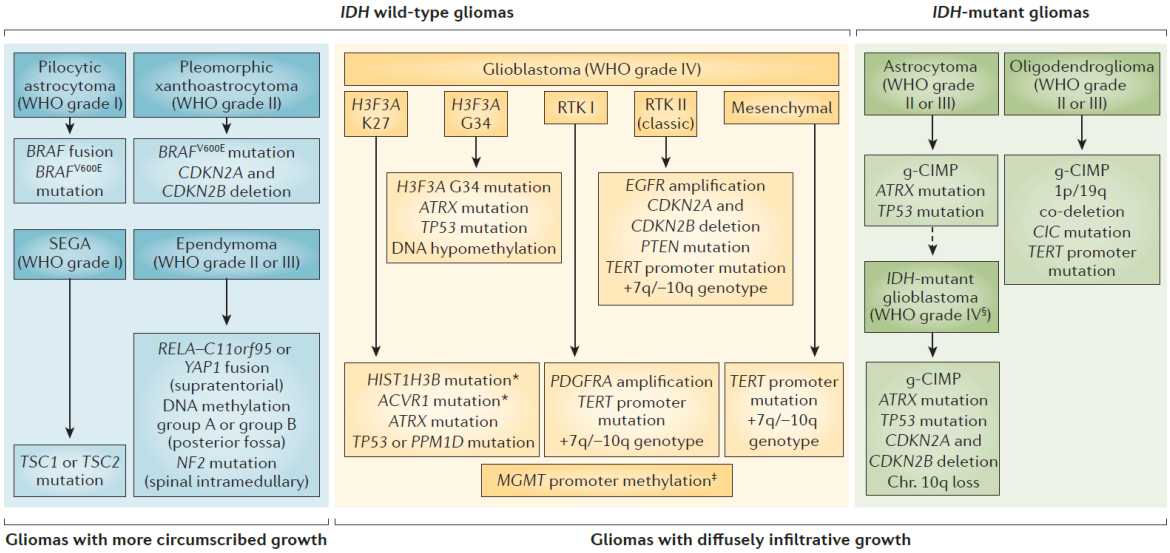

Figure 1. Genetic and epigenetic alterations of gliomas.
(Adapted from Weller *et al.,* 2015)

3.1.2 Genetic and molecular signatures of glioblastoma

In recent years, many studies have described the complexity and heterogeneity of human tumors. High-throughput gene expression analysis of tumor samples has provided valuable insights into the features of glioblastoma. It is now clear that histological evaluation by itself cannot accurately classify the inherent complexity of glioblastoma. Consequently, four different molecular signature have been described to better classify glioblastomas helping to define patients' prognosis: classical, mesenchymal, proneural and neural (Cancer Genome Atlas Research, 2008; Verhaak *et al.*, 2010). Yet, this classification has had no implication on clinical decision making so far.

The classical subtype is characterized by aberrant expression of the epidermal growth factor receptor (EGFR) and lacks mutations in the *IDH* genes and *TP53*. The mesenchymal subtype is featured by mutations of the *neurofibromatosis type 1* (*NF1*)

and the *phosphotensin homolog* (*PTEN*) tumor suppressor genes, and high expression of the *MET* proto-oncogene, and is usually associated with a poorer outcome. The proneural subtype is associated with high expression levels of platelet-derived growth factor receptor (PDGFR) A expression, and mutations in the *IDH* and *TP53* genes, which are usually linked with secondary glioblastoma. Lastly, the neural subtype shows an expression signature similar to those of the normal brain tissue, and displays expression of several neuronal markers; its existence remains doubtful (Cancer Genome Atlas Research, 2008; Verhaak *et al.*, 2010; Vitucci *et al.*, 2011; Reifenberger *et al.*, 2014).

3.1.3 Glioblastoma current standard of care

Gliobastomas are the most aggressive and deadly adult primary brain tumors (Ostrom *et al.*, 2015). Although patients are treated with multi-modal approaches, the prognosis remains poor with a median survival of 16 months within clinical trial populations (Weller *et al.*, 2014). The standard of care for patients below 70 years with newly diagnosed glioblastoma is tumor resection as feasible, followed by radiotherapy and concomitant and maintenance chemotherapy with the alkylating agent temozolomide (TMZ) (Stupp *et al.*, 2005). In patients above 70 years, treatment is based on the O^6-methyl guanine methyl transferase (MGMT) promoter methylation status. Hypofractionated radiotherapy (15 doses, 2.66 Gy) alone is used in patients with MGMT-unmethylated status whereas in MGMT-methylated patients, combined radiochemotherapy or TMZ alone can be used (Malmstrom *et al.*, 2012; Wick *et al.*, 2012; Perry *et al.*, 2017). For patients with tumors that recur after concomitant radiochemotherapy, nitrosureas, alternative TMZ dosing regimens or the anti-vascular endothelial growth factor (VEGF) antibody, bevacizumab, are administered depending on regional guidelines status (Weller *et al.*, 2014).

3.2 Molecular mechanisms driving the malignant phenotype of glioblastoma

3.2.1 Glioma cell of origin and glioma cancer stem cell theory

Historically, two main theories have been postulated regarding the origin of tumors: the stochastic or clonal evolution model, and the hierarchical model or cancer stem cell model. The first theory proposes that all cells within a tumor have the same potential to proliferate, self-renew and drive *de novo* tumor growth. In other words, every cell

within the tumor can acquire new mutations allowing for an increased tumor heterogeneity and probability of generating a tumor clone, which can either re-generate the entire tumor or resist to therapies. Differently, the cancer stem cell hypothesis postulates that tumors bear a rare cell population with stem cell characteristics, which is able to resist standard therapies and propagate a heterogeneous progeny through its unlimited self-renewal potential (Rich, 2008; Shackleton *et al.*, 2009). To date, the second hypothesis seems to be more widely accepted.

In the brain, neural and glial stem cell progenitors exist and possess multi-potency features, and these cells have been indicated as possible glioma cells of origin. In mice, these cells have been isolated mainly from the subventricular region, the dentate gyrus and the hippocampus, and the subcortical white matter (Gage, 2000; Fukuda *et al.*, 2003; Kim and Morshead, 2003). The first evidence in humans of the existence of glioma stem cells (GSC) came from a work published by Ignatova *et al*, where cells with stem cells properties were isolated from human glioblastoma samples. These cells were highly clonogenic, able to form neuro-spheres, expressed neural stem-cell fate determining factors and expressed astroglial and neuronal markers after differentiation (Ignatova *et al.*, 2002). Studies by Singh and colleagues demonstrated that GSC are significantly enriched in the $CD133^+$ population and able to initiate and propagate tumors. The orthotopic injection of only 100 cells was enough to establish tumors in non-obese diabetic, severe combined immunodeficient (NOD-SCID) mouse brains whereas even 10,000 $CD133^-$ cells did not (Singh *et al.*, 2003; Singh *et al.*, 2004). CD133 as a marker of stemness remains the most widely used to isolate GCS even though its specificity has remained controversial. Since the initial publication of Singh *et al*, several other studies explored the importance and the role of GSC in brain tumor pathogenesis and demonstrated that these cells share many similar features with neuronal stem cells (NSC). In fact, they can self-renew, give rise to different cell lineages, and localize in highly specialized niches (Kim and Morshead, 2003; Gilbertson and Rich, 2007). Importantly, the nomenclature “stem cell” referred to glioma indicates the features and abilities of this tumor cell population and not the function of these cells as “cell of origin” of the tumor.

An important characteristic of GSC is their ability to be resistant to conventional treatment modalities, namely radio and chemotherapy. Indeed, $CD133^+$ cells can efficiently activate the DNA damage response (DDR) and are protected from the deleterious effects of irradiation compared to their CD133 negative counterparts. Also,

GSC may express high levels of MGMT, which renders them resistant to TMZ treatment (Liu *et al.*, 2006; Binello and Germano, 2011; Venere *et al.*, 2014). However, this remains controversial as another study showed that TMZ preferentially targets GSC in glioblastoma (Beier *et al.*, 2008).

Some data suggest that GSC reside in vascular niches. Calabrese *et al* showed that brain endothelial cells orchestrate a perivascular niche where they supply critical factors to maintain brain tumor cells in a stem cell-like phenotype (Calabrese *et al.*, 2007). Furthermore, a paper from Bao and colleagues found out that GSC secrete high levels of the pro-angiogenic molecule VEGF and a report from Hamerlik *et al* shed light on autocrine VEGF/VEGF receptor (VEGFR)2 signalling in GSC, which can protect this population from anti-angiogenic therapies. Of note, silencing of VEGFR2 did not only affect VEGF secretion but also stem cell properties and tumorigenicity of GSC (Bao *et al.*, 2006; Hamerlik *et al.*, 2012). Lastly, some studies propose GSC as possible cells of origin of the tumor endothelium, whereas other suggest that these cells can differentiate into pericytes stabilizing vessels and thus supporting tumor growth (Ricci-Vitiani *et al.*, 2010; Wang *et al.*, 2010; Cheng *et al.*, 2013). All these studies support the cancer stem cell model and highlight the importance of GSC in the malignant phenotype of glioblastoma.

3.2.2 Glioblastoma-associated signalling pathways

Several pathways are involved in the malignant phenotype of glioblastoma cells. Aberrant expression and function of key proteins belonging to important signalling pathways are thought to be responsible for tumor-promoting features such as proliferation, survival and invasion.

3.2.2.1 RTK/PI3K/Akt pathway

The receptor tyrosine kinase (RTK)/phosphoinositide 3-kinase (PI3K)/Akt pathway can regulate a plethora of cellular processes and their deregulation may be crucial for glioblastoma initiation and progression. The most frequently mutated RTK in glioblastoma is EGFR. *EGFR* amplification is present in 40% of all glioblastomas and deregulated expression in up to 60% (Libermann *et al.*, 1984; Ekstrand *et al.*, 1991; Wong *et al.*, 1992). Moreover, amplification of the *EGFR* gene is often associated with the expression of a peculiar receptor variant, EGFR variant III (EGFRvIII), which is characterized by an in-frame deletion of the exons 2 to 7, resulting in a truncated

protein. EGFRvIII is constitutively active and can deliver intense intra-cellular signalling due to ineffective receptor endocytocis, recycling and protein degradation via the ubiquitination system (Ekstrand *et al.*, 1992; Grandal *et al.*, 2007; Huang *et al.*, 2009). Downstream of the RTK, the activation of the PI3K pathway is crucial to activate multiple cellular processes, including key tumor cell traits such as survival and motility. This pathway can be augmented by activating mutations or amplifications of the *PI3K subunit alpha* (PI3KCA) catalytic subunit, or by homozygous deletion or mutations of the *PTEN* gene, which negatively regulates PI3K functions (Furnari *et al.*, 1998; Kita *et al.*, 2007). *PTEN* deletion or mutation is one of the most common genetic alterations in glioblastoma, and it is present in 15 to 40% of all tumors (Li *et al.*, 1997; Cancer Genome Atlas Research, 2008).

Not surprisingly, the Akt serine/threonine kinase family, which is a fundamental hub downstream of the RTK/PI3K pathway, is hyper-activated in around 80% of human glioblastomas (Haas-Kogan *et al.*, 1998). This report is in line with the finding that RTK/PI3K/Akt signalling is deregulated in 88% of human glioblastomas (Cancer Genome Atlas Research, 2008).

3.2.2.2 TP53 pathway

The TP53 pathway is probably the most frequently mutated pathway in cancer. TP53 protein, also called the genome guardian, responds to many intra- and extracellular stimuli, and regulates various processes that control cell cycle progression, DNA repair, and apoptosis (Bogler *et al.*, 1995). Disruption of this pathway can occur by mutation of the *TP53* gene itself, or amplification of the *mouse double minute* (*MDM*)-*2* or *-4*, or deletion/mutations of the *p14 alternative reading frame* (*ARF*) gene (Reifenberger *et al.*, 1993; Ichimura *et al.*, 2000). Interestingly, mutations of this pathway are observed mainly in IDH mutant glioblastomas, with a percentage of 65% versus 30% of IDH wild type tumors. Lastly, another mechanism of pathway's disruption is promoter methylation of the $p14^{ARF}$ gene. Indeed, promoter methylation or homozygous deletion happens in 50 and 75% of wild type and mutant IDH glioblastomas, respectively (Nakamura *et al.*, 2001; Ohgaki and Kleihues, 2009).

3.2.2.3 RB pathway

The retinoblastoma (RB) pathway is a critical gatekeeper, which regulates cell cycle entry and progression from the G1 to the S phase (Serrano *et al.*, 1993). During cell

cycle progression, the cyclinD1/cyclin-dependent kinase (CDK) 4 complex can inhibit the RB protein by phosphorylation, releasing the molecular break that controls the activity of the E2F transcription factor. Once activated, E2F readily accelerates the transition from G1 to S phase of the cell cycle. Importantly, the initial cyclinD1/CDK4 complex can be inhibited by two master tumor suppressors; the CDKN2A ($P16^{INK4a}$) and the CDKN2B ($P15^{INK4b}$) proteins. Thus, mutations occurring in any of these genes can disrupt cell cycle control and lead to unchecked proliferation. The Cancer Genome Atlas Network work has unveiled that the RB pathway is deregulated in 77% of glioblastomas and the most frequently mutated genes are CDKN2A and CDKN2B, which are deleted or mutated in 52 and 47% of the analyzed tumors, respectively (Cancer Genome Atlas Research, 2008).

3.3 Angiogenesis in glioblastoma

3.3.1 Mechanisms of brain tumor vessel formation

In physiological conditions, the normal brain vasculature is highly specialized. The blood brain barrier (BBB) is composed of endothelial cells, pericytes, astrocytes and perivascular macrophages, which all together form the neurovascular unit (Abbott *et al.*, 2006). It finely regulates the access of molecules to the central nervous system (CNS), maintains the correct ionic composition of the brain, thereby preserving neurons physiological function, and blocks the entrance of undesirable and possibly toxic molecules. Conversely, glioblastoma vessels are highly tortuous, permeable and bear many abnormalities in endothelial wall, pericyte coverage and basement membrane (Plate and Mennel, 1995; Jain *et al.*, 2007a). Moreover, tumor vessels within brain tumors have a larger diameter and thicker basement membrane compared to those of the normal brain, and harbor peculiar microvasculature structures termed “glomeruloid tufts”, which are composed of multi-layered, proliferative endothelial cells (Robson, 2001).

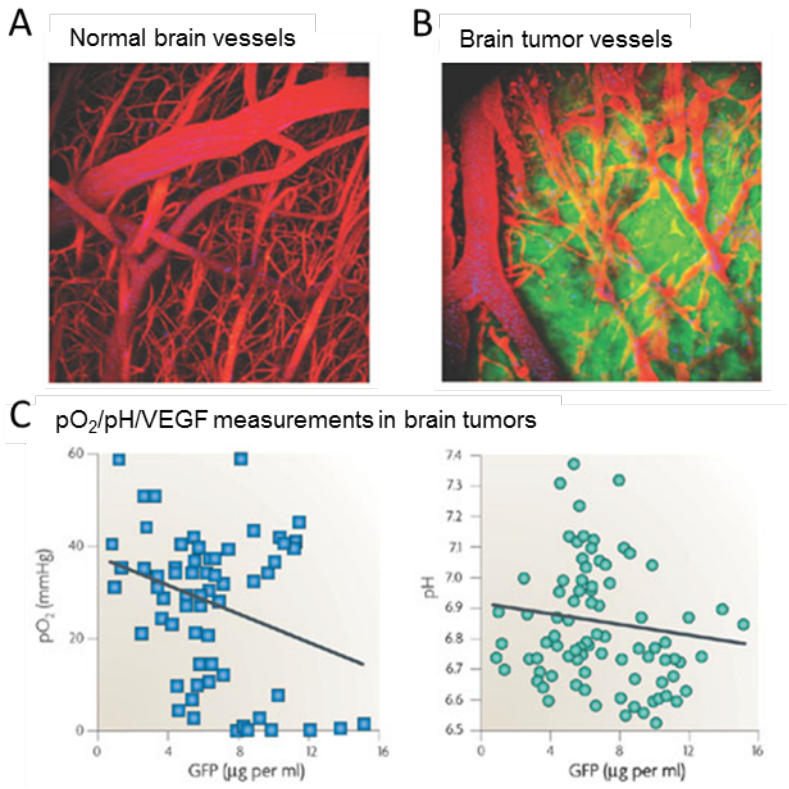

Figure 2. Brain tumor vasculature. A. Normal vasculature is structurally organized and built to provide even nutrient distribution to all surrounding cells. B. Vasculature of a glioma xenograft model is highly disorganized and vessels are not anymore finely connected and organized. Vessels are displayed in red, red blood cells in blue and cancer cells in green. C. Correlation between vascular endothelial growth factor (VEGF) promoter activity in glioblastoma xenograft tumor cells (expressed as GFP produced upon VEGF promoter activation) and oxygen and pH levels (Adapted from Jain *et al.,* 2007)

Despite the fact that the brain tumor vasculature loses its ability to regulate the selective passage of molecules through the BBB, it still partly possesses the physiologic function. Indeed, tumors growing in the brain have significantly reduced trans-vascular transport compared to the same tumors grown subcutaneously (Yuan *et al.*, 1994; Hobbs *et al.*, 1998). It has to be noted nevertheless that magnetic resonance imaging (MRI) studies have shown a 20-fold increase in vascular permeability between normal and tumoral vessels within the brain (Jain *et al.*, 2007a). This highlights that the loss of the BBB function is heterogeneous and spatial, conformational, and tumoral cues impact the entire process. The main problem associated to heterogeneous vessels leakiness is represented by an unstable blood flow, which in turn, can increase interstitial fluid pressure (IFP). An increased IFP is a major problem in glioblastoma patients' care; it increases intracranial edema that can be responsible for many complications, and hinders the correct and homogeneous delivery of therapeutic drugs (Jain, 1994; Jain *et al.*, 2007b) (Figure 2).

Interestingly, studies by Harold Dvorak's group have found that in human and mice tumors at least 6 different types of vessels can be generated by two main processes: angiogenesis and arterio-venogenesis. It has been shown that all six types can be recapitulated in normal mouse tissues by adenoviral vector-mediated expression of VEGF-A protein, and importantly, 4 out of 6 vessel types become VEGF-independent (Nagy *et al.*, 2007; Sitohy *et al.*, 2012). This concept is important since, as already mentioned, brain tumor vascular networks are highly heterogeneous and comprise different types of vessels.

To date, six main pathways of vessel formation have been described in glioblastoma. Initially, brain tumor cells can co-opt (1) existing normal vasculature (Holash *et al.*, 1999). While tumors grow, cells compress the endothelium causing a marked vessel shrinkage and reduced blood flow (Padera *et al.*, 2004). This process eventually leads to the induction of hypoxia, in turn, generating a harsh microenvironment where tumor cell clones with the ability to secrete pro-angiogenic factors are selected. These factors elicit the generation of new vessels from pre-existing ones, via angiogenic processes (2) (Carmeliet and Jain, 2000). Another mechanism, although poorly understood, is the formation of a new vascular network through vasculogenesis (3). Glioma cells can express stromal-derived factor (SDF)-1 that can recruit bone marrow-derived cells into the brain parenchyma. These cells can be incorporated and stabilize nascent vessels within the tumor (Aghi *et al.*, 2006; Santarelli *et al.*, 2006). Intussusception (4) is a process by which tumor vessels can remodel and expand inside the interstitial tissue columns and into the lumen of pre-formed vessels. It has been initially noted in mouse models of brain metastasis; however, the underlying molecular mechanisms are still unknown (Yano *et al.*, 2000; Nagy *et al.*, 2002). Tumor cells can also fuse into the endothelium in a process termed vasculogenic mimicry (5), and GSC have been shown to trans-differentiate into endothelial cells (6), which bore peculiar chromosomal abnormalities (Ricci-Vitiani *et al.*, 2010; Wang *et al.*, 2010; Carmeliet and Jain, 2011).

3.3.2 Vascular endothelial growth factor signalling pathway

Dvorak and colleagues discovered the main ligand of this pathway as vascular permeability factor (VPF) in 1983. Later on, this factor was termed as VEGF for its ability to act as endothelial cell mitogen (Senger *et al.*, 1983; Leung *et al.*, 1989). The importance of this gene was highlighted by the observation that the germline deletion of a single VEGF allele was enough to cause embryonic lethality caused by severe

vascular deficiencies (Carmeliet *et al.*, 1996; Ferrara *et al.*, 1996). Since then, many different ligands and splice variants have been discovered, and these can bind with different affinities to three VEGFR1-3. In humans, VEGF-A, VEGF-B, VEGF-C, VEGF-D, and placental growth factor (PlGF) can bind to VEGFR 1-3 and modulate angiogenic processes (Maglione *et al.*, 1991; Tammela *et al.*, 2005; Koch *et al.*, 2011) (Figure 3). Notably, the VEGF-A gene can undergo alternative splicing mechanisms, which can generate many isoforms with different functions. In particular, splicing isoforms generated via proximal splice site (PSS) selection in exon 8 (VEGFXXXa) are pro-angiogenic, whereas those formed from the exon 8 distal slice site (DSS) (VEGFXXXb) are weakly angiogenic (Harper and Bates, 2008; Catena *et al.*, 2010).

VEGFR1 can bind VEGF-A with 10 fold higher affinity than VEGFR2, nevertheless, it has a poor tyrosine kinase activity compared to VEGFR2. *VEGFR1*$^{-/-}$ mice die at day 9 of the embryonic stage due to a defective vascular system and aberrant endothelial proliferation (Fong *et al.*, 1995). Differently, *VEGFR2*$^{-/-}$ mice have a similar phenotype to *VEGF* knockout mice. These mice die at embryonic day 8.5 due to disrupted endothelial and hematopoietic lineage cells development, with consequent severe vascular impairments (Shalaby *et al.*, 1995).

3.3.3 VEGF signalling in glioma cells

VEGF-A is the most important pro-angiogenic factor released by glioma cells. Its expression correlates with tumor malignancy and the major transcription factor regulating its expression is hypoxia-inducible factor 1α (HIF1α) (Bulnes *et al.*, 2012). Interestingly, TP53 that is frequently mutated in glioblastoma, can form transcriptional complexes with SP1 thereby inhibiting VEGF-A transcription (Kargiotis *et al.*, 2006). In addition, the EGFR signalling pathway, which is hyperactive in around 60% of high-grade gliomas, can up-regulate VEGF-A expression via MAPK/extracellular signal-regulated kinase (ERK) pathway (Woods *et al.*, 2002). Notably, EGFRvIII has been demonstrated to sustain VEGF expression via Ras-dependent signalling in glioblastoma cell lines (Feldkamp *et al.*, 1999).

VEGF-A plays a fundamental role in the GSC niche, where it regulates survival, resistance to therapy, and invasion of GSC (Gorski *et al.*, 1999; Knizetova *et al.*, 2008; Hlobilkova *et al.*, 2009; Hamerlik *et al.*, 2012). VEGF-A secreted by tumor cells, can also fuel proliferation of tumor associated microglia/macrophage, and promoting glioma growth in experimental models (Forstreuter *et al.*, 2002; Kerber *et al.*, 2008).

Furthermore, VEGF-A can act autocrinally on glioma cells themselves, thereby promoting tumor cell survival (Mentlein *et al.*, 2004; Szabo *et al.*, 2016).

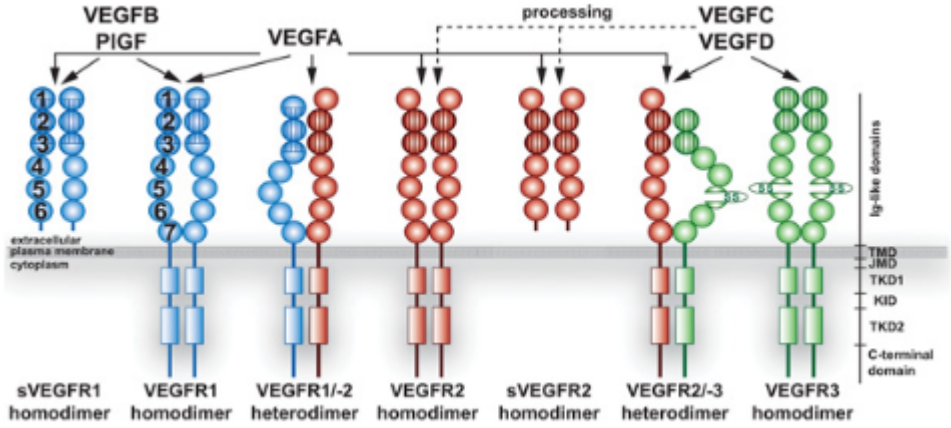

Figure 3: VEGF pathway ligands and receptors. The five VEGF pathway ligands, VEGF-A, -B, -C, -D and PlGF, bind their cognate receptors with different specificities and affinities. Upon binding, VEGF receptors can either homo- or –heterodimerize allowing signal transduction into the cell. VEGF-C and VEGF-D can bind VEGFR2 only after proteolytic processing. VEGFR2 extracellular domain can be cleaved to produce a soluble form. Abbreviations: JMD, juxtamembrane domain; KID, kinase insert domain; TMD, transmembrane domain; TKD1, ATP-binding domain; TKD2, phosphotransferase domain.
(Adapted from Koch *et al.,* 2011)

3.3.4 Anti-angiogenic therapies in glioblastoma

VEGF-A represents the most important target of anti-angiogenic therapies for its prominent role in physiological and pathological angiogenesis. The first approved drug targeting the VEGF-A protein was the humanized monoclonal antibody bevacizumab (Avastin). Despite great expectations, two large phase III clinical trials, RTOG 0825 and AVAGlio, demonstrated a prolongation in progression-free survival, but failed to impact overall survival (Chinot *et al.*, 2014; Gilbert *et al.*, 2014). Bevacizumab remains a drug of interest for its ability to reduce cerebral edema and to normalize the tumor vasculature, which in turn, can relieve IFP and increase the delivery of co-administered drugs (Jain, 2005; Gerstner *et al.*, 2009). Another approach is represented by the targeting of VEGFR tyrosine kinase activity. The pan-VEGFR inhibitor cediranib was shown to normalize the vasculature and to reduce edema in glioblastoma patients (Batchelor *et al.*, 2007). Interestingly, analysis of response to cediranib in newly diagnosed glioblastoma patients revealed that improved perfusion and tumor oxygenation was achieved in a subset of patients associated with improved overall survival. The observed improved survival was linked to increased efficacy of concomitant chemoradiotherapy and resistance to therapy was associated with post-

therapy heightened plasma levels of interleukin (IL)-8 and soluble form of VEGFR1 (sVEGFR1) (Batchelor *et al.*, 2013).

Enzastaurin is a protein kinase Cβ (PKCβ) inhibitor, which blocks neo-angiogenesis by silencing VEGF transcriptional expression. Yet, clinical trials showed that enzastaurin failed to improve overall survival compared to lomustine in recurrent glioblastoma (Wick *et al.*, 2010).

Many other strategies beyond inhibition of the VEGF pathway have been employed. Targeting of the mechanistic target of rapamycin (mTOR)/Akt pathway, cMET inhibition, integrin inhibition, EGFR and PDGFRβ blockade are all strategies that besides targeting tumor cell-core pathways, also affect vessel formation in glioblastoma to a different extent (Batchelor *et al.*, 2014). None of these approaches significantly changed overall survival of glioblastoma patients. However, anti-angiogenic agents remain of interest in clinical neuro-oncology, especially to design combinatorial strategies aimed at blocking multiple angiogenic pathways.

3.3.5 Resistance to anti-angiogenic therapies

Resistance mechanisms to anti-angiogenic therapies have been divided in two major groups: adaptive resistance and intrinsic non-responsiveness (Figure 4). The former occurs when a tumor initially shrinks and regresses due to the therapy, but then develops resistance either by adopting new angiogenic pathways to restore the vasculature or by becoming less dependent from the targeted factor. The latter occurs when the tumor never responded to the therapy and continued growing undisturbed (Bergers and Hanahan, 2008). Studies in preclinical models as well as glioblastoma patients treated with anti-angiogenic agents have shed light on several escape mechanisms. Increased invasiveness of glioblastoma cells has been described as the most prominent escape pathway. For example, this escape mechanism has been noted in models where factors required for the tumor vasculature, such as HIF-1α, matrix metalloproteinase (MMP)-2, and MMP-9, were ablated (Du *et al.*, 2008a; Du *et al.*, 2008b). Also, angiogenesis inhibitors or genetic ablation of tumor-derived VEGF-A increase invasiveness and progression in a glioblastoma orthotopic model (Paez-Ribes *et al.*, 2009). Similarly, in a clinically relevant patient-derived xenograft (PDX) model, anti-VEGF treatment reduces tumor blood supply, which in turn changes cancer cell metabolism, inducing invasion toward normal brain parenchyma (Keunen *et al.*, 2011). Remarkably, retrospective analysis of clinical trials employing anti-VEGF

molecules showed that relapsed tumors were highly infiltrative and in one study, this was correlated with tumor displaying of mesenchymal markers. However, anti-VEGF-induced invasiveness remains controversial since other studies have not confirmed this assumption (Wick *et al.*, 2011; Soda *et al.*, 2013; Wick *et al.*, 2013). VEGF blockade can also induce a more invasive and aggressive tumor phenotype through hypoxia-dependent c-MET upregulation and phosphorylation, and in a xenograft glioblastoma model via significant increase of mesenchymal markers such as transforming growth factor (TGF)-β2 and zinc finger e-box binding homeobox (ZEB)2 (Lu *et al.*, 2012; Piao *et al.*, 2012b). A hypoxic microenvironment can increase the SDF-1/C-X-C motif chemokine receptor (CXCR)-4 pathway activity, inducing the recruitment of pro-angiogenic bone marrow-derived precursors. These cells can drive vasculogenic processes to restore radiation-damaged vasculature, and in another study, specific deletion of MMP-9 in bone marrow-derived cells impaired the ability of the tumor to rebuild vessels lost after irradiation (Kioi *et al.*, 2010; Tseng *et al.*, 2011). Hypoxia can also induce an autophagic response in glioblastoma cells *in vivo*, promoting tumor survival and refractoriness to anti-angiogenic treatments. Deletion of *autophagy related* (*Atg*)*7*, an essential autophagy gene, prevented tumor resistance to bevacizumab (Hu *et al.*, 2012). Another resistance mechanism involves the up-regulation of other molecules involved in angiogenic processes. Angiopoietin (Ang)-2 ectopic expression in tumor cells compromises the efficacy of anti-VEGFR2 therapy, and in glioblastoma patients up-regulation of fibroblast growth factor (FGF)-2 and SDF-1 were associated with glioblastoma progression in patients treated with cediranib (Batchelor *et al.*, 2007; Chae *et al.*, 2010). From the metabolic perspective, Fack et al demonstrated that bevacizumab treatment elicited tumor cell metabolic reprogramming toward anaerobic glycolysis. This finding was corroborated by subsequent analysis of paired glioblastoma patient biopsies pre- and post-bevacizumab treatment (Fack *et al.*, 2015a).

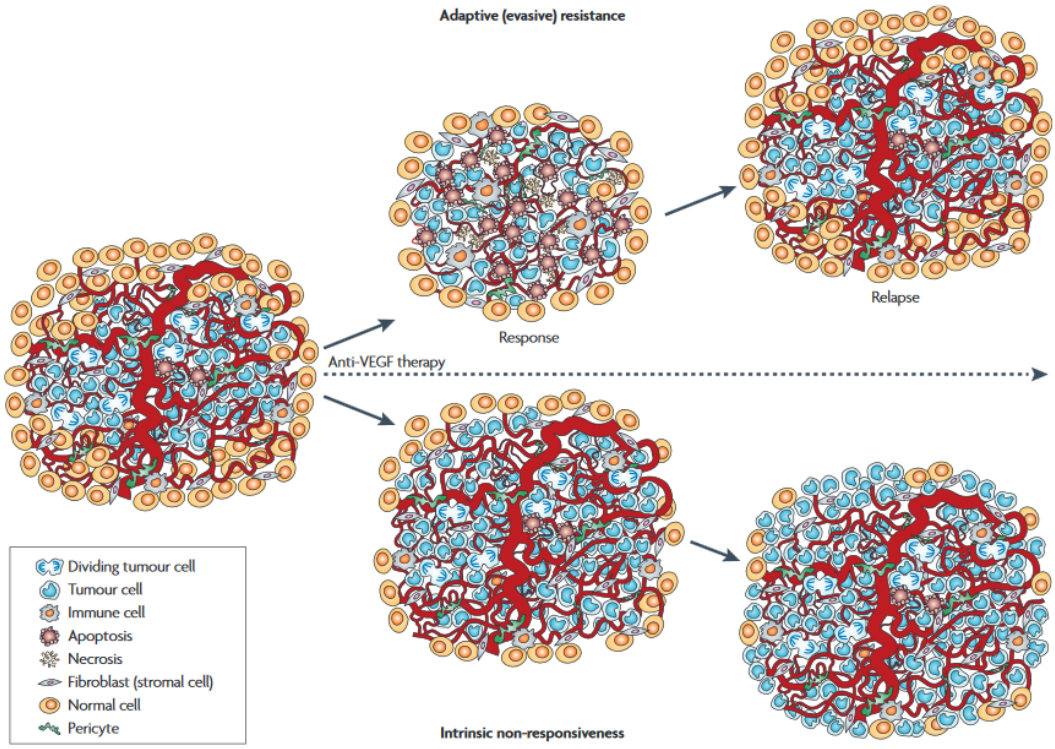

Figure 4. General mechanisms of resistance to anti-angiogenic therapies. Adaptive resistance versus intrinsic non-responsiveness. (Adapted from Bergers and Hanahan*.*, 2008)

3.4 Immunosuppression in glioblastoma

The immune system plays an important role during cancer pathogenesis. Seminal studies have shown in methylcholanthrene-induced cancer models that knockout mice for key components of the interferon (IFN)-γ pathway or the *perforin* gene are significantly more susceptible to tumor formation (Kaplan *et al.*, 1998; Street *et al.*, 2001). Later, it became clear that T cells can actively respond to genetic and cellular alterations occurring in cancer, and can eliminate arising cancer cells. It has been demonstrated that tumor-specific T cells exist against mutated or over-expressed tumoral proteins and can respond to these antigens mounting an effector response (Coulie *et al.*, 2014). However, the high selective pressure imposed by T cells on developing tumors, may eventually lead to immuno-edited clones, which escape from immune tumor-surveillance (Dunn *et al.*, 2004). Glioblastoma is paradigmatic for its ability to evade immunesurveillance and actively suppresses nascent immune responses against the tumor. Major hurdles in the glioblastoma immunotherapeutic context are thus the profound local immunosuppression established by glioma cells and the location of the tumor within the CNS, which is believed to be immunologically privileged.

3.4.1 Blood brain barrier and principles of neuro-immunology

The BBB is a highly specialized barrier that regulates molecules and cells entry within the CNS. More specifically, this barrier function is achieved through a perpetual interaction between the cellular components of the neurovascular unit. Astrocytes are fundamental for the maintenance of the endothelium, while pericytes wrap up the endothelium preserving its structural stability and have a key role during development by inducing endothelium barrier properties (Abbott *et al.*, 2006; Daneman *et al.*, 2010; Alvarez *et al.*, 2013; Obermeier *et al.*, 2013). Lastly, perivascular macrophages work as scavengers and activators of the immune responses at the barrier interface (Polfliet *et al.*, 2001; Serrats *et al.*, 2010). The ability of the endothelium to act as a barrier relies on two main features: tight junction proteins and ATP binding cassette (ABC) efflux transporters. Tight junctions are key structures to prevent the migration of molecules between the endothelial cells forming the BBB. The most important tight junction-associated proteins present in the BBB are occludin, claudin-1, and claudin-5 (Wolburg and Lippoldt, 2002; Abbott *et al.*, 2010). Claudin-1 and occludin are linked through the zonula occludens (ZO) protein to other tight junction-associated proteins (e.g. cingulin) and to the cellular cytoskeletal system.

All these complex interactions are critical to generate a tight closure between endothelial cells, regulating the passage of substances from the blood compartment to the CNS and *vice versa* (van Tellingen et al., 2015). Differently, ABC transporters actively efflux unwanted compounds out of the brain (Pardridge, 2005). The firstly discovered and most active ATP transporter is ABCB1 (also known as P-glycoprotein). It mediates multidrug resistance in tumor cells (Juliano and Ling, 1976). Since then, it has been shown that around 60% of all anticancer drugs are effluxed out by ABCB1, in turn, reducing the amount of drug accumulation in the tumor cells (van Tellingen *et al.*, 2015). Accordingly, ABCB1 heavily impacts the brain penetration of several anticancer agents (Demeule *et al.*, 2002).

The BBB also strictly regulates the access of immune cells to the brain. This tight regulation, along with the lack of a classical lymphatic system, and the observation that cells in the brain express low levels of the major histocompatibility complexes (MHC) proteins, led to the assumption that the CNS is an immunoprivileged site (Lampson and Hickey, 1986). Nonetheless, although at steady state, only few immune cells are present in the brain parenchyma, during injuries or other pathological conditions,

inflammatory stimuli render the BBB more permeable, which in turn, allows the brain trafficking of immune cells (Hickey *et al.*, 1991; Claudio, 1996; Lou *et al.*, 1997).

Several lines of evidence have demonstrated that antigens released in the CNS are drained into the peripheral cervical lymph nodes, where they can be taken up by professional antigen-presenting cells (APC) and be presented to naïve T cells. Only when activated in the cervical lymph nodes, T cells can up-regulate the specific expression of α4 and β1 integrins. These integrins allow for the passage of activated T cells through the BBB via specific interaction with vascular cell adhesion molecule (VCAM)-1 expressed on the surface of the brain endothelium (Calzascia *et al.*, 2005; Dunn *et al.*, 2012).

In the brain cancer context, it has been long assumed that most of the cancer immune-surveillance happens in the meningeal compartment. However, recent studies have shed new light on this matter and changed the view of the immune cell trafficking in and out of the brain. Studies performed independently by two laboratories showed the existence of a dural lymphatic vascular system, which drains fluids, macromolecules and immune cells from the cerebrospinal fluid, and is ultimately connected to the cervical lymph nodes in animal models (Aspelund *et al.*, 2015; Louveau *et al.*, 2015) (Figure 5). Although functional experiments are still required to fully assess the importance of immune cell trafficking during physiological and pathological conditions along the dural lymphatic system, this discovery shifts a long-held paradigm on CNS immunity, re-designing the brain as an immune distinct rather than immune privileged organ.

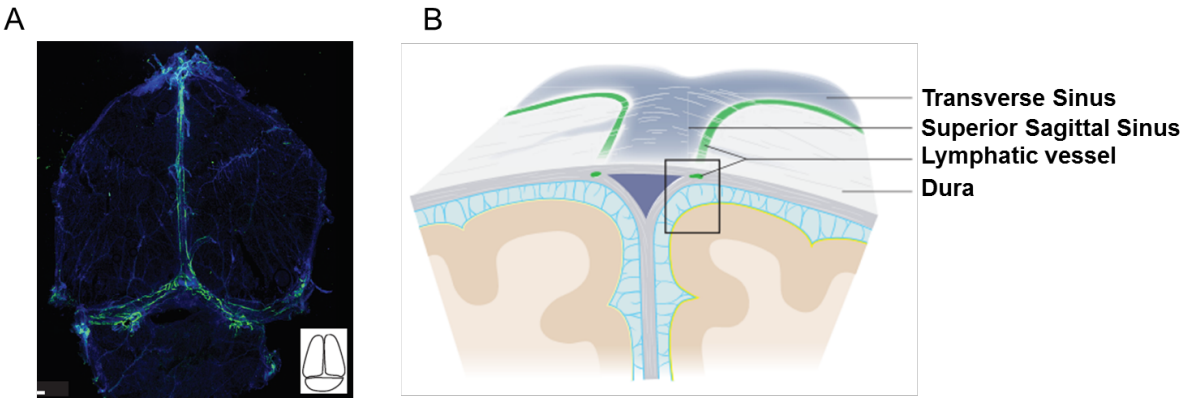

Figure 5. Newly discovered dural lymphatic system. A. Lymphatic vessel endothelial hyaluronan receptor 1 (LYVE-1) staining of whole-meninges section shows the existence of lymphatic vessels adjacent to the dural sinuses. B. Schematic graphic representation of dural lymphatic vessels position within the brain architecture.
(Adapted from Louveau *et al.,* 2015)

To a variable extent, immune cell infiltration within the brain tumor parenchyma has been found (Masson *et al.*, 2007; Donson *et al.*, 2012; Han *et al.*, 2014). During tumor development, the BBB can be partially disrupted, becoming more permeable to immune cell entry and administered drugs. Yet, intact zones of the BBB can protect tumor cells invading the brain parenchyma from anticancer agent delivery (Figure 6). This represents a major therapeutic problem and may likely be a possible explanation for the disappointing results achieved by targeted therapies against glioblastoma (Agarwal *et al.*, 2013; Olson *et al.*, 2014; Becker *et al.*, 2015). Many efforts are currently ongoing to thwart BBB drug-extrusion activity, which in turn, may improve the efficacy of several targeted treatments (van Tellingen *et al.*, 2015).

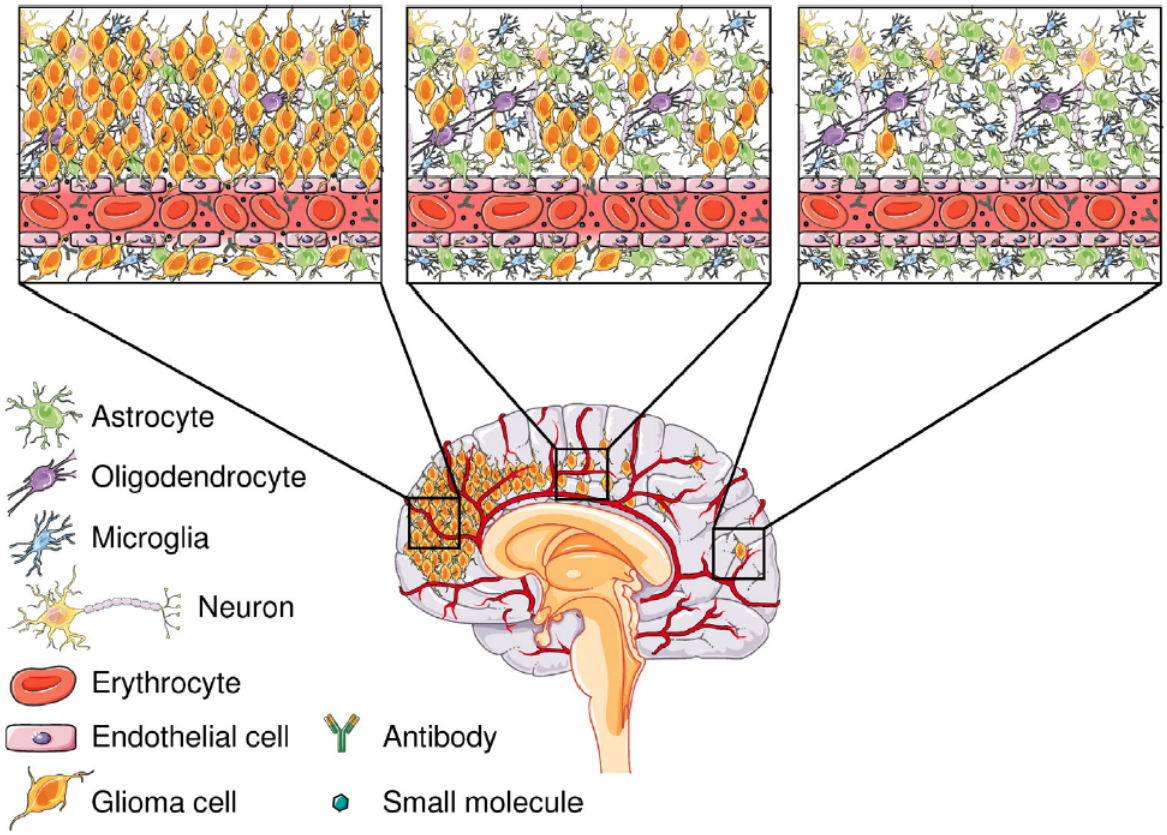

Figure 6. Blood brain barrier (BBB) integrity and composition in glioblastoma. During glioblastoma progression, the BBB possesses a heterogeneous structure: In the left panel, barrier integrity is completely compromised. The middle panel illustrates few zones of leakiness and the presence of some glioblastoma-infiltrating cells. Lastly, in the right panel, the BBB is intact and single invasive tumor cells may be present. Importantly, while disrupted zones of the BBB allow small molecules and antibodies penetrance within the tumor, intact zones may protect tumor cells infiltrated in the brain parenchyma distant from the primary tumor. These cells cannot be resected via surgical procedures and most likely are responsible for tumor recurrence and resistance to therapy. (Adapted from Van Tellingen *et al.,* 2015)

3.4.2 Immunosuppressive immune cell subsets

3.4.2.1 Regulatory T cells

Around 5-10% of all circulating $CD4^+$ T cells are regulatory T cells (Treg). This T cell subset is a key modulator of immune system's activity playing a central role in controlling tolerance to self and host antigens and impeding outbreak of autoimmune processes by resolution of inflammation (Sakaguchi, 2004). Treg display specific markers that distinguish these cells from other T cell subsets. Specifically, Treg are defined by interleukin-2 receptor alpha chain (also known as CD25), glucocorticoid-induced tumor necrosis factor receptor (GITR), and cytotoxic T lymphocyte antigen (CTLA)-4 expression (Wainwright *et al.*, 2013). Moreover, Treg can be further subdivided into two functional classes: natural Treg (nTreg) that developed in the thymus, and induced Treg (iTreg), which emerge from conventional T cells that start to express forkhead box P3 (FoxP3) in an immunosuppressive micro-milieu. In glioblastoma patients, Treg percentages are increased in the peripheral blood and tumor biopsies and this is associated with higher tumor grade and worse prognosis (Fecci *et al.*, 2006; El Andaloussi and Lesniak, 2007; Heimberger *et al.*, 2008). Other studies suggest that the presence of Treg in the blood or tumor is not a negative prognostic factor (Lohr *et al.*, 2011; Han *et al.*, 2014; Thomas *et al.*, 2015). Contradictory data may be due to the existence of different Treg subsets, which can be distinguished only through multi-marker panels and not only via FoxP3 detection. In murine models, infiltrating Treg within gliomas are mainly thymus-derived nTreg. The recruitment of these cells was significantly impaired in mice previously thymectomized (Wainwright *et al.*, 2011). These data suggest that glioma cells can readily recruit nTreg from the periphery, principally through the chemokine/chemoreceptor pathway C-C motif chemokine ligand (CCL)22/C-C motif chemokine receptor (CCR)4 (Jacobs *et al.*, 2010). In a spontaneous astrocytoma model, Thang and colleagues demonstrated that at pre-symptomatic tumor stages, there was a significant infflux of $CD4^+$ and $CD8^+$ cells, with a significant fraction being $CD4^+$ $CD25^+$ T cells which include Treg (Thang *et al.*, 2010). The importance of this cell subset in disrupting anti-tumor immunity has been shown in several pre-clinical models. In the syngeneic SMA-560 orthotopic VM/Dk model, treatment with a monoclonal antibody against CD25 led to functional inactivation of Treg and restored anti-tumor activity (Fecci *et al.*, 2006). Likewise, blockade of the TGF-β pathway

resulted in heightened anti-glioma immunity, partly via diminished intratumoral Treg infiltration most probably due to impaired trafficking from the periphery (Ueda *et al.*, 2009). Treg blockade has also been translated in clinical settings and daclizumab, a humanized monoclonal antibody against CD25, has shown promising preliminary data in glioblastoma patients (Sampson *et al.*, 2012). More recently, Treg have been attributed with new intriguing roles. Lowther and colleagues have detected a dysfunctional Treg cell population, which displays high expression of programmed cell death 1 (PD-1) and has weak suppressive activity and produces IFN-γ (Lowther *et al.*, 2016). Also, in accordance with the role of Treg in resolving inflammatory states, these cells can induce tissue repair by secreting the EGF family ligand amphiregulin (Arpaia *et al.*, 2015; Leavy, 2015). These new findings highlight a wider role played by these cells during physiological and pathological conditions, and possibly challenge the view of an exclusive inhibitory effect on antitumor immunity.

3.4.2.2 Glioma-associated microglia/macrophages and myeloid-derived suppressor cells

Microglia and macrophages represent the most prominent immune infiltrate in glioblastoma and great attention has been posed on their role in tumor development and progression (Morantz *et al.*, 1979; Morimura *et al.*, 1990). These cells can build up to 12% of the tumor mass and their presence correlates with higher tumor grade (Nishie *et al.*, 1999; Badie and Schartner, 2000). Importantly, infiltrated microglia/macrophages are re-programmed to support tumor growth and resistance to therapeutic intervention. Experimentally, microglia and macrophages have been defined by differential expression of the CD45 surface marker. Microglia cells have been distinguished as $CD45^{low}$ whereas macrophages are $CD45^{high}$. However, during inflammatory states, microglia can upregulate CD45 expression making distinctions between these two population challenging (Parney *et al.*, 2009; Muller *et al.*, 2015). To date, it is still not possible to clearly separate these two populations as they are characterized by a wide phenotypic plasticity. Nonetheless, from the functional perspective, these populations have been divided in two phenotypic classes: the classically activated M1 and the alternatively activated M2 state. M1-polarized microglia/macrophages have a pronounced anti-tumor activity and produce high amounts of pro-inflammatory cytokines, whereas M2 skewed cells tune down inflammatory responses, activate tissue remodeling, and repair programs (Mantovani

et al., 2002). Importantly, these two functional polarizations are rather extremes of a wide phenotypic continuum.

In glioblastoma, tumor-associated macrophages show a M2 immunosuppressive phenotype and secrete a plethora of pro-tumorigenic molecules such as TGF-β, VEGF, EGF and MMP-2, which drive various oncogenic features (Platten *et al.*, 2001; Markovic *et al.*, 2005; Komohara *et al.*, 2008; Wesolowska *et al.*, 2008; Coniglio *et al.*, 2012; Riabov *et al.*, 2014). Targeting of colony stimulating factor-1 receptor (CSF-1R), a key receptor that promotes macrophage differentiation, survival, and pro-tumorigenic functions, significantly increased the survival of glioma-bearing mice by the re-polarization of microglia/macrophages to an anti-tumor M1 phenotype (Pyonteck *et al.*, 2013).

Myeloid-derived suppressor cells (MDSC) are another important immunosuppressive cell subset in glioblastoma. In mice, MDSC are usually referred to as $CD11b^{+}$ $Gr\text{-}1^{int}$ $Ly6C^{+}$ and comprise immature cells containing common precursors of both monocytic and granulocytic lineages (Peranzoni *et al.*, 2010). This immature cell subset is recruited by tumors from the bone marrow and directly inhibits cytotoxic T cells through nitric oxide (NO) release in a rat glioma model (Jia *et al.*, 2010). Hypoxia is a main driver for MDSC recruitment and its presence is linked to decreased number of tumor-infiltrating T cells in human and murine gliomas (Corzo *et al.*, 2010; Raychaudhuri *et al.*, 2015). Interestingly, hypoxia-driven HIF-1α up-regulates PD-ligand 1 (PD-L1) expression in glioma-infiltrating MDSC. This finding links the cellular immunosuppressive function of MDSC to the PD-1 pathway (for details see section 3.6.1 and 3.6.2) (Noman *et al.*, 2014). Importantly, despite their prominent role in tumor-associated immunosuppression, the existence of some MDSC subsets remains controversial and requires further investigation (Marvel and Gabrilovich, 2015).

In conclusion, tumor-associated microglia/macrophages and MDSC have many overlapping inhibitory functions and possess an intrinsic high phenotypic plasticity.

3.4.3 Glioma-derived soluble immunosuppressive factors

Glioma cells can secrete a variety of soluble molecules, which contribute to the harsh immune-inhibitory microenvironment (Figure 7). Among the most prominent immunosuppressive factors are TGF-β family ligands, which are thoroughly discussed in section 3.5.2.

VEGF it is not only involved in glioma angiogenesis. Indeed, it can dampen APC maturation and function, and can induce the expression of PD-1 and CTLA-4 on the surface of $CD8^+$ T cells, impairing their antitumor activity (Gabrilovich *et al.*, 1996; Voron *et al.*, 2015). Glioma cells can also produce IL-10, which can induce PD-L1 expression on monocytes and regeneration and tolerance factor (RTF) that can shield glioblastoma cells from natural killer cell attack (Roth *et al.*, 2006; Bloch *et al.*, 2013). Other immunosuppressive secreted molecules are arginase I, NO and prostaglandin E (PGE)-2. Arginase I presence in the sera of glioblastoma patients is strongly associated with general immunosuppression and NO and PGE-2 can be secreted by adult neural stem/progenitor cells suppressing T cell effector functions (Wang *et al.*, 2009; Sippel *et al.*, 2011).

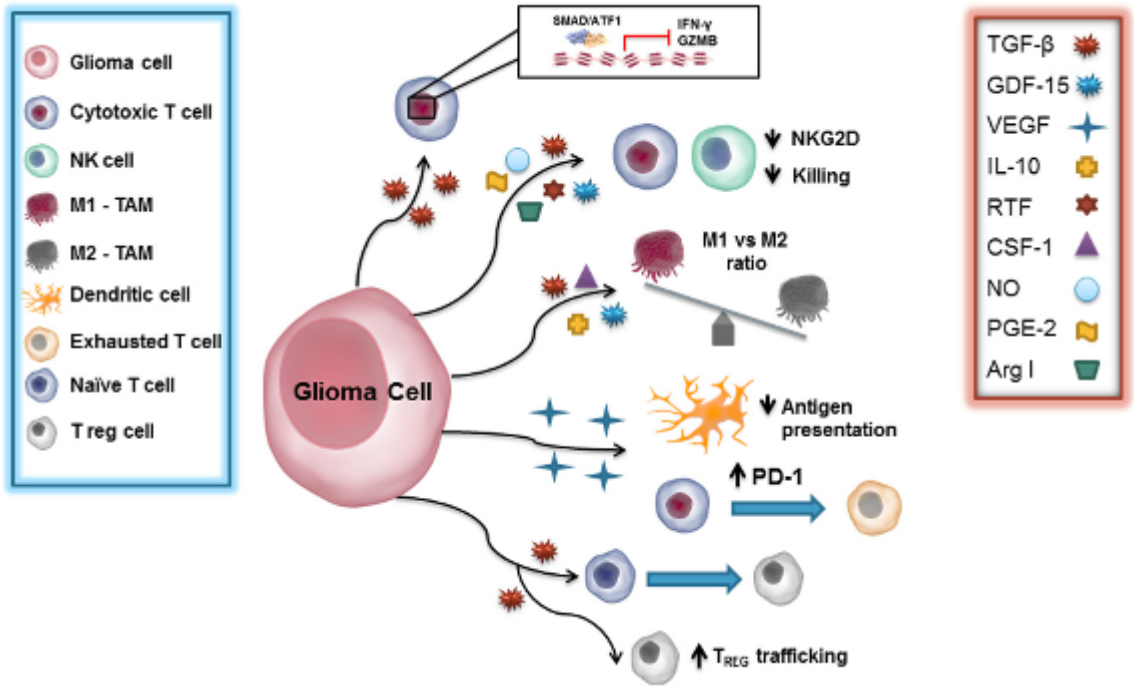

Figure 7. Soluble immunosuppressive factors secreted by glioma cells. Glioma cells employ various soluble factors to generate an immunosuppressive microenvironment. TGF-β impairs T cell cytotoxic functions by inhibiting IFN-γ, granzyme B (GZMB) and NKG2D, shifts macrophages polarization toward an M2 tumor-promoting phenotype, and stimulates Treg induction and recruitment to the tumor. VEGF hinders efficient antigen presentation, and rise the expression of immune checkpoint receptors on $CD8^+$ effector cells. IL-10, RTF, colony stimulating factor (CSF)-1, arginase (Arg) I, NO, andPGE2 altogether contribute to glioma cell-induced immunosuppression. (Adapted from Mangani *et al.,* 2016)

3.5 TGF-β superfamily

The TGF-β superfamily comprises around 30 members. TGF-β ligands, bone morphogenetic proteins (BMP), activins, nodal, growth and differentiation factors (GDF), and anti-Müllerian hormone (AMH) are all superfamily members and play fundamental roles in various processes spanning from the early developmental stages to tissue maintenance and homeostasis in adult mammals (Wakefield and Hill, 2013).

3.5.1 TGF-β pathway

In mammals three main TGF-β ligand isoforms exist: TGF-β_1, TGF-β_2, and TGF-β_3. All the ligands of the family are produced as precursors and are activated by pro-protein convertase mediated-cleavage (Akhurst and Hata, 2012). Activated ligands can homo- or heterodimerize through disulphide bonds and can initiate a transduction cascade via membrane receptors. Usually, two main types of serine/threonine membrane receptors are required: a type I and a constitutively active type II receptor. Upon ligand binding, the constitutive active type II trans-phosphorylates the type I, which then recruits SMAD proteins initiating the signal transduction to the nucleus (Figure 8). TGF-β ligands can also commence a non-canonical signalling via activation of several intracellular mediators such as the RAS pathway, PI3K, TGF-β-activated kinase (TAK)-1 and nuclear factor kappa B (NF-Kb), which all together can generate the pleiotropic responses mediated by this pathway (Akhurst and Hata, 2012) (Figure 9). Of note, signalling activity and strength can be further modulated by the co-receptors endoglin and betaglycan, adding another layer of complexity (Bernabeu *et al.*, 2009).

Knockout mice for *TGF-β_1* are embryonic lethal due to vascular defects (Dickson *et al.*, 1995). *TGF-β_2* null mice possess multiple developmental defects, which do not recapitulate the *TGF-β_1* or *TGF-β_3* knockout mice phenotype suggesting that these ligands have also non-overlapping functions (Sanford *et al.*, 1997). In humans, mutation of the TGFβRI activing receptor-like kinase (ALK)-1 or of the co-receptor endoglin cause an autosomal dominant disorder termed Hereditary Haemorrhagic Teleangiectasia (HHT), which is characterized by vascular dysplasia (McAllister *et al.*, 1995; Johnson *et al.*, 1996).

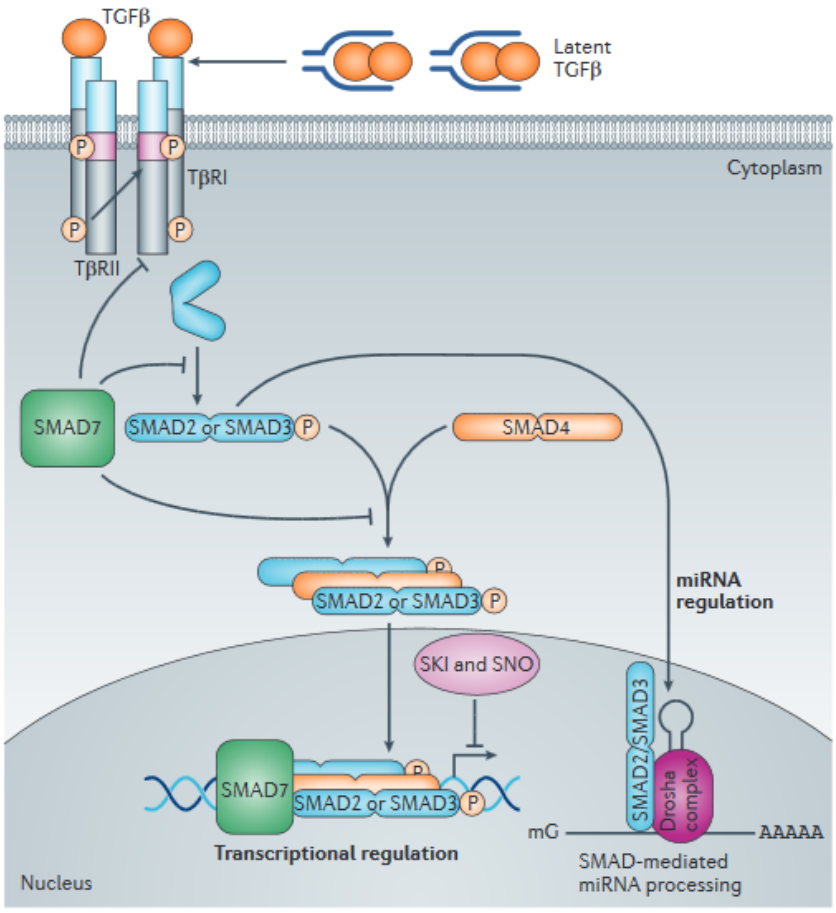

Figure 8. Canonical TGF-β pathway. TGF-β is activated by pro-protein convertase cleavage and can dimerize and thereafter bind its receptors. Upon binding, type II and type I receptors heterodimerize and recruit SMAD2 or SMAD3, which are phosphorylated and bind the common mediator SMAD4. The formed complex can translocate into the nucleus where it can either induce or repress target genes expression. SMAD complexes can also influence the biogenesis of microRNA. SMAD7, and the nuclear proteins SKI and SNO, are negative regulators of the pathway. (Adapted from Akhurst and Hata 2012)

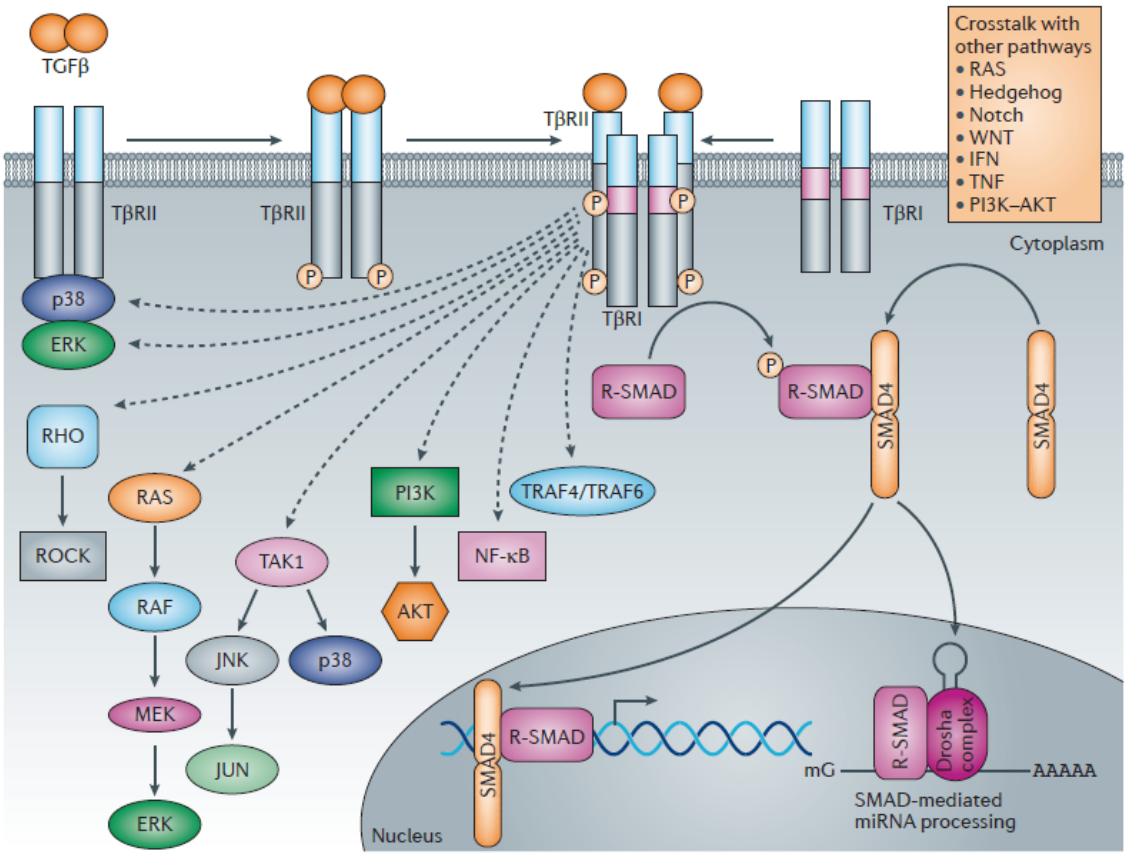

Figure 9. Non-canonical TGF-β pathway.
TGF-β signalling can activate multiple downstream pathways. Besides the classical SMAD-mediated signalling, TGFβR can signal through the RAS/MAPK pathway, TAK1, p38 mitogen-activated protein kinase (p38), PI3K/AKT pathway, RHO/ROCK axis, tumor necrosis factor receptor associated factor (TRAF)-4 and -6, and NF-κB. All these pathways are activated in a context-specific cell-dependent manner, and regulate most of the pleiotropic TGF-β-induced responses.
(Adapted from Akhurst and Hata 2012)

3.5.2 The TGF-β pathway in glioblastoma

TGF-β is a multifunctional cytokine implicated in several physiological processes in a cell-specific and context-dependent manner. Despite the fact that TGF-β initially functions as a "barrier" against cancer development, a strong correlation between this molecule and the level of malignancy, as well as poor prognosis has been demonstrated in glioma in some studies, although this has not been confirmed in our laboratory (Bruna *et al.*, 2007; Massague, 2008; Hau *et al.*, 2011; Frei *et al.*, 2015).
TGF-β_2 was initially discovered as *glioblastoma derived T cell suppressor factor* (GsT) due to its ability to disrupt IL-2-mediated T cell survival (Schwyzer and Fontana, 1985). Since then, many other immunosuppressive and tumor-promoting functions have been

attributed to TGF-β. All three isoforms are expressed in glioblastoma, yet, while TGF-β_1 and TGF-β_2 have been attributed clear roles in repressing immune functions within the tumor microenvironment, fewer data have been collected for TGF-β_3 (Pickup *et al.*, 2013; Frei *et al.*, 2015; Seystahl *et al.*, 2017). When exposed to TGF-β, $CD4^+$ T cells can differentiate into Treg by up-regulating the lineage-defining nuclear transcription factor FoxP3 (Chen *et al.*, 2003; Fu *et al.*, 2004). Moreover, the function of $CD8^+$ cytotoxic T cells are greatly suppressed by TGF-β via activation of a repressive transcriptional circuit. Indeed, a complex formed by SMAD/ATF1 proteins can inhibit the expression of *IFN-γ* and *granzyme B*, which are required to carry out T cell-mediated anti-tumor responses (Thomas and Massague, 2005). Also, TGF-β activity can shield tumor cells from an immune attack by down-modulating the expression of NKG2D, an activating receptor for NK cells and co-stimulatory molecule for $CD8^+$ cells, and by reducing the expression of the NKG2D ligands MICA and ULBP2 on the cell surface of glioma cells (Friese *et al.*, 2004; Eisele *et al.*, 2006). Other immune-repressing activities orchestrated by TGF-β include polarization of myeloid cells toward a pro-tumorigenic phenotype and diminished antigen presentation by dendritic cells (DC) (Fridlender and Albelda, 2012; Gong *et al.*, 2012). Of note, other members of the TGF-β superfamily such as GDF-15 may also suppress immune effector mechanisms (Roth *et al.*, 2010).

Pleiotropic activity of the TGF-β pathway encompasses multiple pro-tumorigenic features, far beyond immunosuppression. TGF-β activity may be crucial for tumorigenicity, self-renewal, survival, and resistance of GSC to radiotherapy (Ikushima *et al.*, 2009; Penuelas *et al.*, 2009; Anido *et al.*, 2010; Hardee *et al.*, 2012). Also, TGF-β fosters the malignant phenotype of glioblastoma through induction of angiogenesis, proliferation, migration, and invasion (Platten *et al.*, 2001; Wick *et al.*, 2001; Ishihara *et al.*, 2008; Dieterich *et al.*, 2012; Krishnan *et al.*, 2015).

Due to its extensive role in the malignant phenotype of glioblastoma, TGF-β has been regarded as a promising molecular target. Although TGF-β inhibition has proven remarkable efficacy in various preclinical glioma models, translation of these results into the clinic has been disappointing (Uhl *et al.*, 2004; Ueda *et al.*, 2009). A phase II trial in recurrent glioblastoma with the TGFβRI inhibitor galunisertib was ineffective to prolong progression-free or overall survival (Brandes *et al.*, 2016). However, TGF-β inhibition is still of interest, especially, in combinatorial approaches targeting different glioblastoma-relevant pathways (such as angiogenesis or immune checkpoints).

3.6 Immune checkpoints

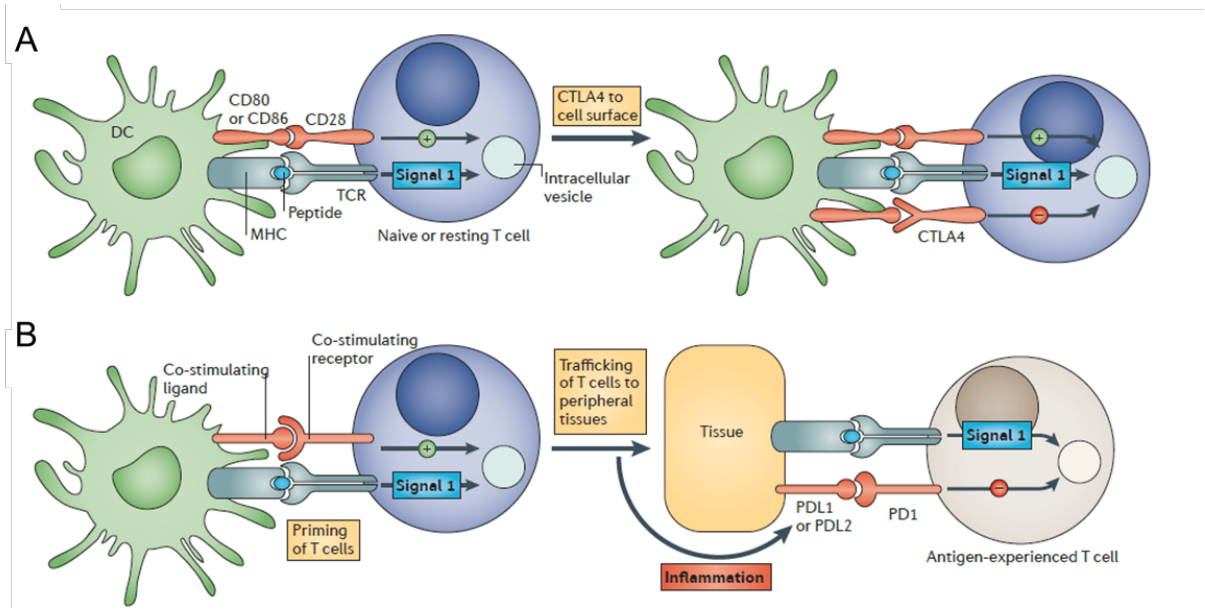

Figure 10. CTLA-4 and PD-1 immune checkpoint pathways.
A. CTLA-4 acts at the initial stages of the immune response. It is induced in an amplitude-dependent manner during T cell activation, and competes with the CD80/CD86 costimulatory molecules for CD28 binding, dampening T cell responses. B. The PD-1 pathway regulates inflammatory T cell responses in peripheral tissues. Activated T cells start to express increasing levels of PD-1 in time, while inflammatory signals induce the expression of PD-L1 and PD-L2 in tissues. When PD-1 engages its ligand expressed by cells present within the inflamed tissue, T cells receive a negative signal that dampens their effector activity.
(Adapted from Pardoll 2012)

Lafferty and Cunningham proposed the widely accepted model of naïve T cell activation in 1975 (Lafferty and Cunningham, 1975). This model postulates that T cells require a double positive signal in order to become fully activated. The first signal is highly specific and dictated by the interaction between a peptide loaded on a MHC-complex with the T cell receptor (TCR). The second stimulus, also called costimulatory signal, is antigen-independent and is delivered by APC to induce all the characteristic features possessed by activated T cells such as clonal expansion or cytokine secretion. Without the second signal, T cells cannot respond to antigen stimulation and rather become anergic and subsequently even tolerant to that antigen. The classical costimulatory signal happens when CD80 or CD86 present on the mature APC membrane bind to CD28 found on T cells, delivering the second signal and inducing full T cell activation (Pardoll, 2012). Costimulatory molecules that deliver negative signals also exist and are referred as to immune checkpoints. These molecules are regulators of T cell activation, are critical for preserving self-tolerance, and modulate

duration and magnitude of immunological responses. To date, two major checkpoints have been regarded as the most relevant for cancer immunotherapy: CTLA-4 and PD-1 (Figure 10).

CTLA-4 acts in the initial steps of T cell activation and its inhibitory function depends on the magnitude of the initial response; MHC-peptide complexes with high affinity for the TCR produce higher induction of CTLA-4 expression. This mechanism allows the maintenance of a fine balance between positive and negative signals and permits a constant T cell activation that is less dependent from antigen concentration and ligand affinity (Pardoll, 2012). Differently from CTLA-4, PD-1 acts after the initial step to regulate T cell activation in peripheral tissues, limiting inflammation-related collateral damages.

3.6.1 PD-1 pathway

In 1992, Ishida and colleagues discovered the PD-1 receptor as a molecule that was up-regulated in a T cell hybridoma cell line during apoptosis (Ishida *et al.*, 1992). The first compelling evidence of the role of PD-1 in immune regulation comes from the phenotype displayed by *Pdcd1*-null mice, which are prone to develop different autoimmune diseases in a strain-dependent manner (Nishimura *et al.*, 1999; Nishimura *et al.*, 2001). The phenotypes exhibited by PD-1 knockout mice show the role of this receptor in controlling the induction and maintenance of T cell tolerance, thus acting mainly as an immunological rheostat and highlight the differences with *CTLA-4* null mice, which die from fatal multi-organ failure caused by uncontrolled lymphoproliferation (Tivol *et al.*, 1995; Waterhouse *et al.*, 1995).

Upon binding to one of its ligands, PD-L1 or PD-L2, PD-1 is phosphorylated in its intracellular tail and recruits the SH2-domain containing tyrosine phosphatase (SHP)-2 protein, which in turn, hinders TCR signalling and subsequent T cell activation (Sheppard *et al.*, 2004). Mechanistically, PD-1 activation leads to inhibition of the anti-apoptotic protein B cell lymphoma-extra large (Bcl-xL) and reduced expression of transcription factors implicated in T cell effector mechanisms such as GATA-3, Tbet and Eomes (Chemnitz *et al.*, 2004; Nurieva *et al.*, 2006).

PD-L1 is present on almost all human and mouse cells and its constitutive and inducible expression is regulated by interferon signalling, since two IFN regulatory factor (IRF)-1 binding sites are present in the promoter region (Lee *et al.*, 2006; Keir *et*

al., 2008). Differently, PD-L2 expression is rather restricted to few hematopoietic cells, such as DC and macrophages, and mainly inducible by inflammatory stimuli.

PD-1 ligands can also have different binding partners. Recently, it has been shown that PD-L1 can also bind CD80 with higher affinity than CD28, but lower than CTLA-4. Interestingly, PD-L1 can be found on the surface of T cells and knockout studies have shown that signalling through this ligand exert an additional inhibitory signal (Latchman *et al.*, 2004).

Although PD-L2 cannot bind CD80, another binding partner has been identified. Repulsive guidance molecule b (RGMb), a coreceptor for BMP signalling, can bind PD-L2 and this engagement is fundamental in promoting respiratory tolerance, adding an ulterior layer of complexity to this pathway (Xiao *et al.*, 2014).

3.6.2 The PD-1 pathway in glioblastoma

Given that PD-1 transduces an inhibitory signal to the activated T cell, PD-L1-expressing tumor cells can protect themselves from an immune attack by a mechanism called “molecular shield” (Azuma *et al.*, 2008). The relevance of this pathway lies in the observation of so far unseen clinical responses achieved by PD-1 blockade in hitherto unresponsive tumors such as advanced metastatic melanoma and non-small cell lung cancer (Wolchok *et al.*, 2013; Rizvi *et al.*, 2015). Efficacy of PD-1 targeting agents are yet to be determined in glioblastoma, however, they are being currently evaluated in both newly diagnosed and recurrent glioblastoma (Preusser *et al.*, 2015; Weiss *et al.*, 2015).

Various preclinical studies *in vitro* and *in vivo* have confirmed PD-L1 expression in glioma cells (Wintterle *et al.*, 2003; Wilmotte *et al.*, 2005; Jacobs *et al.*, 2009; Berghoff *et al.*, 2015; Nduom *et al.*, 2016). At the molecular level, PD-L1 expression in glioblastoma has been linked with PTEN loss and NF1 mutation with subsequent MAPK pathway activation (Parsa *et al.*, 2007; Heiland *et al.*, 2017). Conversely, no evidence so far has been provided for PD-L2 expression in glioblastoma. Importantly, PD-L1 levels are dramatically enhanced by IFN-γ stimulation. This mechanism, called adaptive resistance, has a crucial role during inflammatory response as it protects normal tissues from collateral damages that can be caused by uncontrolled T cell activation. Tumors can efficiently hijack this process shielding themselves from immune recognition and elimination (Tumeh *et al.*, 2014). Therapeutic efficacy by PD-1 blockade, and even complete tumor eradication, have been demonstrated in several

preclinical glioma models. Best results were achieved when PD-1 inhibition was administered in combination with radiotherapy or other checkpoint inhibitors (Zeng *et al.*, 2013; Wainwright *et al.*, 2014; Reardon *et al.*, 2016). As already mentioned, PD-L1 is ubiquitously expressed and induced by inflammatory stimuli. As a consequence all cell types residing in the tumor micro-milieu can provide negative signals to infiltrated T lymphocytes. Gliomas can mediate an IL-10-dependent paracrine loop that induces PD-L1 expression in tumor-associated macrophages, which results in heightened immunosuppression (Bloch *et al.*, 2013). In another study, an IFN-β-mediated autocrine loop in human neurons enhances PD-L1 expression and this was linked with induction of apoptosis in glioma cells and improved survival of glioma patients (Liu *et al.*, 2013). Accordingly, a recent paper has shown that PD-L1 from different cell type sources within the tumor microenvironment can non-redundantly contribute to immunosuppression (Lau *et al.*, 2017).

Intriguingly, several reports have shown that the role of PD-L1 may extend beyond immunosuppression. In fact, this ligand provides reverse signalling into the cell, which may provide anti-apoptotic stimuli to the tumor cell (Azuma *et al.*, 2008). Moreover, membrane-bound PD-L1 can increase tumor cell glycolytic activity, thereby sustaining tumor cell immune escape by withdrawing glucose bioavailability from T cells, which highly depend on this molecule to efficiently activate their effector phenotype (Chang *et al.*, 2015). Mechanisms by which PD-L1 regulates tumor cell metabolism are poorly understood and have never been investigated in glioblastoma warranting further investigation. In conclusion, these studies highlight that the PD-1/PD-L1 pathway may represent a key tumor-promoting hub, which plays a dual role in protecting tumor cells from immune attack while promoting their metabolic activity and survival.

4. Materials and Methods

Reagents

Recombinant human TGF-β2 was purchased from R&D systems (Minneapolis, MN), murine VEGF (VEGF120) from biolegend (San Diego, CA) and murine IFN-γ from peprotech (Rocky Hill, NJ). B20 was kindly provided by T. R. Schwartz (Genentech, South San Francisco, CA), cediranib by AstraZeneca (London, UK), LY2157299 (LY) by Eli Lilly & Co. (Indianapolis, MN), SD-208 by Scios Inc. (Freemont, CA) and anti-PD-1 (78AFS) by Merck (Boston, MA).

Cell lines

Murine SMA-497, SMA-540 and SMA-560 glioma cells were kindly provided by D.D. Bigner (Durham, NC). GL-261 cells were received from the National Cancer Institute (Frederick, MD). The cells have been characterized extensively in our laboratory (Ahmad *et al.*, 2014) and are commonly cultured as adherent monolayers in Dulbecco`s modified Eagle medium (DMEM) (Gibco, Invitrogen AG, Basel, Switzerland) supplemented with 10% heat-inactivated fetal calf serum (FCS) (Biochrom KG, Zug, Switzerland) and 2 mM glutamine (Biochrom KG) (DM medium). Hypoxia treatment was done in a hypoxia chamber 1% O2 atmosphere at 37°C.

Viability and clonogenicity assays

Viability was assessed after pooling adherent and floating cells by trypan blue dye exclusion. Clonogenicity was assessed as previously described (Happold *et al.*, 2014). Briefly, 100 cells per well were seeded in 96-well or 6-well plates, allowed to adhere overnight, and treated for 24 h with either LY2157299 (Eli Lilly & Co, 1 µm), cediranib (AstraZeneca, 100 nM), or B20 (Genentech, 100 µg/ml) in fresh medium followed by an observation period for 10 to 14 days in serum-containing medium. Cell density was assessed by counting crystal violet stained cultures.

Real-time PCR (RT-PCR)

Total mRNA for baseline gene expression analyses was extracted from murine glioma cells or from *in vivo* tumor tissue (Seystahl *et al.*, 2015). For RT-PCR, gene expression was measured using the Real Time PCR System 7300 (Applied Biosystems, Foster City, CA) with SYBR Green Master Mix (AppliChem, Darmstadt, Germany) and primers

at optimized concentrations. The conditions for RT-PCR were 40 cycles, 95°C/15s, 60°C/30s, 72°C/30s. Relative quantification of gene expression was determined by comparison of cycle threshold values. Hypoxanthine phosphoribosyltransferase 1 (HPRT1) was used as a housekeeping gene and specific target gene expression was normalized to HPRT1 and calculated with the ΔCT-method for relative quantification with respect to primer efficiency calculated by the standard curve method. The following mouse-specific primers were used: HPRT1 (forward 5'-TTGCTGACCTGCTGGATTAC-3', reverse 5'-TTTATGTCCCCCGTTGACTG-3'), VEGF (forward 5'-CACGACAGAAGGAGAGCAGA-3', reverse 5'-GGGCTTCATCGTTACAGCAG-3'), VEGFR1 (forward 5'-AGAGGAGGATGAGGGTGTCT-3', reverse 5'-GGGAACTTCATCTGGGTCCA-3'),VEGFR2 (forward 5'-GCTCCTGACTACACTACCCC-3', reverse 5'-AGGAAACAGGTGAGGTAGGC-3'), TGF-β_1 (forward 5′-TGGAGCAACATGTGGAACTC-3′, reverse 5′- GTCAGCAGCCGGTTACCA-3′), TGF-β_2, (forward 5′-GCCCACTTTCTACAGACCCT -3′, reverse 5′-CCTTGCTATCGATGTAGCGC-3′), ALK-5 (forward 5'-TGGGACTTGCTGTGAGACAT-3', reverse 5'- CCACCAATAGAACAGCGTCG-3') and TGF-βR2 (forward 5'-CTGTTGCCTGTGTGACTTCG-3', reverse 5'-AACGACTCCACGTTTTC-3'), PD-L1 (forward 5'-CTCCTCGCCTGCAGATAGTT-3', reverse 5'-ATCGTGACGTTGCTGCCATA-3'), PD-L2 (forward 5'-GTGCTGGGTGCTGATATTGAC-3', reverse 5'-AAAATCGCACTCCAGGCTCA-3') (all Microsynth, Balgach, Switzerland).

Immunoblot analyses

For immunoblot analysis, whole cell lysates were prepared using RIPA lysis buffer containing 1% NP-40, 0.5% sodium deoxycholate, 50 mM Tris/HCl pH 8.0, 150 mM NaCl, 5 mM EDTA pH 8.0, 0.1% SDS in Milli-Q water supplemented with 2 µg/mL aprotinin, 10 µg/mL leupeptin, 100 µg/mL phenylmethylsulfonyl fluoride (Sigma Aldrich, St. Louis, MO), phosphatase inhibitor cocktails 2 and 3 (Sigma Aldrich). Protein levels were determined using BCA Protein Assay Kit (Pierce/Thermo Fisher, Madison, WI). After SDS-PAGE (8 – 12 % acrylamide gels, Biorad, Hercules, CA) under reducing conditions with loading of equal amounts of proteins, proteins were transferred to nitrocellulose membranes (Biorad), blocked in Tris-buffered saline containing 5% skim milk and 0.1% Tween 20 and incubated with the following antibodies at concentrations

recommended by the manufacturers: anti-VEGFR1 (R&D Systems, AF471, 1:500), anti-VEGFR2 (Cell Signaling, Leiden, Netherlands, #2479, 1:500), anti-pSMAD2 (Cell Signaling, #3108, 1:1000), anti-ALK-5 (Santa Cruz Biotechnology, Inc., Dallas, TX, sc-9048, 1:500), anti-TGFβR2 (R&D Systems, AF532, 1:500), anti-β-actin (Santa Cruz Biotechnology, Inc., sc-1616, 1:2000). Visualization of protein bands was accomplished using horseradish peroxidase (HRP)-coupled secondary antibodies (Santa Cruz) and enhanced chemoluminescence (Pierce/Thermo Fisher, Madison, WI). For quantitative correlation analyses of baseline expression of total and phosphorylated proteins, band intensity was analyzed via densitometry using ImageJ software (http://imagej.nih.gov/ij/index.html, Open Source).

Enzyme-linked immunosorbent assay (ELISA)

Supernatants were collected from subconfluent glioma cell cultures after the indicated time periods. Treatments were performed in serum-free medium for the indicated time periods. Cellular debris was removed by centrifugation and supernatants were concentrated using 3K-Amicon® Ultra-4 Centrifugal Filter Units (Millipore AG, Zug, Switzerland). ELISA kits for murine VEGF (VEGF, eBiosciences, San Diego, BM5619/2), murine TGF-β_1 (eBiosciences, BMS608/4) and TGF-β_2 (R&D, MB200) were used. Results were normalized to the cell numbers at the time of harvesting.

Animal studies

The standard operating procedures for the animal studies were approved by the Swiss Cantonal Veterinary Office under the Animal license permission number 38/2012 and 132/2011. The care and treatment of all animals was in accordance with the Swiss Federal Law on the Protection of Animals, the Swiss Federal Ordinance on the Protection of Animals and the guidelines of the Swiss confederation. Following anesthesia, a burr hole was drilled in the skull 1.5 mm lateral and 1 mm posterior to the bregma. The needle of a Hamilton syringe (Hamilton, Darmstadt, Germany) was introduced to a depth of 3 mm. A volume of 2 µl of a single cell suspension in PBS was slowly injected into the right striatum. In VM/Dk mice 5 x 10^3 SMA glioma cells were implanted, whereas in C57Bl/6 mice 2 x 10^4 GL-261 cells were implanted (n=10 per group). For project 1 systemic treatment was performed by i.p. injections of B20 (5 mg/kg body weight twice weekly) or the solvent PBS, or by oral gavage delivering the TGF-βR1 inhibitor LY2157299 (150 mg/kg weight/daily) or the solvent (1% w/v

HEC/0.25% v/v Tween 80/ 0.05 v/v Antifoam 1510-US in H2O).The mice were observed daily and euthanized when developing neurological symptoms or at defined time points for histological analysis as indicated. Three mice per group were commonly euthanized using pre-randomization when any mouse in the experiment became symptomatic in order to perform histological studies to assess tumor growth at an early stage. The remaining 7 mice were euthanized when displaying neurological symptoms to obtain survival or histological data (end-stage). Where indicated, mice brains were explanted for snap-frozen samples. All brains were collected upon euthanization, embedded in cryomoulds in Shandon Cytochrome yellow (Thermo Scientific, Waltham, MA) and frozen in liquid nitrogen. Tumor incidences and sizes were determined using hematoxylin and eosin stainings of 8 µm thick cryosections using a Microm HM560 (Microchom HM560, Thermo Scientific).

Immunohistochemical analysis

Cryosections were fixed in 4% formalin, acetone or methanol/acetone for 10 min, air-dried, pretreated with 0.3-3% H_2O_2 and blocked in 10% rabbit or donkey serum or blocking solution (Candor Biosciences, Wangen, Germany). After blocking, the primary antibodies were applied for 1 h at 37°C or overnight at 4°C. Primary antibodies were polyclonal goat anti-CA IX (R&D Systems, AF2344, 1:50), monoclonal rat anti-CD4 (BD Pharmingen, 553727, 1:100), monoclonal rat anti-CD8a (BD Pharmingen, BD550281, 1:50), polyclonal rabbit anti-CD11b (Abcam, Cambridge, UK, ab75476, 1:400), monoclonal rat anti-CD31 (BD Pharmingen, Allschwil, Switzerland, BD550274, 1:50), monoclonal rat anti-CD45 (Biolegend, San Diego, CA, 103102, 1:1000), monoclonal rabbit anti-Ki-67 (Epitomics, Burlingame, CA) and monoclonal rabbit anti-pSMAD2 (Cell Signaling, 3108, 1:1000). Biotinylated secondary antibodies, streptavidin and 3,3′-diaminobenzidine (DAB) were obtained from Dako (Baar, Switzerland). Histofine Simple Stain Mouse MAX PO secondary-labelled antibody system was obtained from Nichirei (Tokyo, Japan). Secondary antibodies were incubated for 30 min at room temperature. The antigen antibody conjugates were then detected by staining with DAB (Dako) for 1-3 min. The nuclei were stained using hematoxylin for up to 4 min, washed in water and dehydrated twice in 96% ethanol, then twice in 100% ethanol and three times in xylol before mounting onto coverslips using Eukitt mounting medium (Sigma Aldrich). Quantification of immunohistological stainings was obtained from 4 regions of interest (ROI) from 3 tumors per group. Within

tumor tissue, percentages of CD11b- and CD45-positive cells of all nucleated cells were determined, microvessel density (MVD) was calculated by counting CD31+ capillaries, and infiltrating CD4 and CD8a positive cells per ROI were counted. Quantification of pSMAD2-positive cells was performed by H scoring in four randomly selected, different microscopic fields of independent hotspots (tumor margin) and tumor centers on the basis of both the percentage of positive tumor nuclei and staining intensity in tumors (Frei *et al.*, 2015). In brief, to obtain scores, staining intensity is scored as absent (0), mild (1), moderate (2) or strong (3) expression. The staining intensity value is multiplied by the percentage of cells showing each grade of positivity, thus, the maximum H score is 300 (Kinsel *et al.*, 1989; Kraus *et al.*, 2012). The surface detection function within the Image J software was used for the quantification of CD11b-, CD45- and Ki-67-positive cells and for carbonic anhydrase (CA) IX-positive areas. Tumor volumes were calculated using an approximation based on ellipsoid geometric primitive (Schmidt *et al.*, 2004).

Immunofluorescence microscopy

Immunofluorescence studies were carried out on cryosections of tumor-bearing mouse brains. The following antibodies were applied overnight at 4°C: polyclonal anti-CA IX (R&D Systems, 1:50), monoclonal anti-CD31 (BD Pharmingen, 1:50), monoclonal pSMAD2 (Cell Signaling, 1:500), monoclonal rat anti-VEGFR1 (Biolegend, 136402, 1:50) and monoclonal rabbit anti-VEGFR2 (Cell Signaling, 2479, 1:200). Binding specificity was controlled by IgG isotype control (Jackson Immunoresearch, West Grove, PA). For visualization, Alexa Fluor 488 goat anti-rabbit IgG (Life Technologies, Zug, Switzerland, A-11008) or Alexa Fluor 594 donkey anti-rat IgG (Life Technologies, A-21209) was applied. All sections were mounted in Dako Fluorescent Mounting Medium (Dako). DNA was stained with 4',6-diamidino-2-phenylindole (DAPI). Pictures were taken with a ×63 oil immersion objective (1.4 numerical aperture; Leica Microsystems, Heerbrugg, Switzerland). A CLSM Leica SP5 microscope (Leica Microsystems) attached to a diode and an argon laser was used to provide excitation at 405 nm, 488 nm and 561 nm wavelengths. The emitted fluorescence light was detected via three adjustable photomultiplier detectors. Per brain section, two single images from randomly selected ROI were recorded and included in the quantification. The surface detection function within the Bitplane Imaris (Bitplane) software (Roth *et al.*, 2013) was used for quantification of pSMAD2 staining.

Analysis of gene expression data

The microarray data have been presented previously (Ahmad *et al.*, 2014). Raw microarray data were calibrated and summarized using the hook method including quantile-normalization (Irizarry *et al.*, 2003; Binder *et al.*, 2008; Binder and Preibisch, 2008). The expression value of each gene was transformed into log10-scale and centered with respect to its mean value averaged over all samples investigated (Wirth *et al.*, 2011). Differential expression analysis was performed using pairwise comparisons of sample classes and by applying a shrinkage t-score combined with false discovery rate multiple test correction for judgement of significance (Wirth *et al.*, 2012). For functional analysis we applied gene set enrichment analysis based on predefined gene sets taken from the literature, from gene ontology classification schemes, or from gene lists determined in this study. All methods were implemented in the program opoSOM that was used for all analyses (Loffler-Wirth *et al.*, 2015).

STRING analysis

Functional gene interactions were analysed with the Search Tool for the Retrieval of Interacting Genes/Proteins (STRING) Version 10 at http://string-db.org (Franceschini *et al.*, 2013). High confidence settings were applied, integrating combined scores higher than 0.700. Cluster analysis was performed by application of the Markov Cluster algorithm (MCL).

Fluorescence-activated cell sorting (FACS) expression analysis

Cells were detached with StemPro Accutase (Thermo Scientific), washed and incubated for 20 minutes in the dark at 4 °C with antibodies targeting the following membrane proteins: rat anti-mouse CD274 (PD-L1) BV421 (564716, BD Pharmingen, 1:50), rat anti-mouse CD273 (PD-L2) APC (560086, BD Pharmingen, 1:50). Dead cell labelling was performed during surface staining by adding Zombie Aqua (423102, Biolegend, 1:100) to the antibodies mix. FACS was performed with a FACSVerse (BD, Biosciences). Dead cells were gated out and signal intensity was calculated as the ratio of the median fluorescence intensity (MFI) of the specific antibody and the isotype control antibody.

Intracellular cytokine staining

Lymphocytes were isolated from the organ of interest or harvested from in vitro culture. For each staining at least 1 million cells were taken. In some cases, lymphocytes were re-stimulated in medium containing ionomycin (1:2000) (I0634, Sigma Aldrich), PMA (1:2000) (P-8139, Sigma Aldrich) and GolgiPlug/GolgiStop (1:1000) (555029, 554724, BD Biosciences) for 4-6 hours at 37°C. Surface staining was performed by incubating cells for 20 minutes at 4 °Cin the dark, using the following antibodies diluted in PBS: anti-mouse CD4 Pacific Blue (100428, Biolegend, 1:100), anti-mouse CD8a APC (100712, Biolegend, 1:100). Dead cell labelling was performed during surface staining by adding Zombie Aqua (423102, Biolegend, 1:100). Cells were then fixed and permeabilized with BD Cytofix/Cytoperm Fixation/Permeabilization Kit (554714, BD Biosciences), and stained intracellularly, following manufacturer's instructions, with the following antibodies: anti-mouse IFN-γ PE (505808, Biolegend, 1:200), anti-mouse IL-2 PerCP/Cy5.5 (503822, Biolegend, 1:25), and anti-mouse IL-10 PerCP/Cy5.5 (505028, Biolegend, 1:25). Samples were analyzed with a FACSVerse (BD, Biosciences) and subsequently, data were analysed with FlowJo software (TreeStar).

Nuclear transcription factor staining

Lymphocytes were isolated from the organ of interest or harvested from *in vitro* culture. For each staining at least 1 million cells were taken. Surface staining was performed incubating cells for 20 minutes at 4 degrees in the dark, using the following antibodies diluted in PBS: anti-mouse CD4 Pacific Blue (100428, Biolegend, 1:100), and anti-mouse CD25 APC (101910, Biolegend, 1:50). Dead cell labelling was performed during surface staining by adding Zombie Aqua (423102, Biolegend, 1:100). Cells were then fixed and permeabilized with FoxP3/Transcription factor staining buffer set (00-5523, eBiosciences) and stained following manufacturer's instructions with rat anti-mouse FoxP3 PE antibody (12-5773-82, eBiosciences, 1:50). Samples were read with a FACSVerse (BD, Biosciences) and subsequently, data were analysed with FlowJo software (TreeStar).

Cell cytotoxicity assay

Immune-mediated glioma cell lysis was determined using a flow cytometry-based cytotoxicity assay. Target cells were stained with PKH-26 (Sigma-Aldrich) for 3 min and then co-incubated with effector cells at different effector to target (E:T) ratios as

indicated for 4-6 h. Subsequently, live/dead staining was performed with Zombie Aqua Fixable Viability Kit (BioLegend) followed by assessment of target cell lysis by flow cytometry. Specific cell lysis was expressed as percentage of dead cells within the PKH-26-positive target cells, corrected for spontaneous background lysis.

Statistical analyses

All in vitro data are representative of experiments performed in three independent experiments with similar results. Statistical significance was assessed using either two-sided unpaired Student's t-test or one-way ANOVA with Tukey's post hoc test for multiple analysis. Quantitative data are represented as mean ± standard deviation (SD) for in vitro or standard error (SEM) of the mean for in vivo experiments. A p value below 0.01 was considered significant. Kaplan Meier survival curves generated from the animal studies were analyzed using the log-rank test or the Gehan-Breslow-Wilcoxon test. A p value below 0.05 was considered significant. All statistical analyses were performed using Prism 5 (GraphPad Software, La Jolla, CA).

5. Aims of the doctoral thesis

Project 1

Previous studies from our laboratory and many pieces of evidence described by others, have established a tight connection between the VEGF and TGF-β pathways. Indeed, they interdependently regulate several glioblastoma malignant features such as angiogenesis, immunosuppression, stem cell maintenance and invasion (described above). Furthermore, TGF-β is a well-known upstream regulator of VEGF expression. All these observations point to the possibility that TGF-β signalling may supply VEGF functions during anti-angiogenic therapy.

Aim 1: To investigate a potential crosstalk between the VEGF and TGF-β signalling pathways in murine glioma cell lines *in vitro*.

Aim 2: To investigate whether co-targeting of VEGF and TGF-β will prevent or delay tumor progression in syngeneic murine experimental glioma models *in vivo*. Moreover, in case co-treatment will provide synergy *in vivo*, we plan to investigate which molecules and cell populations are involved in the process.

Project 2

The activity of checkpoint inhibition in glioblastoma is yet to be determined. Preclinical studies have demonstrated that these therapies may work best when combined with other agents targeting redundant immunosuppressive pathways. Several studies have shown that TGF-β is a master regulator of glioblastoma-induced immunosuppression. Thus, we reasoned that inhibition of the TGF-β pathway could improve the efficacy of PD-1 blockade.

Aim 1: Determine PD-L1 and PD-L2 expression in murine glioma cells and determine whether their expression can be modulated by different stimuli.

Aim 2: To investigate whether dual targeting of the PD-1 and TGF-β pathways elicits T cell effector responses in experimental glioma models.

6. Results

6.1 Limited role for transforming growth factor-β pathway activation-mediated escape from VEGF inhibition in murine glioma models

A related manuscript has been published in Neuro-Oncology 2016, Volume 18, Issue 12 : 1610-1621 ; DOI:https://doi.org/10.1093/neuonc/now112

Davide Mangani[1], Michael Weller[1,2], Emad Seyed Sadr[1], Edith Willscher[3], Katharina Seystahl[1], Guido Reifenberger[4], Ghazaleh Tabatabai[1,2,*], Hans Binder[3], Hannah Schneider[1]

[1]Laboratory of Molecular Neuro-Oncology, Department of Neurology, University Hospital and University of Zurich, Zurich, Switzerland
[2]Center for Neuroscience, University of Zurich, Zurich, Switzerland
[3] Interdisciplinary Center for Bioinformatics, University of Leipzig, Leipzig, Germany
[4] Institute of Neuropathology, Heinrich Heine University, Duesseldorf, and German Cancer Consortium (DKTK), German Cancer Research Center (DKFZ) Heidelberg, partner site Essen/Duesseldorf, Germany

*Current address: Interdisciplinary Division of Neuro-Oncology, University Hospital Tuebingen, Laboratory of Clinical and Experimental Neuro-Oncology, Hertie Institute for Clinical Brain Research, Eberhard Karls University, Tuebingen, Germany

Author contributions

Davide Mangani: Designed the work, acquired the majority of data and interpreted the results; Michael Weller: Designed and supervised the study and interpreted the results; Emad Seyed Sadr: Acquired parts of in vitro and in vivo data; Edith Willscher: Analyzed bioinformatic data and interpreted results; Katharina Seystahl: Acquired parts of *in vivo* data; Guido Reifenberger: Acquired transcriptomic data; Ghazaleh Tabatabai: Designed and supervised parts of the study; Hans Binder: Analyzed bioinformatic data and interpreted results; Hannah Schneider: Designed and supervised the study, acquired in vivo data and interpreted the results; M. Weller and H. Schneider wrote the first draft of the manuscript.

6.1.1 Results project 1

Characterization of VEGF and TGF-$\beta_{1/2}$ ligand/receptor expression in mouse glioma cells

VEGF-A (*VEGF*) mRNA was constitutively expressed by all four murine glioma cell lines, with the highest levels in GL-261 and SMA-560. In contrast, the highest levels of protein release were observed in SMA-540 and SMA-560 (Figure 11A). *VEGFR1* mRNA was expressed in all cell lines and protein levels correlated well, with highest levels in SMA-560. SMA-560 showed the highest *VEGFR2* mRNA levels followed by SMA-540, and protein was only detected in SMA-540 and SMA-560 (Figure 11B). *TGF-$\beta_{1/2}$* mRNA was abundant in all four models. There was no apparent correlation between mRNA and protein levels, and TGF-β_1 consistently exceeded TGF-β_2 protein levels in the supernatant. TGFβR2 and ALK-5 were expressed in all models at variable levels, with correlation between mRNA and protein (Figure 11C,D). We also examined *ex vivo* tumoral mRNA expression of ligands and receptors, using syngeneic normal brain tissue (NBT) of VM/Dk and C57BL/6 mice as a reference. *In vitro* maintained monolayer cultures (MC) and mouse gliomas in vivo (T) showed similar VEGF mRNA levels (Figure 12A). Compared with MC, there were higher VEGFR1 mRNA in SMA-497 and GL-261, and higher VEGFR2 mRNA levels in all models *in vivo* (Figure 12B,C), suggesting a major contribution from tumor blood vessels or up-regulation of expression in tumor cells *in vivo*. Immunohistochemical stainings of VEGFR2 levels revealed a major contribution from tumor cells, even masking a typical vessel staining pattern, which, however, became readily visible in tumors stained for CD31 (see below) (Figure 13A,B).

TGF-β_1 but not *TGF-β_2* mRNA was enhanced *in vivo* in SMA-497, SMA-560 and GL-261. While *ALK-5* mRNA was consistently increased *in vivo*, there was a mixed pattern for *TGFβR2* mRNA expression with increased expression in SMA-560, and a trend for decreased expression in the other models (Figure 14A-D).

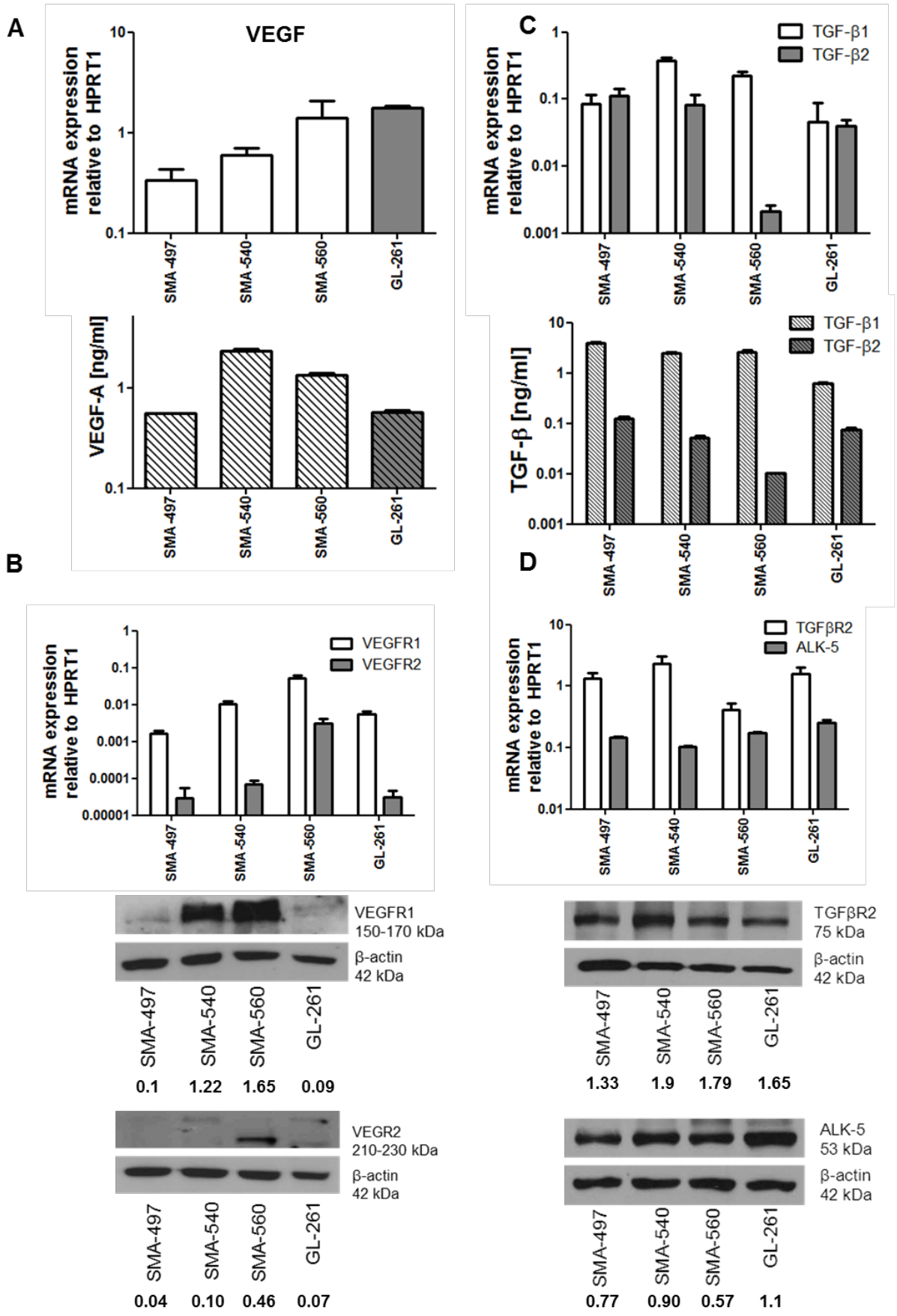

Figure legend 11 on the next page

Figure 11. Expression of VEGF and TGF-β pathway ligands and receptors in mouse glioma models *in vitro*. SMA-497, SMA-540, SMA-560 and GL-261 cells were studied for gene expression. A. VEGF expression determined by RT-PCR for mRNA (top) and by ELISA for protein in the supernatant (bottom) *in vitro*. B. VEGFR1,2 expression determined by RT-PCR (top) and immunoblot (bottom) *in vitro*. C. TGF-$\beta_{1/2}$ expression determined by RT-PCR (top) and ELISA in the supernatant (bottom) *in vitro*. D. TGF-βR2 and ALK-5 expression determined by RT-PCR (top) and immunoblot (bottom) *in vitro*. Values of densitometric analysis relative to β-actin are shown below the immunoblot panels in B and D.

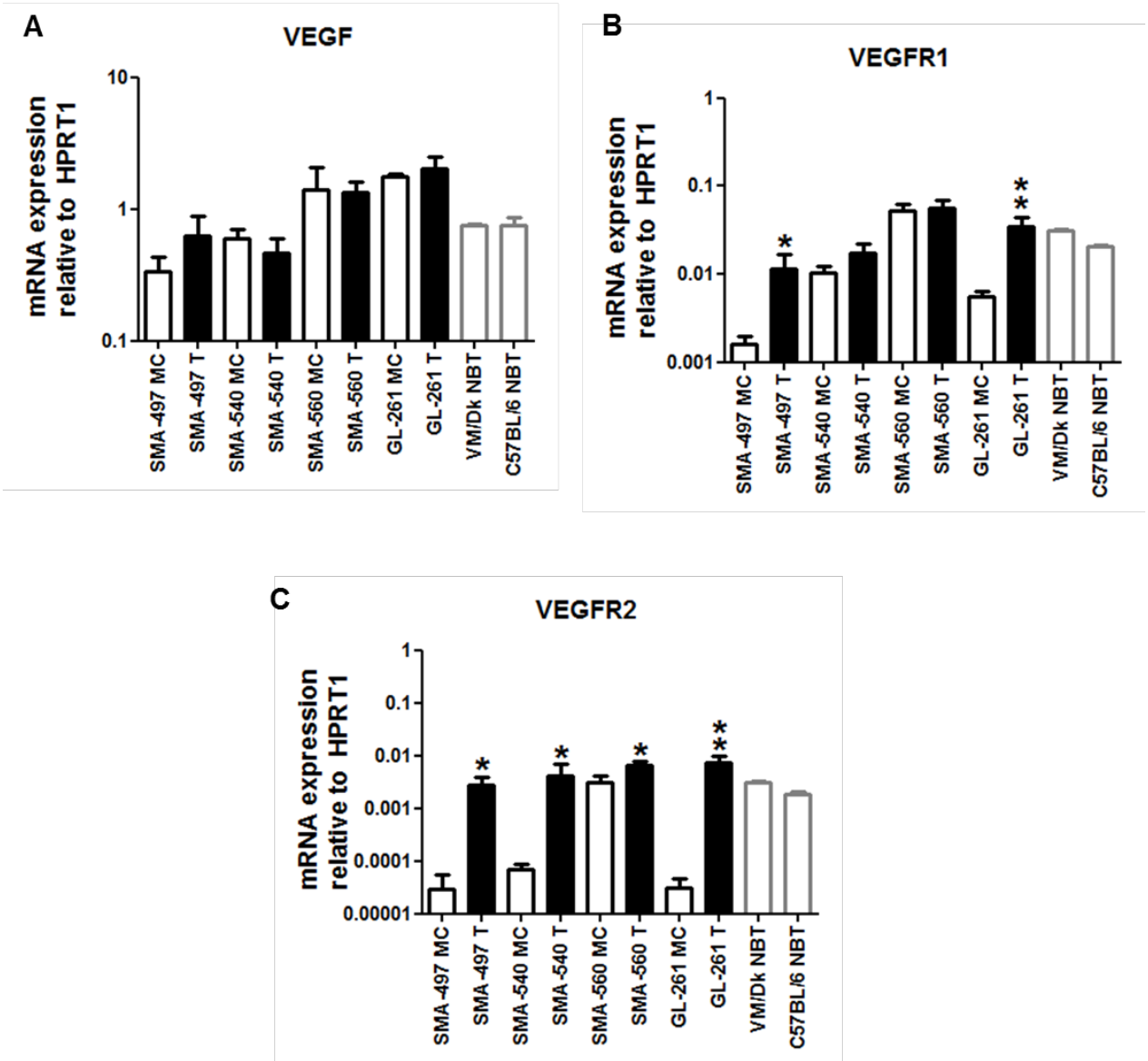

Figure 12. VEGF pathway ligand and receptor expression in experimental mouse gliomas *in vivo*. A-C Explanted SMA-497, SMA-540, SMA-560 or GL-261 mouse tumors (T) were studied for *VEGF* and *VEGFR1,2* mRNA expression. MC and normal brain tissue of the respective mouse strain (VM/Dk or C57BL/6) served as references. (A) *VEGF*, (B) *VEGFR1*, (C) *VEGFR2*. Three ex vivo tissue samples per group were analysed. Data are expressed as mean and SD (*p<0.05, **p<0.01, unpaired student t-test, T versus MC).

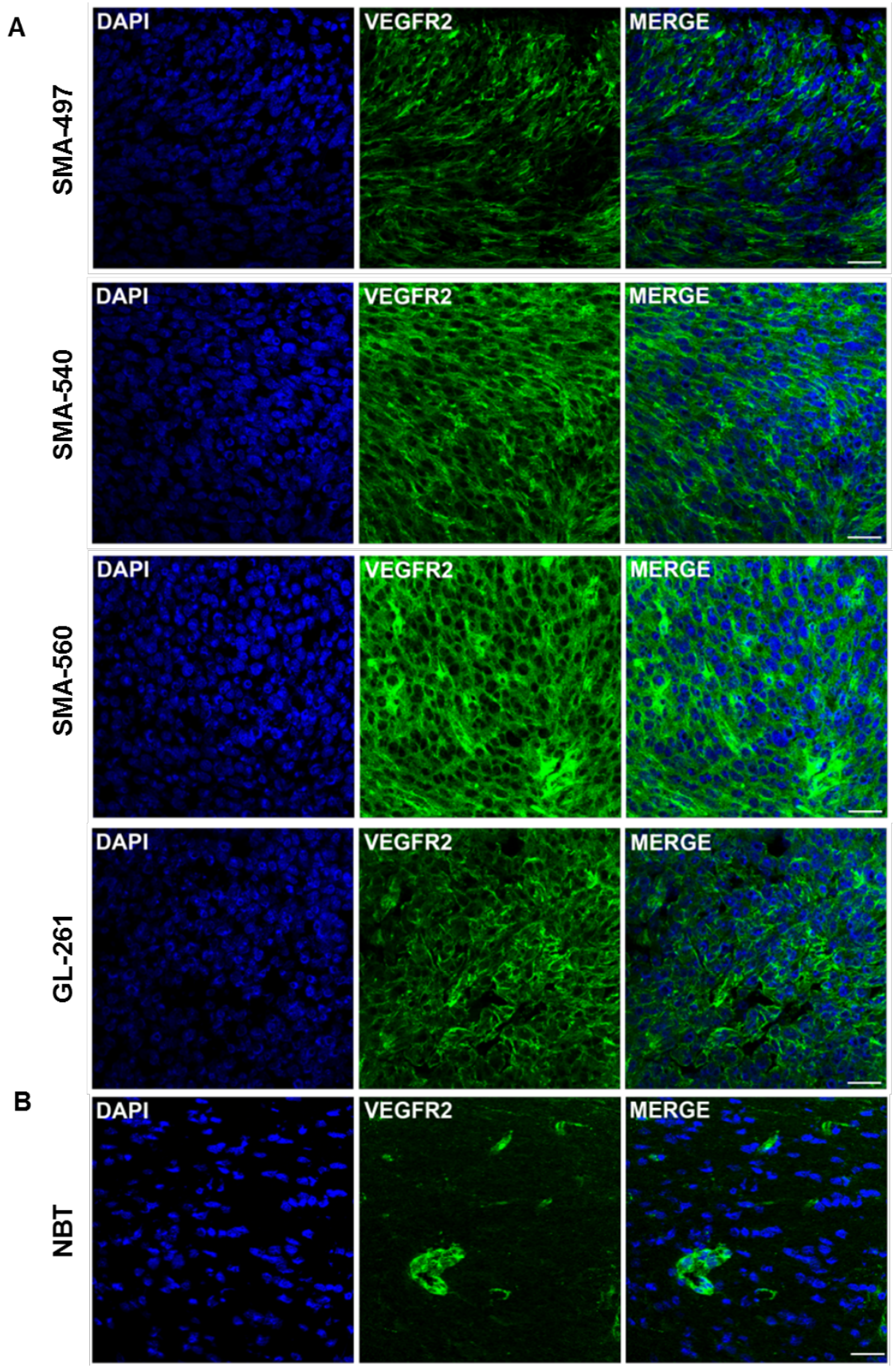

Figure 13. VEGFR2 immunofluorescence in experimental mouse gliomas *in vivo*.
Immunofluorescent stainings of VEGFR2 in mouse glioma tissues (A) and NBT (B) were performed (size bar: 20 µM).

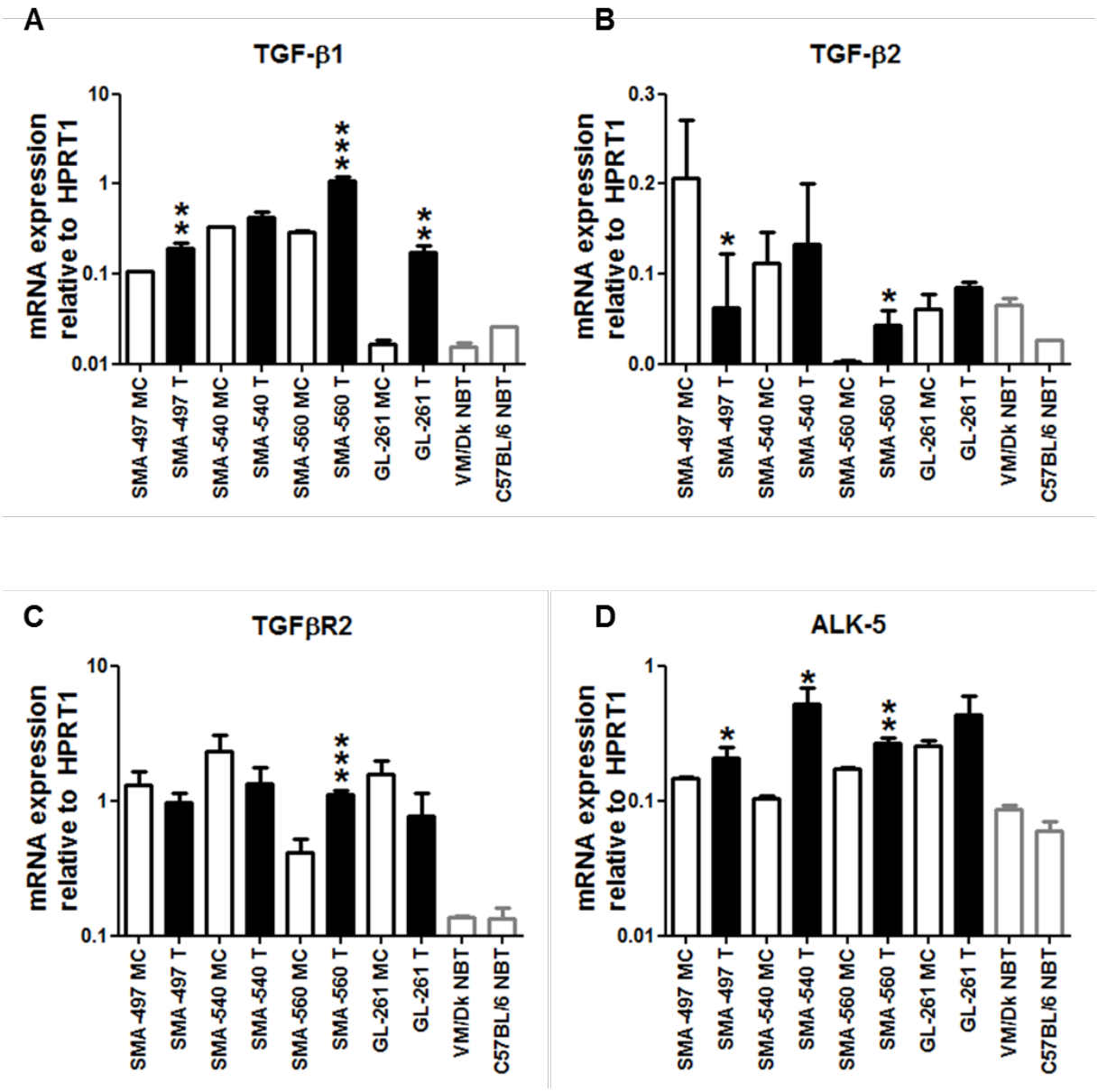

Figure 14. TGF-β pathway ligand and receptor expression in experimental mouse gliomas *in vivo*. A-D Explanted tumors (T) were studied for *TGF-β$_{1/2}$*, *TGFβR2* and *ALK-5* mRNA expression. MC and normal brain tissue of the respective mouse strain (VM/Dk or C57BL/6) served as references. (A) *TGF-β$_1$*, (B) *TGF-β$_2$*, (C) *TGFβR2*, (D) *ALK-5*. Three *ex vivo* tissue samples per group were analysed (*p<0.05, **p<0.01, ***p<0.001, unpaired student t-test, T versus MC).

Modulation of VEGF and TGF-β$_{1/2}$ signaling *in vitro*

We observed an increase in pVEGFR1 levels in response to exogenous VEGF in SMA but not in GL-261 glioma cells. pVEGFR2 was increased upon VEGF stimulation in SMA-540 and SMA-560 (Figure 15A). An increase in pSMAD2 was observed in all models after exposure to exogenous TGF-β$_2$. LY2157299 attenuated constitutive and induced SMAD2 phosphorylation (Figure 15B). Neither VEGF pathway inhibition using

B20 nor relevant concentrations of cediranib nor TGF-β pathway inhibition by LY2157299 affected viability or clonogenicity (Figure 16A,B).

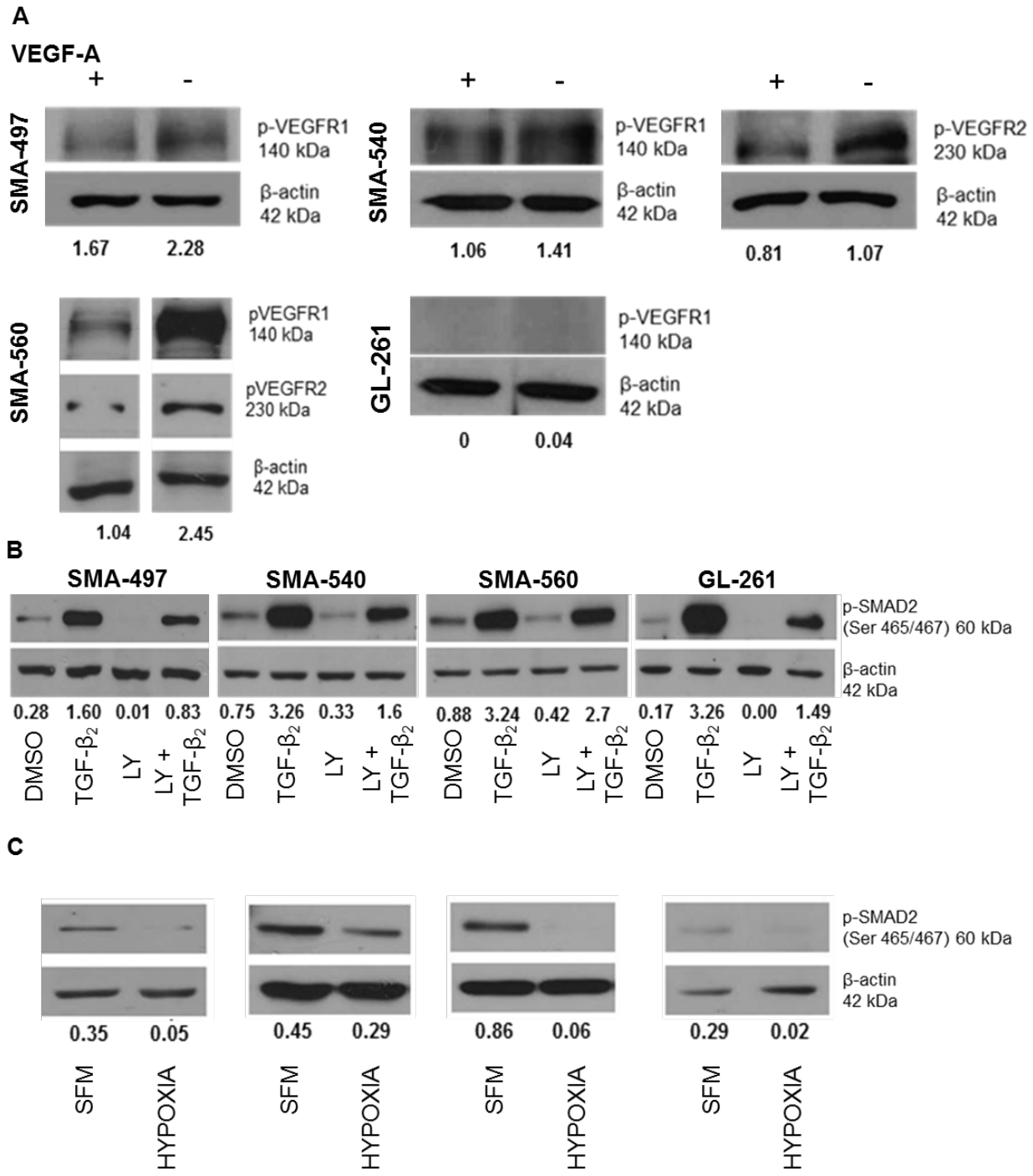

Figure 15. VEGF and TGF-β signaling in mouse glioma cells *in vitro*. A. pVEGFR1,2 levels after VEGF stimulation (400 ng/ml, 5 min) were assessed by immunoblot. B. pSMAD2 levels of cells either treated with 1 μM LY2157299 or 2 ng/ml TGF-β_2 or both (SMA-540, SMA-560 for 3 h, SMA-497, GL-261 for 24 h) were analyzed. C. pSMAD2 levels were assessed under normoxic or hypoxic conditions (24 h, 1% O2). Values of densitometric analysis of pVEGFR and pSMAD2 protein levels, relative to β-actin, are shown below the immunoblot panels.

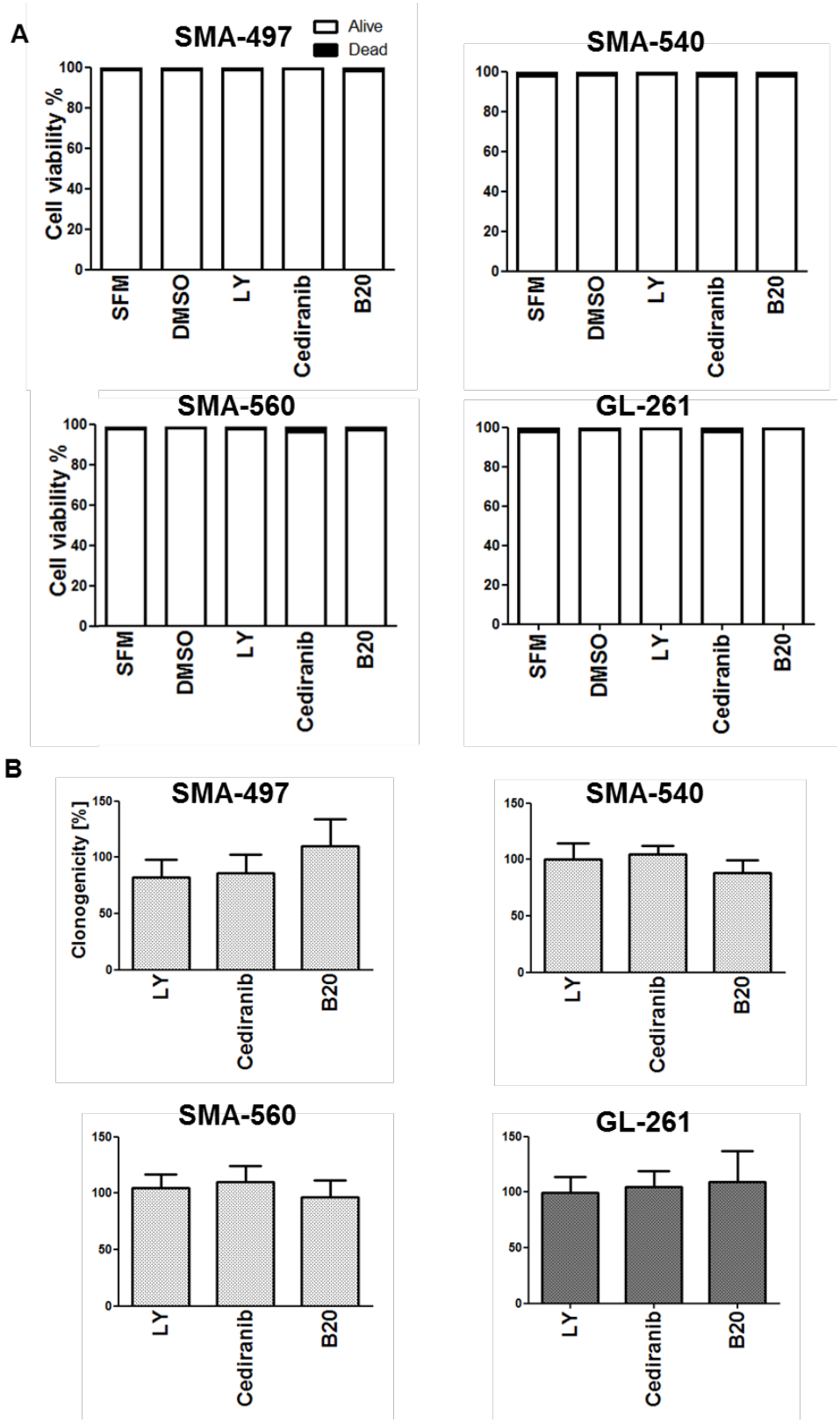

Figure 16. VEGF and TGF-β signaling effects on viability and clonogenicity of mouse glioma cells *in vitro*. Mouse glioma cells were exposed to LY2157299 (24 h, 1 μM), cediranib (24 h, 100 nM) or B20 (24 h, 100 μg/ml) A. Viability was assessed by trypan blue exclusion assay. B. Clonogenic survival was assessed by measuring cell density via crystal violet staining. Quantitative data are expressed as mean and SEM (***p<0.001, one-way ANOVA followed by Tukey's post hoc test, confidence interval 99%, LY2157299 or cediranib versus DMSO)

Murinized bevacizumab prolongs survival in SMA-540, SMA-560 and GL-261 glioma models

We next determined single agent activity of B20 treatment in the four mouse glioma models. Histological analyses of tumors harvested when the first clinical symptoms occurred (early-stage) revealed reduced tumor volumes in all models except SMA-497. Tumor volume reduction was not paralleled by changes in Ki-67 labeling. Solvent-treated tumors possessed well-delineated margins whereas tumor borders in the B20 treatment groups were frayed and surrounded by numerous smaller satellites in all models (Figure 17A,B). The number of intratumoral vessels was decreased in SMA-540, SMA-560 and GL-261, but not in SMA-497 (Figure 17C). Vessel morphology was specifically changed in GL-261 with decreased vessel diameter. CA IX staining as a surrogate marker for hypoxia was strongly induced in SMA-540 and SMA-560, but still not reaching constitutive levels of the SMA-497 model (Figure 17D). In general, CA IX staining was inversely related to CD31 labeling, confirming that hypoxia develops with increasing distance from blood vessels (Figure 18). Finally, B20 prolonged survival in the SMA-540, SMA-560 and GL-261 models, but not in SMA-497 (Figure 19; Table 1). Our hypothesis of induced activation of the TGF-β pathway as an escape route from VEGF inhibition led us to predict increased pSMAD2 levels in B20-treated tumors at least at progression. However, we observed decreased pSMAD2 levels in 2 of 4 mouse models *in vivo,* and no change in the other two models, in fact, there was an association between decreased pSMAD2 levels and benefit from B20 (Figure 20A). This decrease in pSMAD2 levels was observed in tumor cells and tumor-infiltrating leukocytes. Tumor cells were more frequently pSMAD2-positive than host cells indicating that tumor cells may be more responsive to TGF-β than host cells (Figure 20B). Further, we noted that, in sharp contrast to the initial hypothesis of B20-triggered hypoxia followed by hypoxia-induced, TGF-β-mediated invasiveness, induction of hypoxia and reduction of pSMAD2 were seen in the same models. Accordingly, all four cell lines responded to hypoxia with decreased pSMAD2 levels *in vitro*, too (Figure 15C). Bioinformatic analyses of previously published data focusing on angiogenesis gene sets (Table 2) revealed that SMA-497 express high levels of genes involved in angiogenic escape pathways (Figure 21; Table 3) (Ahmad *et al.*, 2014). Unsupervised clustering of significantly regulated genes further revealed that genes up-regulated in SMA-497 were mainly down-regulated in GL-261, and *vice versa* (Figure 21; encircled clusters). Further assessment of these gene clusters by STRING analysis visualized

the differential activation or down-regulation of genes of the angiogenic genesets in SMA-497 and GL-261 (Figure 22A,B).

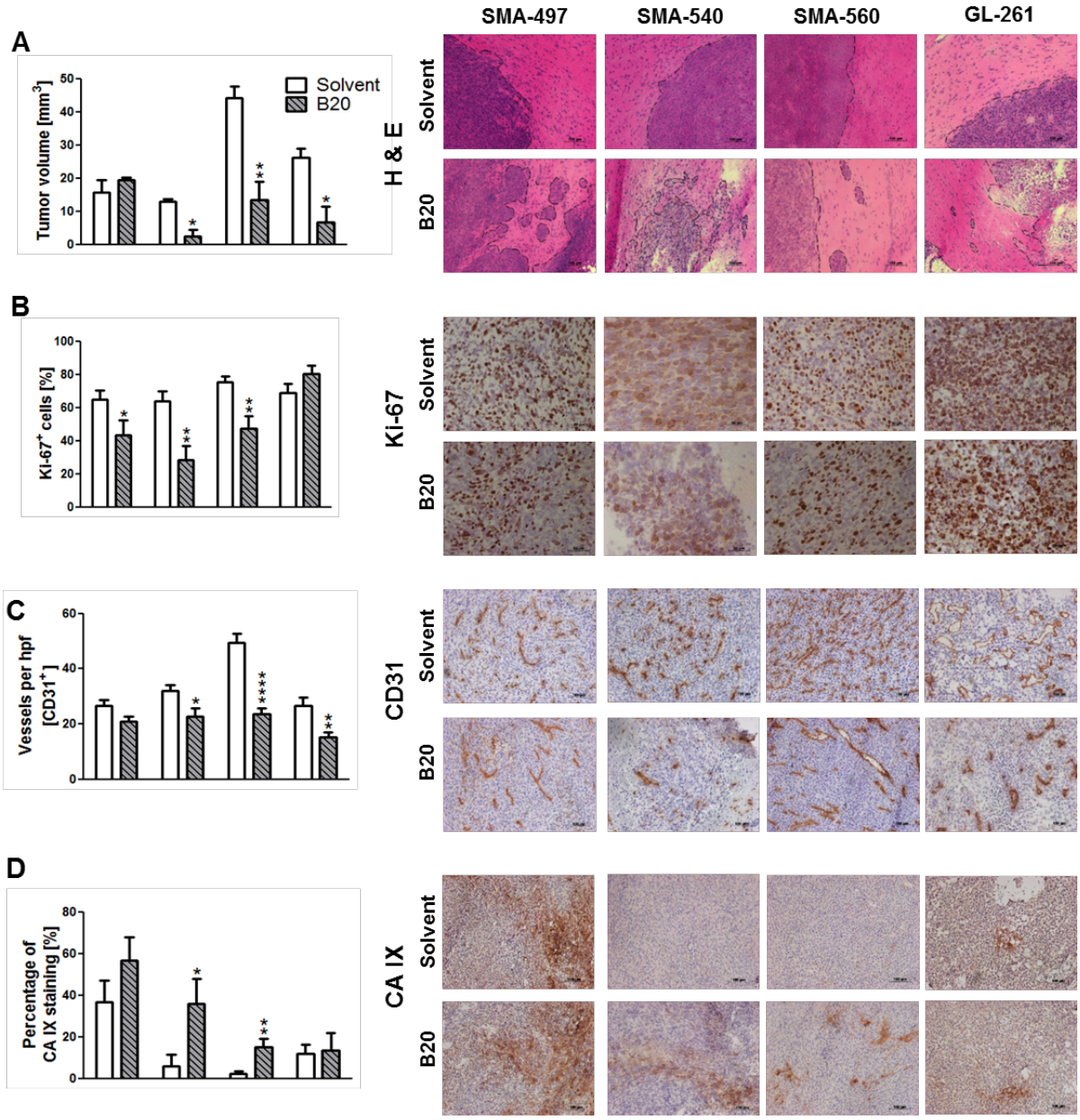

Figure 17. Differential effects of murinized bevacizumab on angiogenesis and growth of murine gliomas. Syngeneic mice intracranially implanted with SMA-497, SMA-540, SMA-560 or GL-261 cells were treated twice weekly with 5 mg/kg B20 or PBS from day 7 on. A-D Brain sections from animals sacrificed when the first mice became symptomatic were stained with (A) H&E or by immunohistochemistry and quantified for (B) Ki-67, (C) CD31, or (D) CA IX. Data are expressed as mean and SEM (*p<0.05, **p<0.01, ****p<0.0001, unpaired student t-test, B20 versus solvent). Size bars correspond to 100 µM A,C,D and 50 µM B.

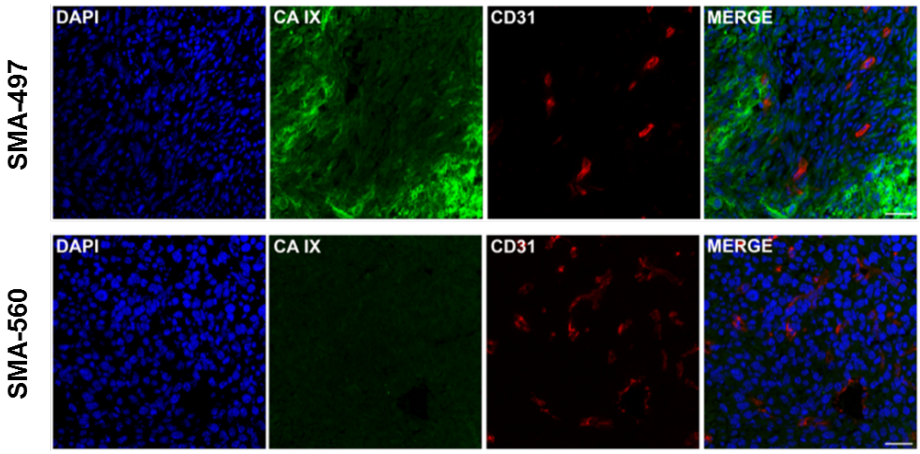

Figure 18. Vessel density and hypoxia in murine gliomas. Vessel density and tumor hypoxia in untreated murine SMA-497 or SMA-560 gliomas were assessed by immunofluorescent stainings for CA IX (green) and CD31 (red), using nuclear counterstaining with DAPI (blue). Merged images are provided as indicated in right images of each row. Size bars correspond to 100 µM.

	Cell line			
	SMA-497	**SMA-540**	**SMA-560**	**GL-261**
	Median survival (range) [days]			
Treatment				
Control	14 (13–17)	31 (27–44)	14.5 (12–14)	20 (19-24)
B20	15 (13–20)	48 (41–55)	32.5 (20->40*)	27.5 (24->40*)
	ns	p=0.0009	p=0.0007	p=0.0025
Control	14 (12–18)	42 (27->60*)	13 (11–14)	17 (15 – 22)
LY2157299	14 (12–19)	>60 (44->60*)	17 (12 – 18)	17 (15–22)
	ns	ns	p=0.014	ns
Control	15 (14–16)			19.5 (17–44)
B20	15 (14–17)			28 (22–41)
LY2157299	15.5 (14–17)			19 (17–32)
B20+LY2157299	16 (15–17)			33 (25–41)
	ns			p=0.0166 (cotreatment vs B20) p<0.0001 (cotreatment vs LY)

* censored because experiment was terminated at day 40 or day 60

Table 1. Sensitivity of mouse glioma models to VEGF antibody B20 or the TGFβR1 (ALK-5) antagonist LY2157299 alone or their combination *in vivo.*

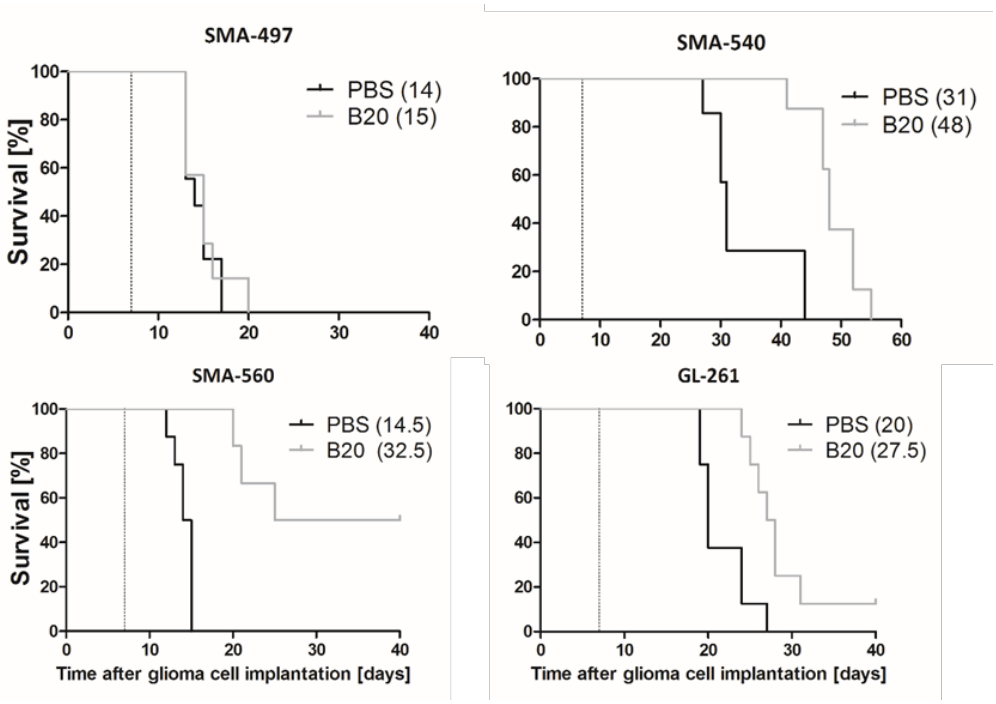

Figure 19. Differential effects of murinized bevacizumab on survival of murine gliomas. Kaplan-Meier survival curves of glioma-bearing mice (log-rank test, considered significant for $p<0.05$).

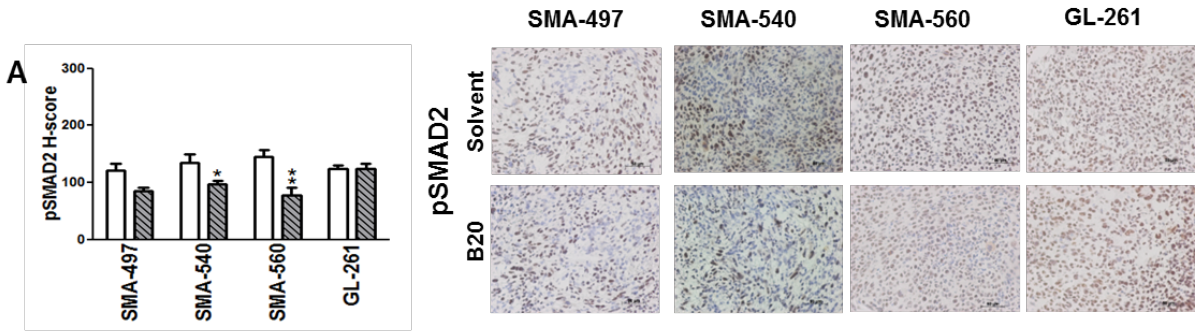

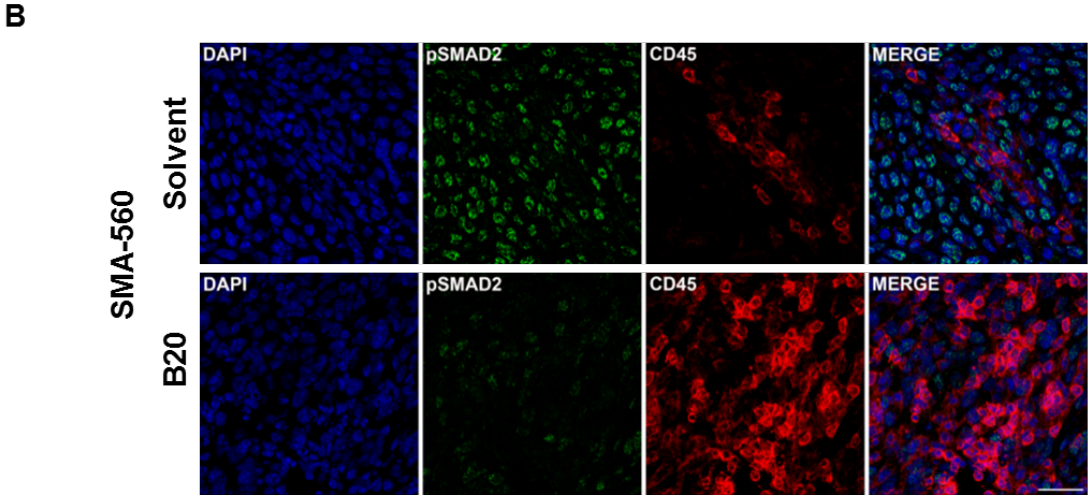

Figure legend 20 on the next page

Figure 20. pSMAD2 levels in murine gliomas. Syngeneic mice intracranially implanted with SMA-497, SMA-540, SMA-560 or GL-261 cells were treated twice weekly with 5 mg/kg B20 or PBS from day 7 on. A. Brain sections from animals sacrificed when the first mice became symptomatic were stained for pSMAD2. B. pSMAD2 levels were determined in tumor cells and leukocytes upon B20 treatment in the SMA-560 model *in vivo*. Immunofluorescent stainings were performed for pSMAD2 (green) and CD45 (red), again using DAPI as a counterstain. Merged images are provided as indicated in right images of each row. Size bars correspond to 50 µM (A) and 100 µM (B).

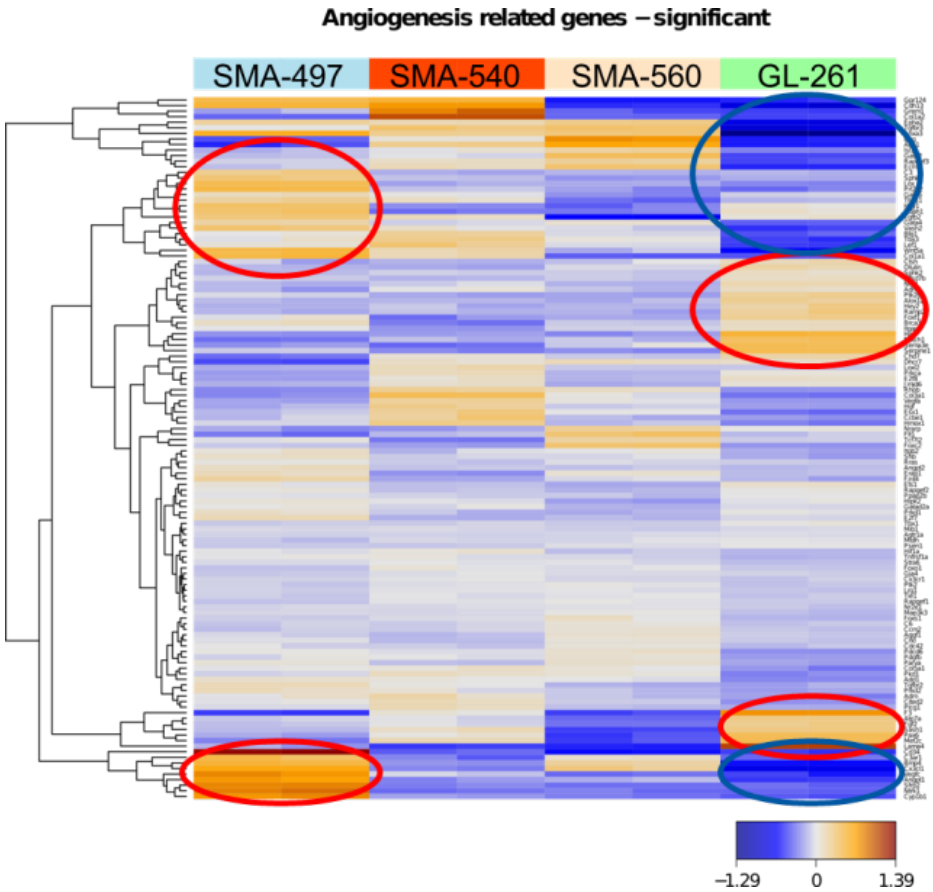

Figure 21. Angiogenic gene expression heatmap. The heatmap was obtained by unsupervised comparison of genes differentially expressed in the four mouse glioma cell lines. The heatmap indicates high to low expression levels as red to blue color coding. Up- or downregulated gene clusters in SMA-497 and GL-261 cells are encircled in red or blue.

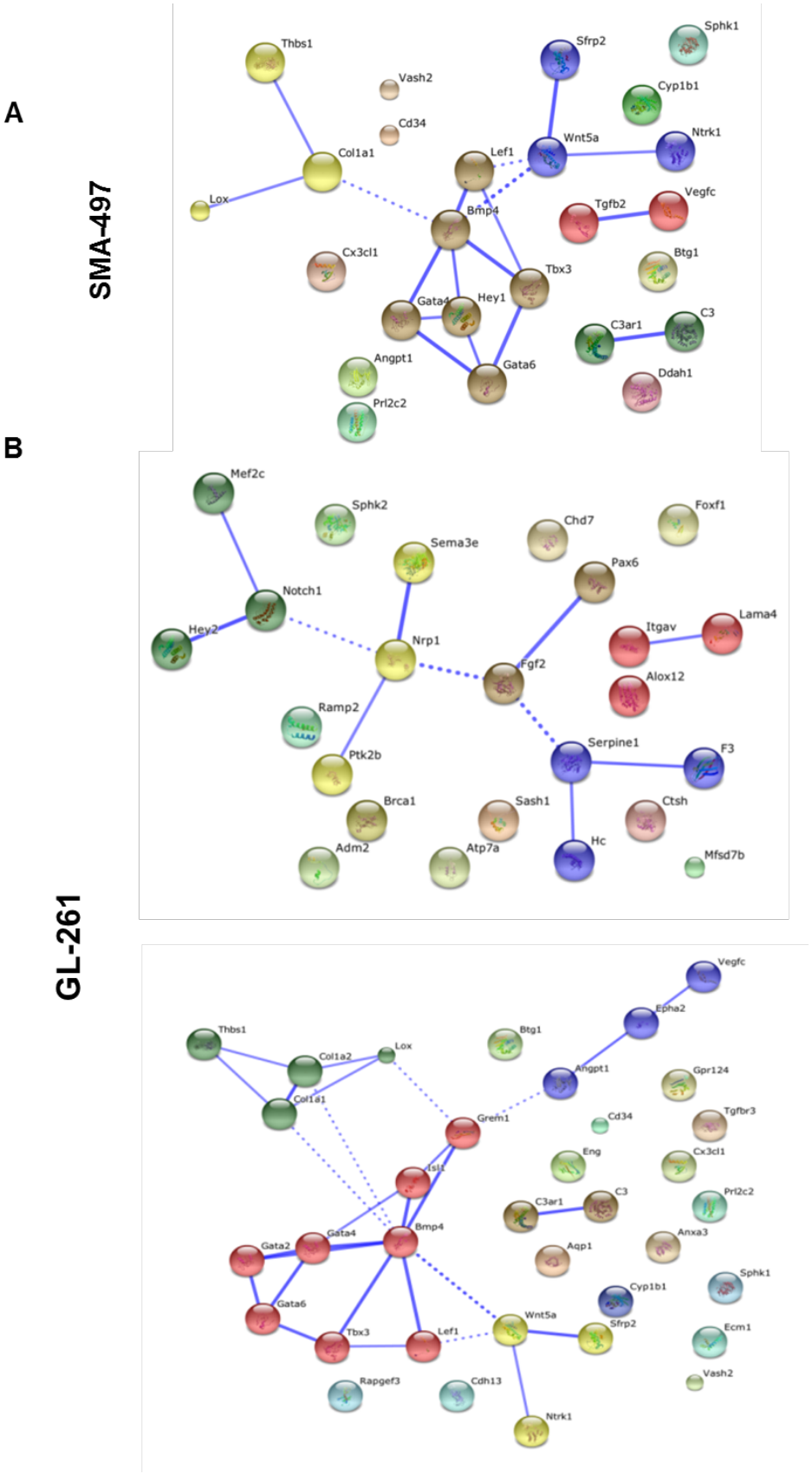

Figure 22. Gene cluster analysis. A.B. Functional interactions between genes up-regulated in the angiogenic profiles of (A) SMA-497 and (B) GL-261 (top) or down-regulated in GL-261 (bottom) were analyzed in Affymetrix micro-array based gene expression profiling by STRING analysis. Interactions with high confidence score of 0.700 were integrated to the interactome. Clusters were determined by MCL algorithm and presented with different node colors. Inter-cluster edges are represented by dashed-lines.

Angiogenesis related genes (all genes analysed)						
Ctsh	*Col1a1*	*Wnt5a*	*Gata6*	*Sfrp2*	*Kdr*	*Hmox1*
Cdc42	*Dlx3*	*Gdf2*	*Fgf1*	*Gja5*	*Tgfbr3*	*Cx3cl1*
Pdcl3	*Ramp2*	*Loxl2*	*Lox*	*F3*	*Ccl24*	*Cdh13*
Col3a1	*Map3k3*	*Bmp4*	*Ccbe1*	*Lef1*	*Serpine1*	*Foxf1*
Cxcr2	*Sphk1*	*Cma1*	*Tcf7l2*	*Ddah1*	*Cdx2*	*Foxc2*
Chil1	*Uts2r*	*Gata4*	*Nrarp*	*Hey1*	*Flt1*	*Nrp1*
Tnfsf4	*Prop1*	*Ptk2b*	*Egfl7*	*Agtr1b*	*Col1a2*	*Angpt2*
Cd34	*Alox12*	*Cysltr2*	*Col5a1*	*Rapgef2*	*Aqp1*	*Gatad2a*
Tgfb2	*Brca1*	*C6*	*Rapgef1*	*Ntrk1*	*Gata2*	*Agt*
Vash2	*Prkca*	*Mtdh*	*Eng*	*Ecm1*	*Tnfrsf1a*	*Ets1*
Mfsd7b	*Jmjd6*	*Adm2*	*Itgav*	*Chd7*	*Hipk2*	*Stra6*
Cited2	*Hif1a*	*Acvrl1*	*Pax6*	*Tek*	*Epha1*	*Aldh1a2*
Lama4	*Psen1*	*Otulin*	*Thbs1*	*Angptl3*	*C3ar1*	*Ccr3*
Nodal	*Rhob*	*Angpt1*	*Angpt4*	*Ppap2b*	*Prkd2*	*Camp*
Itgb2	*Prkd1*	*Ptk2*	*Plcg1*	*Epha2*	*Psg22*	*Tgfbr2*
Tbxa2r	*Pgf*	*Pdgfb*	*Notch1*	*Uts2*	*Rras*	*Cx3cr1*
Btg1	*Agtr1a*	*Rapgef3*	*Hc*	*Shb*	*Fzd4*	*Cdx4*
E2f7	*Foxc1*	*Crkl*	*Grem1*	*Tie1*	*Adm*	*Atp7a*
Sash1	*Erap1*	*Tbx1*	*Il1a*	*Gja4*	*Parva*	*Cxcr3*
Hey2	*Mef2c*	*Pkd1*	*Il1b*	*Sema3e*	*Prkcb*	*Cysltr1*
Nr2e1	*Esm1*	*Vegfa*	*Foxs1*	*Hgf*	*Dhcr7*	*Chm*
Ccm2	*Prl2c2*	*Lrg1*	*Ptgis*	*Nos3*	*Sphk2*	*Esx1*
Flt4	*Pdcd6*	*C3*	*Sox18*	*Add1*	*E2f8*	
Pik3r6	*Aggf1*	*Cyp1b1*	*Fgf2*	*Anxa3*	*Gpr124*	
Ccl11	*Isl1*	*Mib1*	*Foxo1*	*Tbx3*	*Vegfc*	

Table 2. Gene sets of angiogenic profiles as defined by Gene Ontology classification schemes.

Angiogenesis-related genes up-regulated in SMA-497	Angiogenesis-related genes up-regulated in GL-261	Angiogenesis related genes down-regulated in GL-261
C3; Col1a1; Wnt5a; Lef1; Tbx3; Btg1; Vash2; Gata4; Tgfb2; Ddah1 Hey1; Thbs1; Gata6 Prl2c2; Lox; Sphk1 CD34; Cyp1b1; Ntrk1 Sfrp2; Angpt1; Vegfc; Cx3cl1; Bmp4; C3ar1	*Chd7; Serpine1; Sema3e; Notch1; Hc; Itgav; Brca1; Foxf1; Ramp2; Hey2; Alox12; Ptk2b; Adm2; Nrp1; Mfsd7b; Sphk2; Otulin; Ctsh; F3; Lama4; Mef2c; Pax6; Sash1; Fgf2; Atp7a*	*Col1a1; Wnt5a; Lef1; Tbx3; Btg1; Vash2 Gata4; Thbs1; Gata6 Prl2c2; Lox; Sphk1 C3; Ecm1; Rapgef3 Gata2; Isl1; Aqp1;Eng Anxa3; Tgfbr3; Epha2 Col1a2; Grem1;Cdh13 Gpr124; CD34; Cyp1b1; Ntrk1; Sfrp2; Angpt1; Vegfc; Cx3cl1; Bmp4; C3ar1*

Table 3. Differentially regulated genes of angiogenic profiles of SMA-497 and GL-261 mouse glioma cell lines, as defined by Gene Ontology classification schemes.

LY2157299 prolongs survival in the SMA-540 and SMA-560 murine glioma models

Next, we determined single agent activity of LY2157299 in the four mouse glioma models. Histological analyses of tumors harvested when the first clinical symptoms occurred revealed a trend towards reduced tumor volumes only in SMA-560 (Figure 23A). We then explored whether exposure to LY2157299 suppressed pSMAD2 as a surrogate marker of TGF-β pathway activity. pSMAD2 levels were decreased by LY2157299 in all models, confirmed by immunoblot in SMA-560 (Figure 23B). Intratumoral vessel density was unaffected in either model but vessel morphology was changed in all models, except SMA-497, towards a vasculature with decreased vessel diameter and lumina upon LY2157299 treatment (Figure 23C). LY2157299 prolonged survival in SMA-560 and SMA-540, but not SMA-497 or GL-261 (Figure 24;Table 1). Accordingly, transcriptomic analysis of TGF-β receptor signaling pathway gene sets (Table 4) showed SMA-540 and SMA-560 to be the cell lines with the highest TGF-β pathway activity (Fig. 25A, Table 5). The survival differences in the SMA-540 control groups in the studies reported in Figures 2 and 3 is explained by variations in the tumorigenicity in this model which is the least tumorigenic. Transcriptomic profiling also revealed that the most immunogenic tumors as defined by Gene Ontology, SMA-497 and GL-261, exhibited differential clusters of up- and down-regulated genes involved in immune response pathways. Genes up-regulated in SMA-497 were mainly down-regulated in GL-261, and *vice versa* (Fig. 25B encircled; Table 6,7). STRING analysis of the differentially regulated gene clusters visualized the differential activation or

down-regulation of genes of the immune response-related gene sets in SMA-497 and GL-261 (Fig. 26A,B).

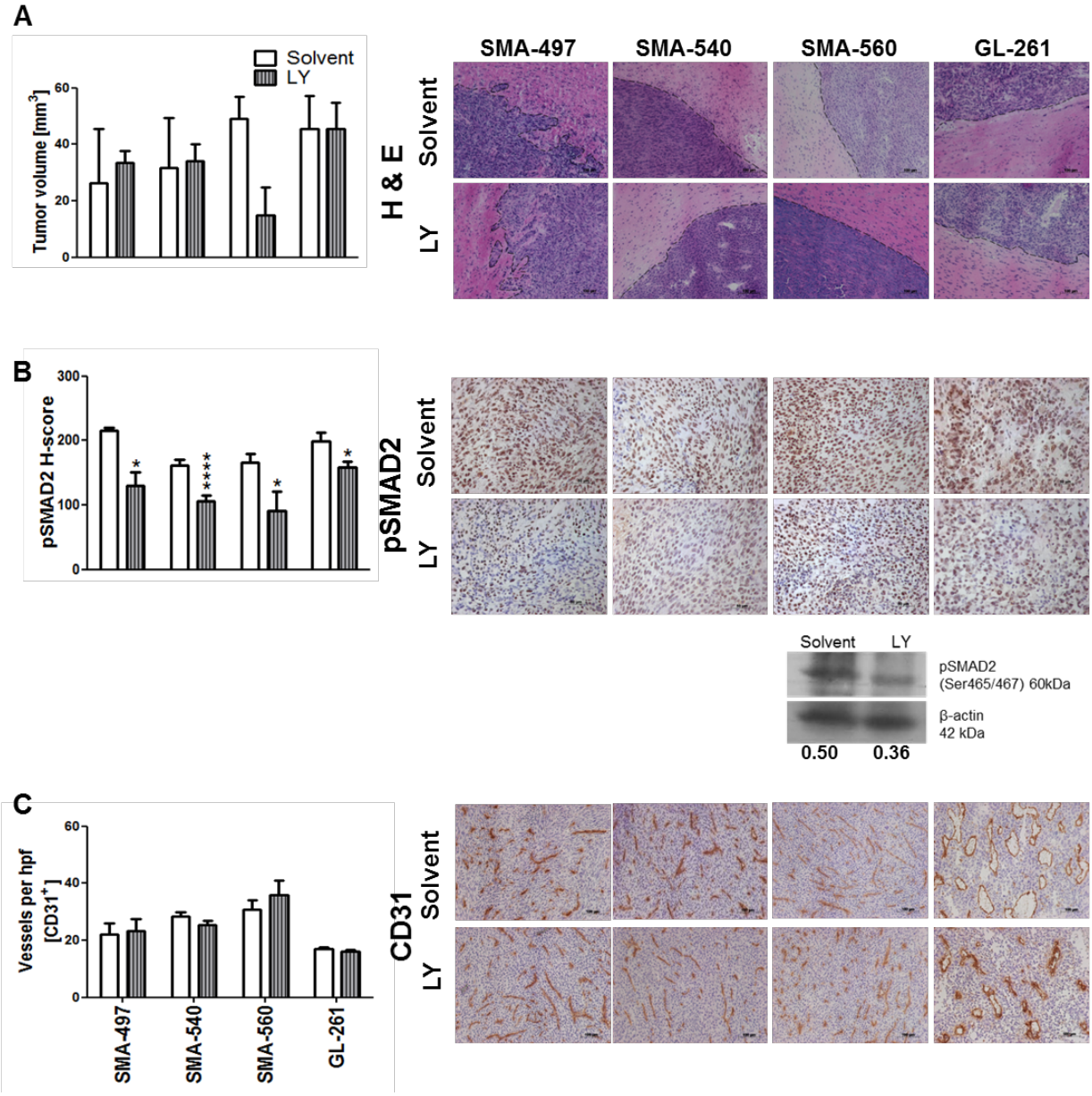

Figure 23. Differential effects of LY2157299 on pSMAD2 levels and angiogenesis of murine gliomas. Mice intracranially implanted with SMA-497, SMA-540, SMA-560 or GL-261 cells were treated daily with LY2157299 at 150 mg/kg or control solvent from day 7 on. A-C Data quantification and displaying of brain sections from animals sacrificed when the first mice became symptomatic. A. H&E. B. Immunohistochemical stainings of pSMAD2 (top) and protein levels determined by immunoblot (bottom). Values of densitometric analysis of pSMAD2 protein levels, relative to β-actin, are shown below the immunoblot panels. C. CD31. Size bars within images correspond to 50 µm (B) and 100 µm (A,C).

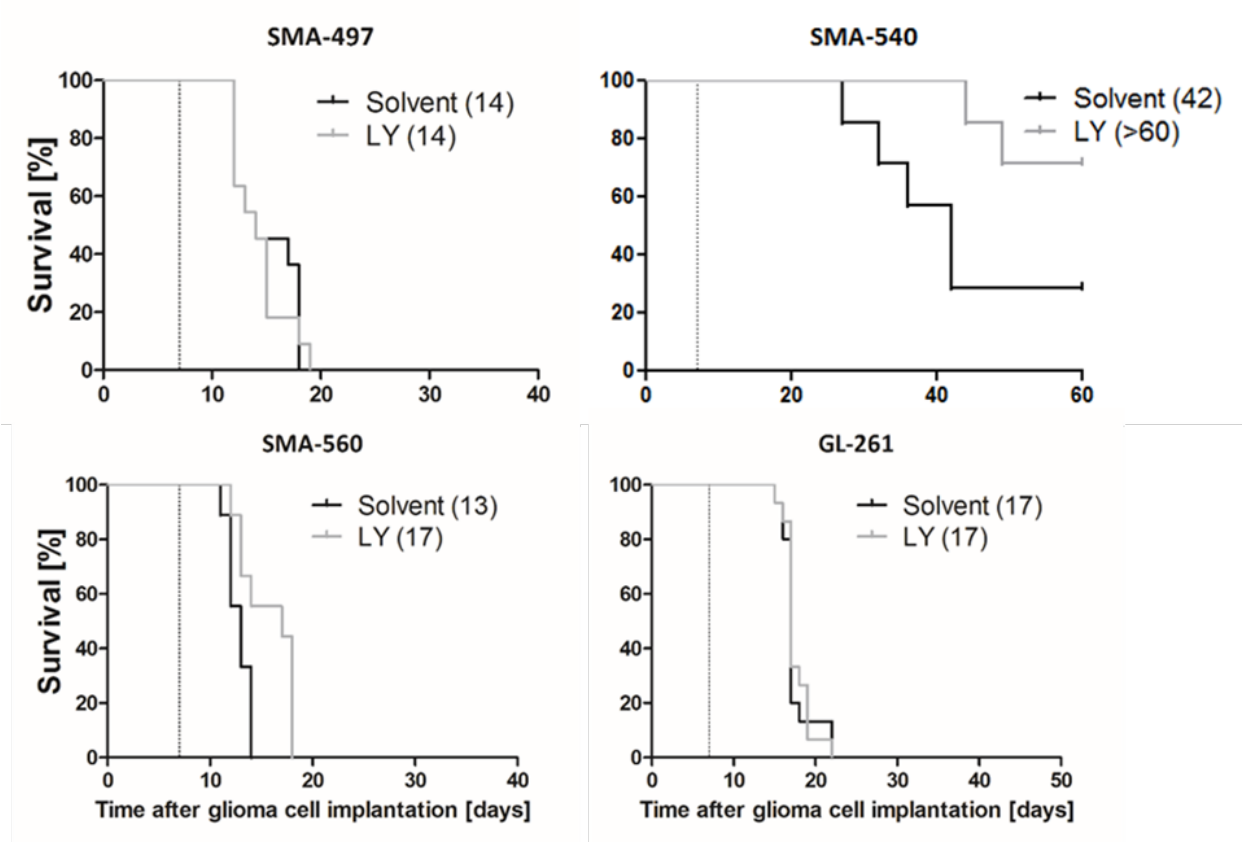

Figure 24. Differential effects of LY2157299 on the growth of murine gliomas. A. Kaplan-Meier survival curves of glioma-bearing mice (log-rank test was considered significant for $p<0.05$).

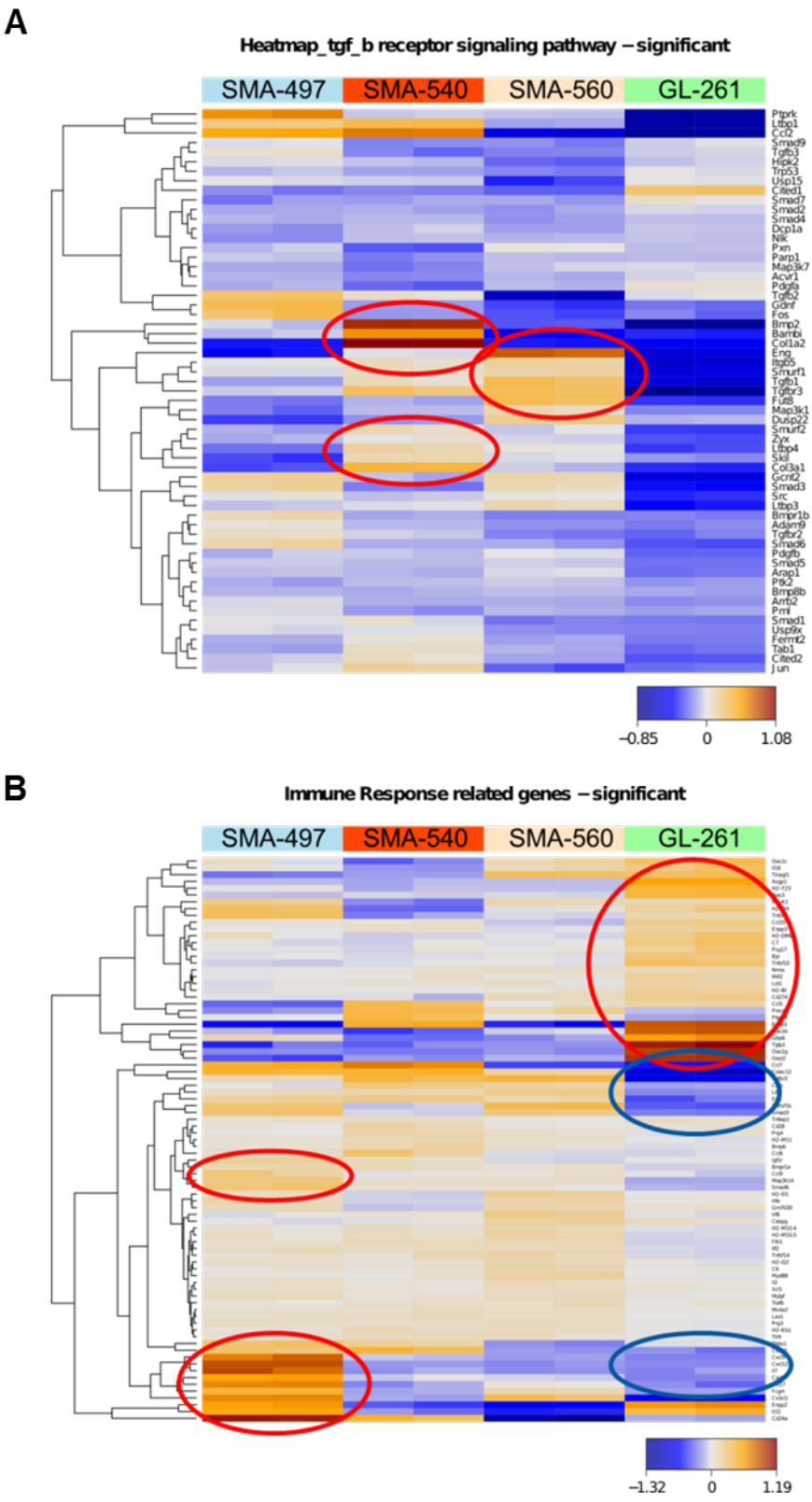

Figure 25. TGF-β and immune response gene expression heatmaps. Heatmaps were obtained by unsupervised comparison of genes differentially expressed in the four mouse glioma cell lines for the TGF-β signaling (A) and immune response (B) pathways. The heatmaps indicate high to low expression levels as red to blue color coding. Up- or downregulated gene clusters in SMA-497 and GL-261 cells are encircled in red or blue.

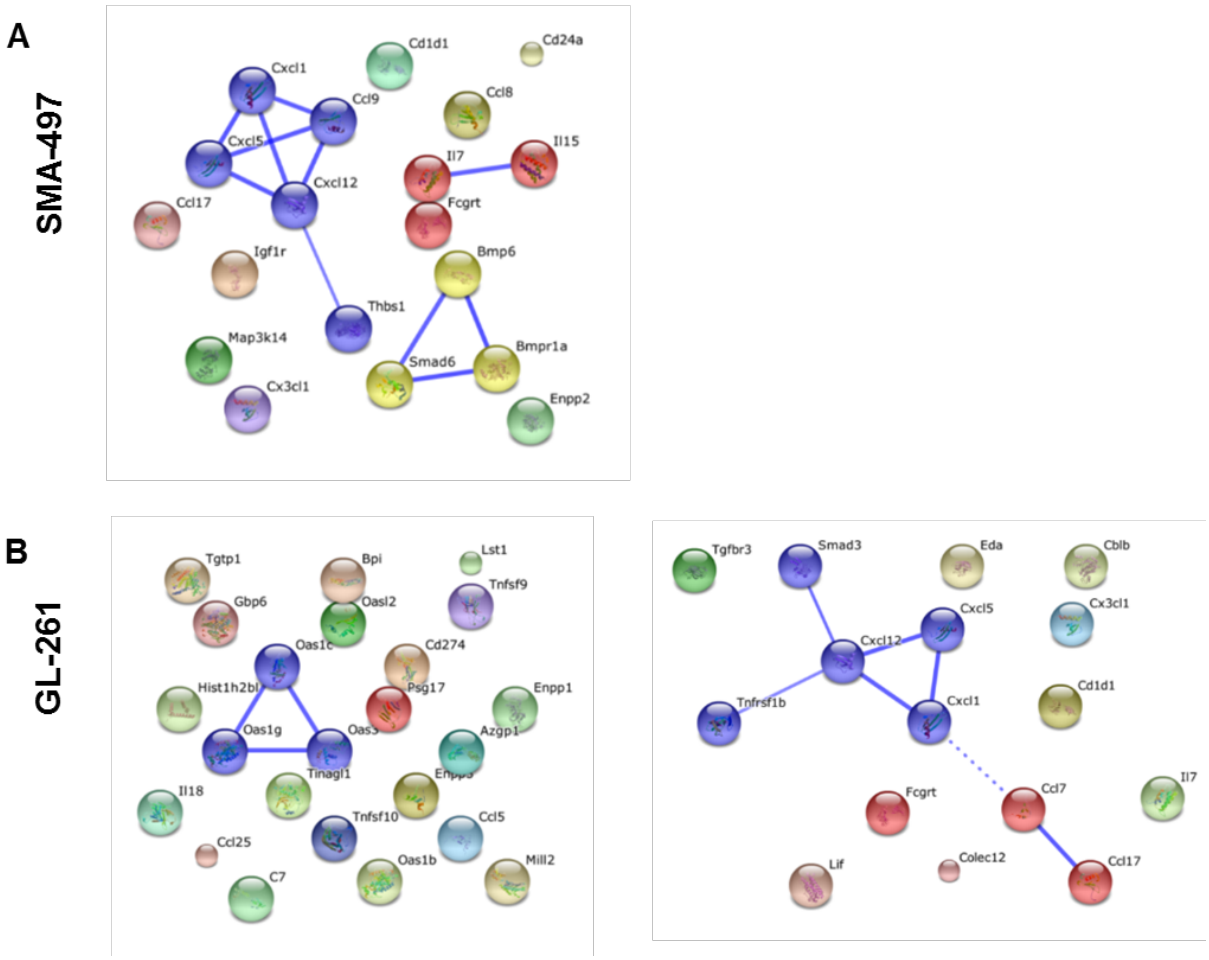

Figure 26. Gene cluster analysis. Functional interactions between genes up-regulated in immune response pathways in SMA-497 (A) and GL-261 (B, left) or down-regulated in GL-261 (B, right) were analyzed by Affymetrix micro-array based gene expression profiling using STRING analysis. Interactions with high confidence score of 0.700 were integrated to the interactome. Clusters were determined by MCL algorithm and presented with different node colors. Inter-cluster edges are represented by dashed-lines.

TGF-β receptor signaling pathway related genes (all genes analysed)					
Col3a1	*Wfikkn2*	*Tab1*	*Eng*	*Bmp8a*	*Smad1*
Mstn	*Smurf2*	*Acvrl1*	*Bmp2*	*Pxn*	*Pml*
Parp1	*Smurf2*	*Amhr2*	*Src*	*Tgfbr3*	*Smad3*
Tgfb2	*Fut8*	*Ptk2*	*Acvr1*	*Pdgfa*	*Smad6*
Cited2	*Fos*	*Foxh1*	*Fshb*	*Smurf1*	*Tgfbr2*
Ptprk	*Tgfb3*	*Pdgfb*	*Dusp15*	*Col1a2*	*Usp9x*
Nodal	*Dusp22*	*Itgb5*	*Skil*	*Zyx*	*Cited1*
Usp15	*Gcnt2*	*Ltbp1*	*Smad9*	*Hipk2*	
Trp53	*Smad5*	*Bambi*	*Bmpr1b*	*Tgfb1*	
Arrb2	*Map3k1*	*Smad7*	*Map3k7*	*Arap1*	
Ccl2	*Dcp1a*	*Smad2*	*Tgfbr1*	*Ltbp4*	
Nlk	*Fermt2*	*Smad4*	*Bmp8b*	*Hpgd*	
Wfikkn2	*Gdnf*	*Ltbp3*	*Jun*	*Adam9*	

Table 4. Gene sets of TGF-β receptor signaling pathways as defined by Gene Ontology classification schemes.

TGF-β-related genes up-regulated in SMA-540	TGF-β-related genes up-regulated in SMA-560
Tgfbr3; Tgfb1; Smurf1; Itgb5;	*Dusp22; Map3k1*
Eng; Col1a2; Bambi; Bmp2;	*Fut8; Tgfbr3; Tgfb1*
Col3a1; Skil; Ltbp4; Zyx: Smurf2	*Smurf1; Itgb5; Eng*

Table 5. Differentially regulated genes of TGF-β signaling pathways of SMA-540 and SMA-560 mouse glioma cell lines, as defined by Gene Ontology classification schemes.

Immune response related genes (all genes analysed)					
Ilf2	*Ccl1*	*H2-M11*	*Thbs1*	*Oas3*	*Myd88*
Oprk1	*Ccl5*	*H2-M10.5*	*Procr*	*Oas1e*	*Ccr1*
Zap70	*Ccl9*	*H2-M10.6*	*Bpi*	*Oas1c*	*Ccr1l1*
Cd28	*Ccl6*	*Tnfsf9*	*Il1a*	*Oas1g*	*Ccr5*
Ctla4	*Ccr7*	*Vav1*	*Il1b*	*Ccl26*	*Ccl28*
Ccl20	*Ccr10*	*H2-K1*	*Tnfsf10*	*Ccl24*	*Eda*
Fcamr	*Map3k14*	*Lst1*	*Il12a*	*Cxcl12*	*Was*
Il10	*Bmp6*	*H2-T24*	*Cd1d2*	*Clec4e*	
Sbspon	*Hfe*	*H2-T23*	*Il7*	*Cd4*	
Prg4	*Cxcl14*	*H2-T22*	*Il2*	*Mill1*	
Fasl	*Il9*	*Gm7030*	*Il21*	*Mill2*	
Xcl1	*Bmpr1a*	*H2-Bl*	*Cd1d1*	*Igf1r*	
Fcgr2b	*Tnfsf11*	*H2-T10*	*Ifi44l*	*Mylpf*	
Cd24a	*C6*	*H2-T3*	*Ccl27b*	*Psg17*	
Zfr2	*C7*	*H2-M10.2*	*Gm13304*	*Cebpg*	
9230019H11Rik	*Ptger4*	*H2-M10.1*	*Tnfsf15*	*Fcgrt*	
Enpp1	*Enpp2*	*H2-M10.3*	*Tnfsf8*	*Lat*	
Enpp3	*Endou*	*H2-M10.4*	*C8a*	*Ccl25*	
Susd2	*Cblb*	*H2-M9*	*Tinagl1*	*Tnfsf13b*	
Osm	*Vpreb1*	*H2-M1*	*Tnfrsf1b*	*March1*	
Lif	*Nrros*	*H2-M5*	*Cxcl5*	*Ccl22*	
Il5	*Ccr6*	*H2-M2*	*Cxcl3*	*Cx3cl1*	
Vtn	*H2-Oa*	*Cd70*	*Cxcl15*	*Ccl17*	
Ccl7	*H2-DMb2*	*Tnfsf14*	*Cxcl1*	*Irf8*	
Ccl11	*H2-Ob*	*Colec12*	*Cxcl2*	*Il15*	
Ccl12	*H2-Ab1*	*Fth1*	*Cxcl13*	*Il18*	
Ccl8	*H2-Eb1*	*Cd274*	*Oasl2*	*Tlr9*	
Ccl4	*H2-Eb2*	*Nkx2-3*	*Oas1b*	*Ccr8*	
Csf3	*Ltb*	*Ms4a2*	*Oas1f*	*Ccr9*	
Tgtp1	*H2-D1*	*Lax1*	*Oas1h*	*Ccr2*	
Il13	*H2-Q1*	*Il1f8*	*Oas1d*	*Cxcr5*	
Csf2	*H2-Q2*	*Il1f6*	*Azgp1*	*Smad3*	
Il3	*H2-Q4*	*Prg2*	*Cxcl9*	*Smad6*	
Tnfsf12Tnfsf13	*H2-Q6*	*Prg3*	*Gbp6*	*Tinag*	
Tnfaip1	*H2-Q10*	*Traf6*	*Tgfbr3*	*Ccr4*	

Table 6. Gene sets of immunogenic profiles as defined by Gene Ontology classification schemes.

Immune response-related genes up-regulated in SMA-497	Immune response-related genes up-regulated in GL-261	Immune response-related genes down-regulated in GL-261
Smad6; Map3k14	*Oasl2; Oas1g; Tgtp1*	*Smad3; Tnfrsf1b; Eda*
Ccl9; Bmpr1a; Igf1r;	*Gbp6; Oas1b; Enpp1*	*Lif; Cblb; Tgfbr3*
Bmp6; Ccl8; Cd24a; Il15; Enpp2;	*Ccl5; Cd274; H2−Bl*	*Colec12; ccl7 ; Cx3cl1; Fcgrt;*
Cx3cl1; Fcgrt; Ccl17; Cxcl1; Il7;	*Lst1; Mill2; Nrros*	*Ccl17 ; Cxcl1; Il7; Cxcl12 ;*
Cxcl12	*Tnfsf10; Bpi; Psg17*	*Cxcl5; cd1d1*
Cxcl5; Cd1d1; thbs1	*C7; H2−DMb2; Enpp3*	
	Ccl25; Tnfsf9; H2−Q4	
	H2−K1; Oas3; H2−T23	
	Azgp1; Tinagl1; Il18	

Table 7. Differentially regulated genes of immunogenic profiles of SMA-497 and GL-261 mouse glioma cell lines, as defined by Gene Ontology classification schemes.

Reciprocal modulation of the VEGF and TGF-β pathways in vitro

We next assessed the expression of ligands and receptors of the VEGF and TGF-β pathways in the mouse glioma models after reciprocal stimulation. First we explored whether modulation of VEGF signalling in glioma cells affected the TGF-β pathway. Exposure to exogenous VEGF, B20 or cediranib had no effect on TGF-$\beta_{1/2}$ mRNA and protein levels (Figure 27A,B) or pSMAD2 levels (Figure 27C). Conversely, VEGF mRNA expression and protein release were induced by TGF-β_2 in a LY2157299-sensitive manner. VEGF mRNA expression was also increased in all cells in response to hypoxia whereas protein levels were increased in SMA-497, SMA-540 and GL-261 and remained similar in SMA-560 (Figure 28A,B). Furthermore, we observed an increase in total *VEGFR1* mRNA expression in response to TGF-β_2 in SMA-497 and SMA-560 glioma cells which was decreased upon co-treatment with LY2157299 only in SMA-560. However, protein levels were increased in all models and this effect was blocked by LY2157299 (Figure 29A). VEGFR2 levels in response to TGF-β_2 stimulation, analyzed in SMA-540 and SMA-560 cells only, were increased upon stimulation in a LY2157299-sensitive manner (Figure 29B). Although LY2157299 alone reduced constitutive pSMAD2 levels (Figure 15B), it had no effect on constitutive VEGF ligand or receptor mRNA expression or protein release in either cell line.

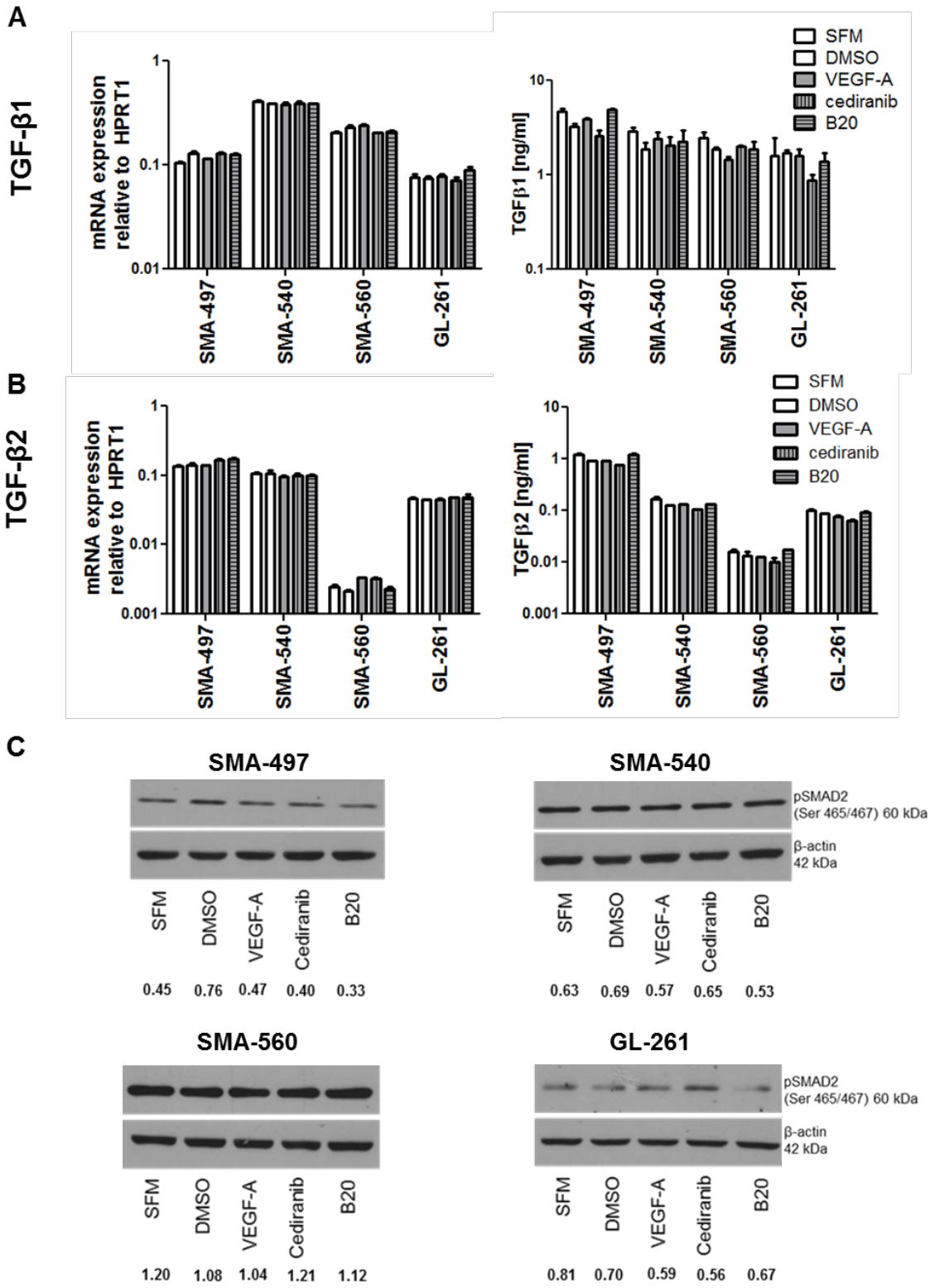

Figure 27. Modulation of the TGF-β signaling pathway by VEGF *in vitro*. A.B. Modulation of TGF-β_1 (A) or TGF-β_2 (B) mRNA (left) expression was determined by RT-PCR 24 h after exposure to VEGF (400 ng/ml), cediranib (100 nM) or B20 (100 µg/ml). Protein levels (right) were detected in corresponding supernatants by ELISA. Data are expressed as mean and SD (n=3) (one-way ANOVA followed by Tukey's post hoc test, confidence interval 99%). C. pSMAD2 levels were assessed by immunoblot. Values of densitometric analysis of pSMAD2 protein levels relative to β-actin are shown below the immunoblot panels.

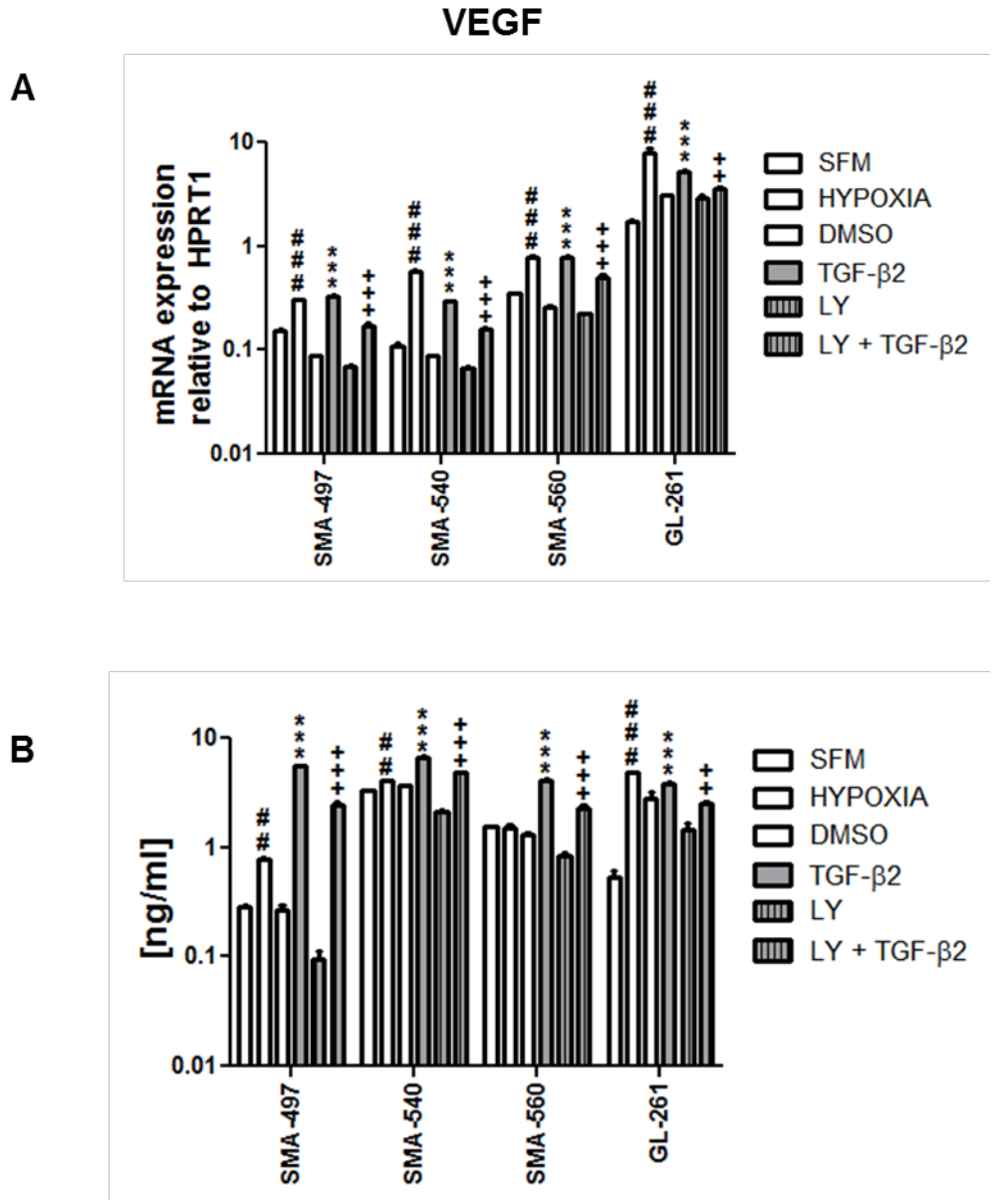

Figure 28. Modulation of VEGF-A by TGF-β signaling pathway *in vitro*. A.B. The cells were treated with TGF-β_2 (2 ng/ml) or LY2157299 (LY) (1 µM) or both for 24 h. *VEGF* mRNA expression was assessed by RT-PCR (A). In parallel, VEGF protein levels were determined by ELISA (B). Hypoxia served as positive control for VEGF-A expression (***p<0.001, one-way ANOVA followed by Tukey's post hoc test confidence interval 99%, treated versus SFM, ++p<0.01, +++p<0.001, LY2157299 + TGF-β_2 versus TGF-β_2, ##p<0.01, ###p<0.001, hypoxia versus SFM).

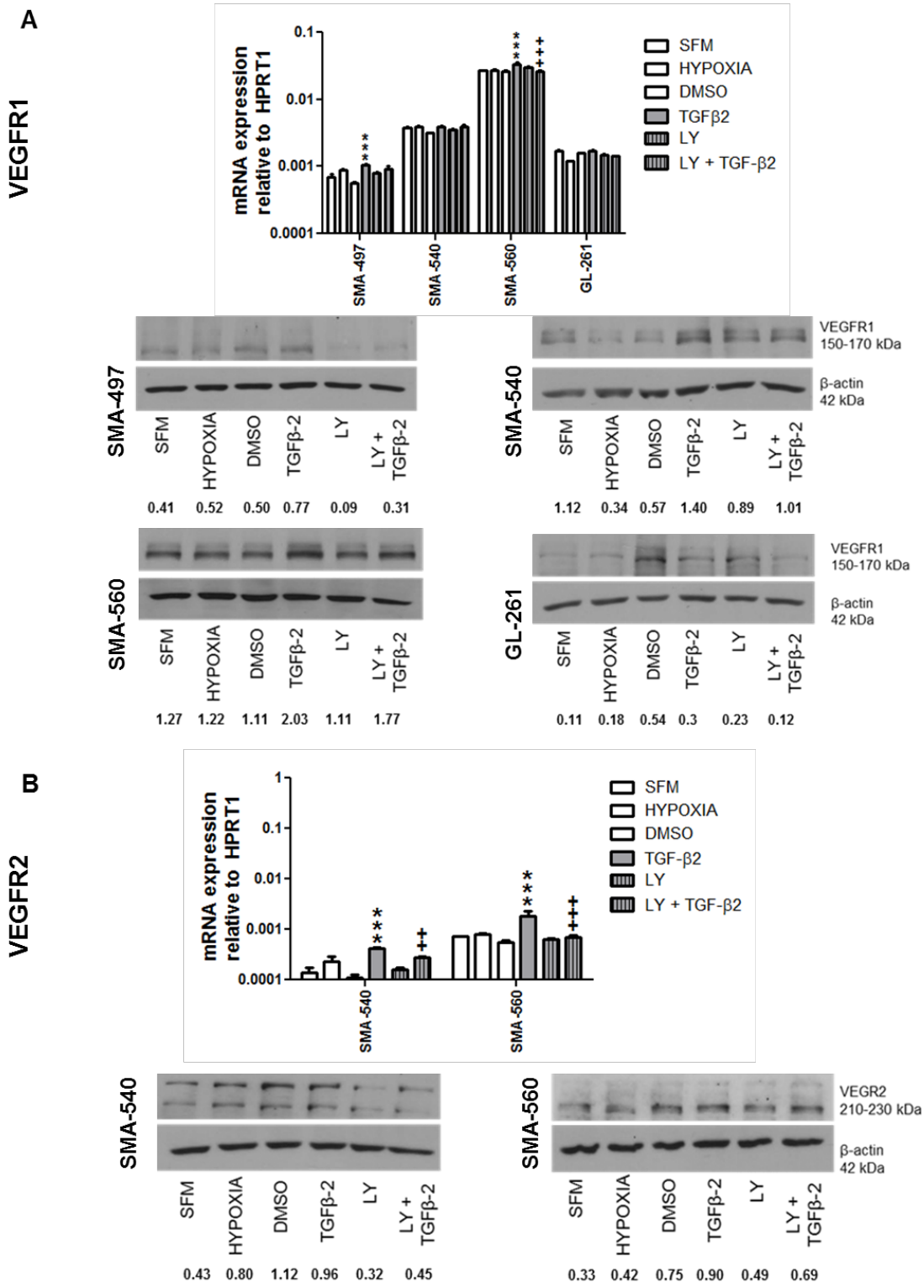

Figure 29. Modulation of VEGFR1-2 by TGF-β signaling pathway *in vitro*. A.B. VEGFR1/2 mRNA (top) and protein (bottom) levels were assessed by RT-PCR and immunoblot, respectively. mRNA and ELISA data are expressed as mean and SD (n=3) (***p<0.001, one-way ANOVA followed by Tukey's post hoc test confidence interval 99%, treated versus SFM, ++p<0.01, +++p<0.001, LY2157299 + TGF-β_2 versus TGF-β_2). Values of densitometric analysis of VEGFR protein levels, relative to β-actin, are shown below the immunoblot panels in A and B.

Co-targeting of the VEGF and TGF-β pathways in vivo

SMA-497 and GL-261 were chosen to explore a potential synergy between VEGF and TGF-β pathway inhibition. SMA-497 was chosen because it was refractory to either treatment as single agent, facilitating the detection of any possible synergy. GL-261 was chosen because LY2157299 alone was not active whereas B20 was. A gain from co-treatment would indicate that the TGF-β pathway assumes a different role in the context of VEGF inhibition. There was no survival benefit from co-treatment in SMA-497 whereas combination treatment was superior to either treatment alone in GL-261 (Figure 30; Table 1).

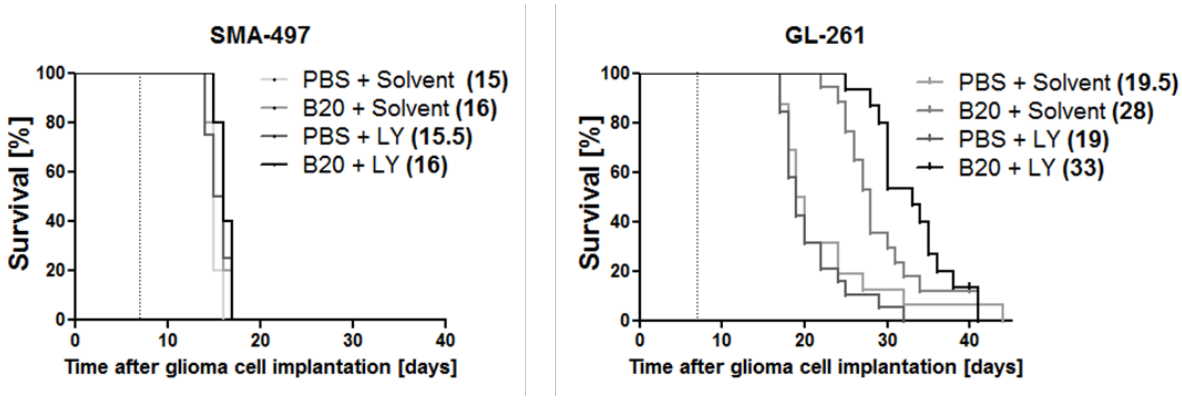

Figure 30. Effect of combined B20 and LY2157299 treatment in SMA-497 and GL-261 syngeneic models *in vivo*. Syngeneic mice were intracranially implanted with SMA-497 or GL-261 cells and treated twice weekly with 5 mg/kg B20 or daily with 150 mg/kg LY2157299 or corresponding solvents or both from day 7 on. Kaplan-Meier survival curves (Gehan-Breslow-Wilcoxon test, considered significant for $p<0.05$).

Early reductions of tumor volumes and blood vessel density were seen in GL-261, but not SMA-497, and only in the B20-containing regimens, with no modulation by LY2157299. The volume differences in early-stage GL-261 tumors were abolished in end-stage tumors. However, reduced blood vessel density was only maintained in the co-treatment group, but not in the B20-only end-stage tumors. Decreased vessel diameter and increased vessel wall thickness were observed with all therapeutic regimens in GL-261 (Figure 31A,B). ZO-1 was used as a marker for tight junction staining showing a more regular staining pattern indicative for a restoration of endothelial barrier integrity (Figure 32A-D). Co-treatment with LY2157299 prevented B20-induced increased tumor invasiveness in early stages, but this effect was abolished in end-stage tumors (Figure 31A, bottom). In GL-261, but not SMA-497 gliomas, the reduction of pSMAD2 levels by LY2157299 alone was enhanced by co-

treatment with B20 in early-stage responsive and in end-stage resistant tumors. In contrast, pSMAD2 levels were increased in B20-treated end-stage tumors, consistent with the TGF-β pathway as an escape route from VEGF inhibition, and this was not seen with combined treatment (Figure 33A). There was no significant CA IX induction in either model in early-stage tumors whereas treatment resistance in the GL-261 co-treatment group was accompanied by an increase in CA IX staining from 18% to 39% positive tumor areas (Figure 33B). Assessment of the role of TGF-$\beta_{1/2}$ within angiogenesis gene clusters up-regulated in SMA-497 and GL-261 by STRING analysis revealed that TGF-$\beta_{1/2}$ may interact with only a small subset of up-regulated genes in SMA-497. Conversely, both molecules are integrated in the main network of functional gene interactions in GL-261 (Figure 34), indicating a possible role of TGF-β in mediating resistance to B20 therapy.

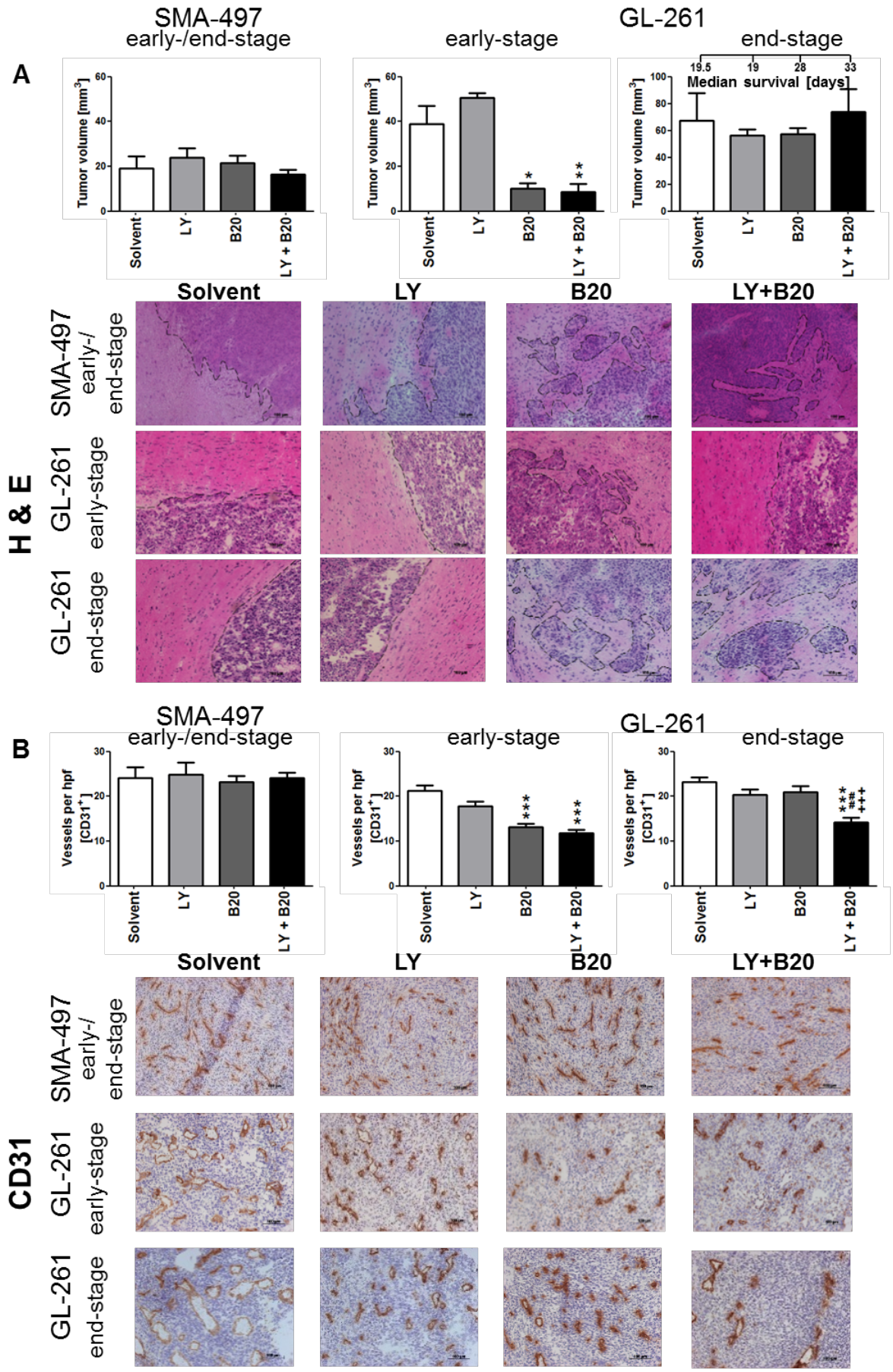

Figure legend 31 on the next page

Figure 31. Analysis of morphology and angiogenesis patterning in SMA-497 and GL-261 syngeneic models treated with combined B20 and LY2157299 *in vivo*. Syngeneic mice intracranially implanted with SMA-497 or GL-261 cells were treated twice weekly with 5 mg/kg B20 or daily with 150 mg/kg LY2157299 or corresponding solvents or both. Early-stage refers to brain sections from animals sacrificed when the first mice became symptomatic and end-stage at the time point when each specific mouse developed neurological symptoms. A. Tumor volume (top) and morphological analysis by H&E (bottom). B. CD31+ capillaries density quantification (top) and immunohistochemical staining (bottom). Size bars corresponds to 100 µm. (***p<0.001, one-way ANOVA followed by Tukey's post hoc test confidence interval 95%, treated versus solvent, +++p<0.001, B20+LY2157299 versus B20, ##p<0.01, B20+LY2157299 versus LY2157299).

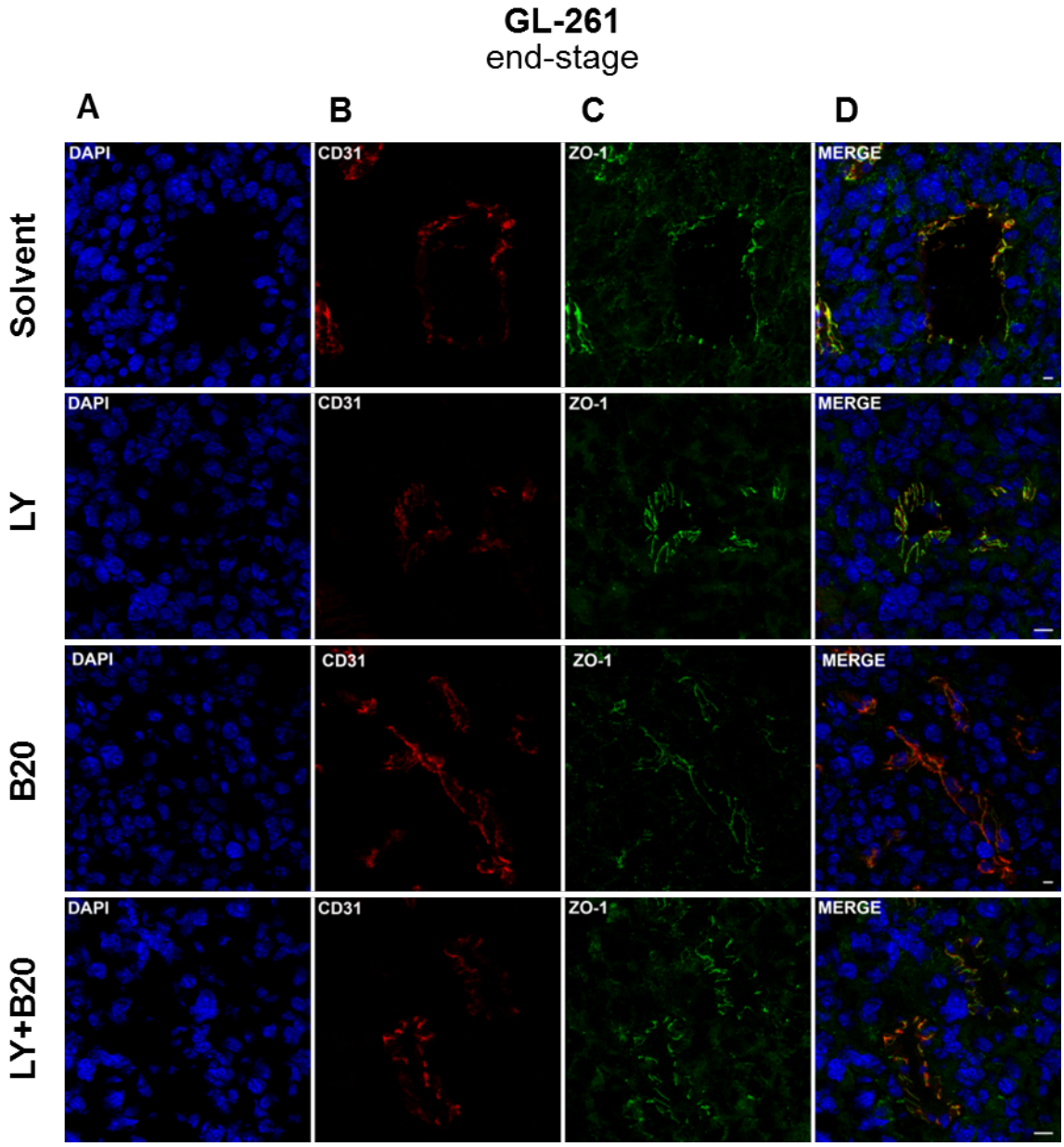

Figure 32. Analysis of tight junctions patterning in SMA-497 and GL-261 syngeneic models treated with combined B20 and LY2157299 *in vivo*. Syngeneic mice were intracranially implanted with SMA-497 or GL-261 cells and treated twice weekly with 5 mg/kg B20 or daily with 150 mg/kg LY2157299 or corresponding solvents or both from day 7 on. A-D Staining of tumor sections to visualize vessel normalization was performed with DAPI (A. blue), CD31 (B. red) and ZO-1 (C. green). Merged images are shown in (D). Size bars correspond to 10 µm.

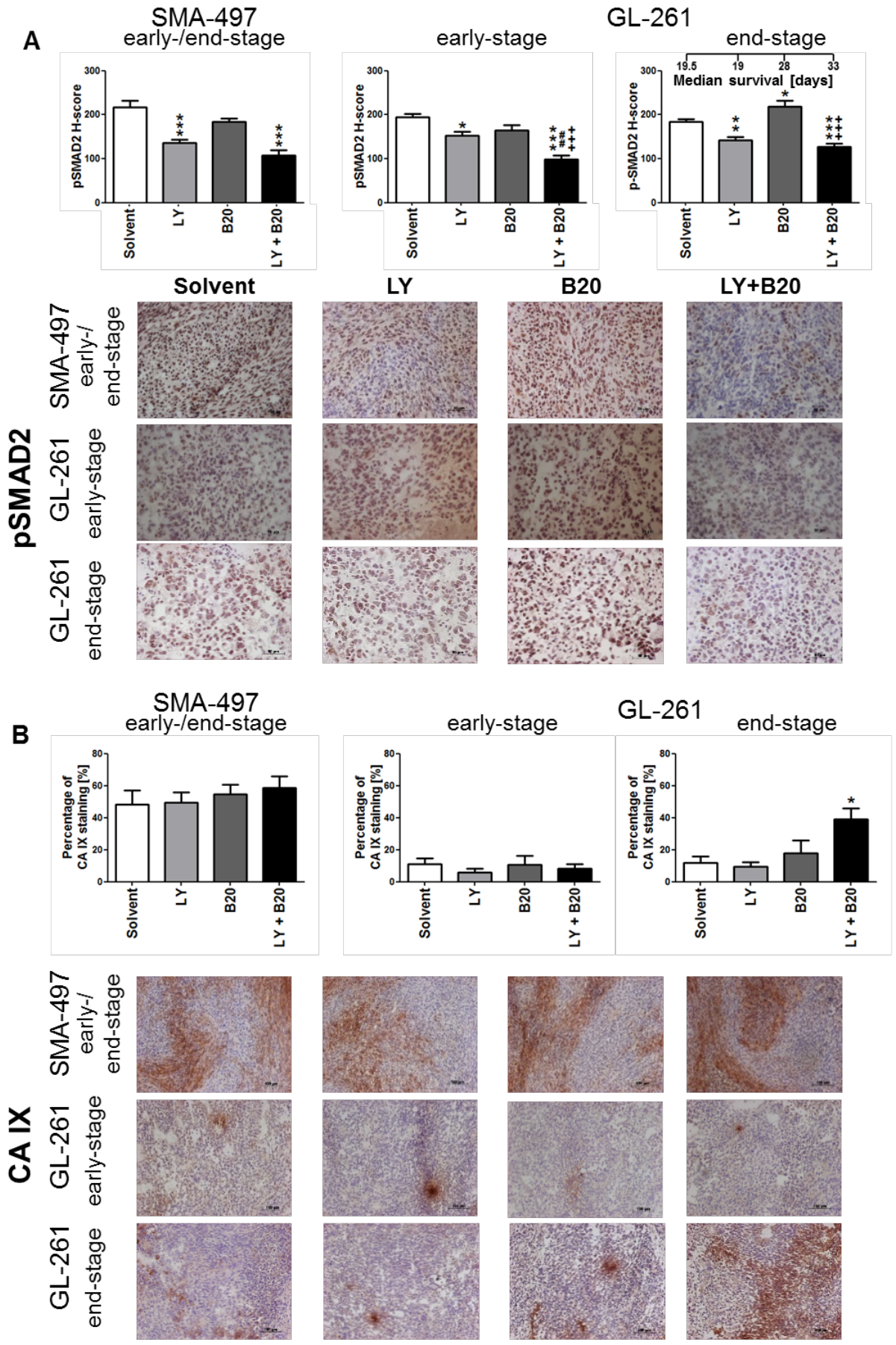

Figure legend 33 on the next page

Figure 33. Analysis of pSMAD2 levels and hypoxia patterning in SMA-497 and GL-261 syngeneic models treated with combined B20 and LY2157299 *in vivo*. Syngeneic mice intracranially implanted with SMA-497 or GL-261 cells were treated twice weekly with 5 mg/kg B20 or daily with 150 mg/kg LY2157299 or corresponding solvents or both. Early-stage refers to brain sections from animals sacrificed when the first mice became symptomatic and end-stage at the time point when each specific mouse developed neurological symptoms. A. pSMAD2 H-score quantization (top) and immunohistochemistry representative images (bottom). B. CA IX percentage of stained area (top) and representative immunohistochemistry images (bottom). Size bars correspond to 50 µm (A) and 100 µm (B). (*p<0.05, **p<0.01, ***p<0.001, one-way ANOVA followed by Tukey's post hoc test confidence interval 95%, treated versus solvent, +++p<0.001, B20+LY2157299 versus B20, ##p<0.01, B20+LY2157299 versus LY2157299).

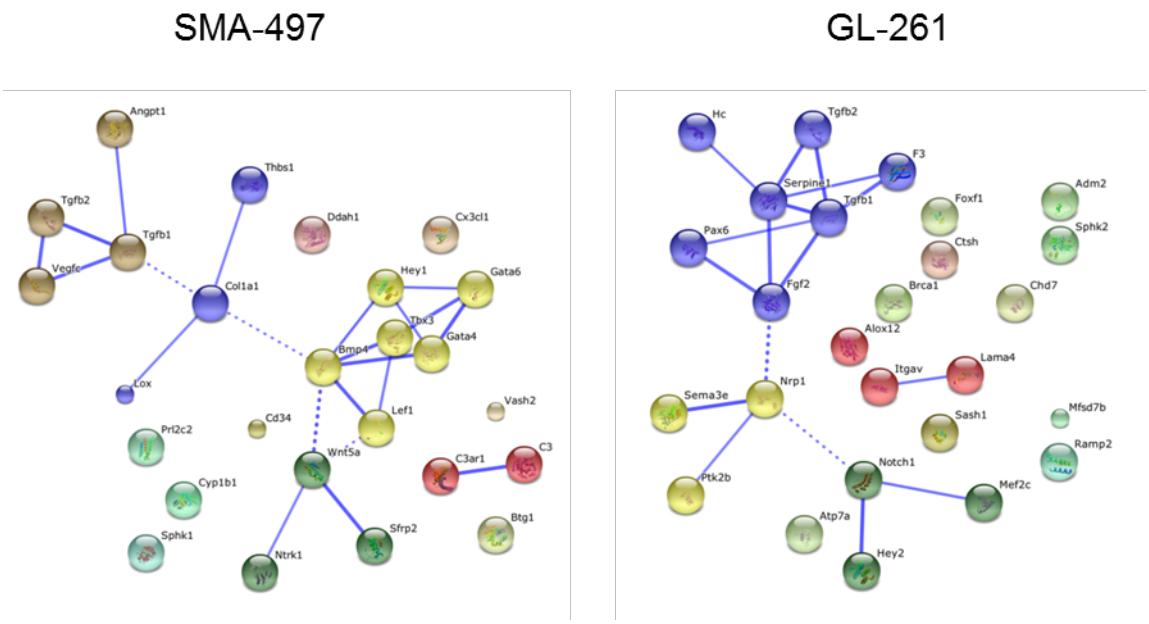

Figure 34. Bioinformatic analysis of TGF-$\beta_{1/2}$ interactome within angiogenesis gene clusters up-regulated in SMA-497 and GL-261. Gene cluster analysis. Functional interactions between TGF-$\beta_{1/2}$ and genes upregulated in angiogenic profiles in SMA-497 (left) and GL-261 (right) were analyzed in Affymetrix micro-array based gene expression profiling by STRING analysis. Interactions with high confidence score of 0.700 were integrated to the interactome. Clusters were determined by MCL algorithm and presented with different node colors. Inter-cluster edges are represented by dashed-lines.

Differential host cell responses to VEGF/TGF-β co-targeting

To generate a broad overview on host cell infiltration, we assessed frequencies of leukocytes ($CD45^+$), T cells ($CD4^+$ and $CD8^+$) and macrophages/microglia ($CD11b^+$) in mono- and co-treated SMA-497 and GL-261 early- and end-stage tumors (Figure 35,36). In GL-261, only in early- but not in end-stage tumors, increased infiltration of $CD11b^+$ cells upon B20 alone and increased numbers of cytotoxic T (CD8+) cells upon co-treatment were observed (Figure 36A). Resistance to co-treatment was accompanied by decreased infiltration of $CD45^+$ and $CD11b^+$ cells in GL-261 end-stage gliomas when compared to solvent or B20 mono-treatment (Figure 35A, 36B).

pSMAD2 was detected in tumor cells rather than host leukocytes in GL-261 end-stage tumors. Due to the higher proportion of pSMAD2-positive tumor cells versus infiltrating leukocytes, tumor cells were more affected by decreased pSMAD2 levels, although levels in single leukocytes were altered similarly, with a decrease upon LY2157299 and combined treatment, and an increase by B20 alone (Figure 37A-D).

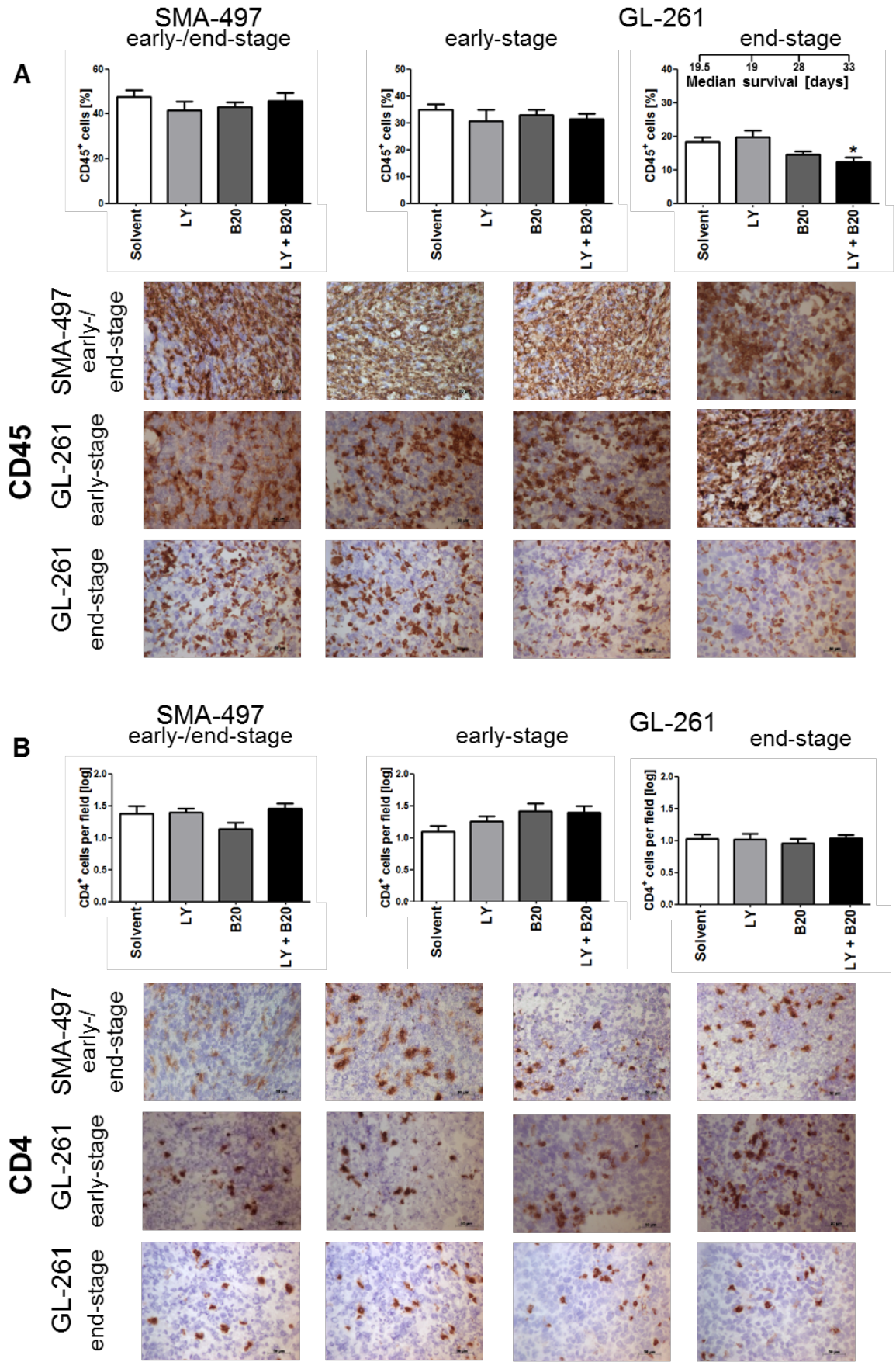

Figure legend 35 on the next page

Figure 35. Modulation of tumor CD45$^+$ and CD4$^+$ cells infiltration in combined B20- and LY2157299-treated syngeneic models *in vivo*. Syngeneic mice intracranially implanted with SMA-497 or GL-261 cells were treated twice weekly with 5 mg/kg B20 or daily with 150 mg/kg LY2157299 or corresponding solvents or both. Early-stage refers to brain sections from animals sacrificed when the first mice became symptomatic and end-stage at the time point when each specific mouse developed neurological symptoms. A. CD45$^+$ cells percentage (top) and representative immunohistochemistry images (bottom). B. CD4$^+$ number of cells per field (top) and representative immunohistochemistry images (bottom). Size bars correspond to 50 µm. (*$p<0.05$ ANOVA followed by Tukey's post hoc test confidence interval 95%).

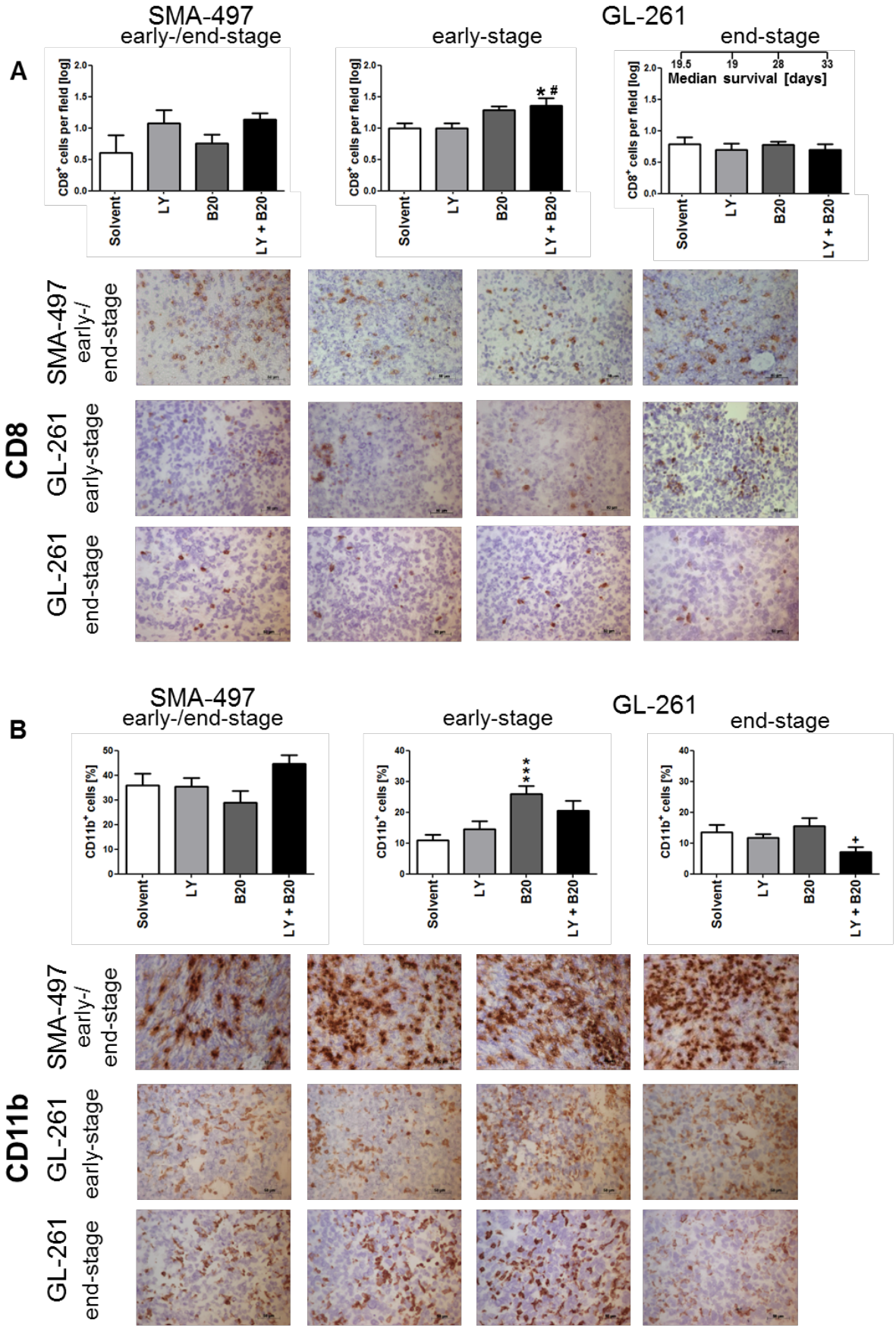

Figure legend 36 on the next page

Figure 36. Modulation of tumor CD8$^+$ and CD11b$^+$ cells infiltration in combined B20- and LY2157299-treated syngeneic models *in vivo*. Syngeneic mice intracranially implanted with SMA-497 or GL-261 cells were treated twice weekly with 5 mg/kg B20 or daily with 150 mg/kg LY2157299 or corresponding solvents or both. Early-stage refers to brain sections from animals sacrificed when the first mice became symptomatic and end-stage at the time point when each specific mouse developed neurological symptoms. A. CD8$^+$ number of cells per field (top) and representative immunohistochemistry images (bottom). B. CD11b$^+$ percentage of cells (top) and representative immunohistochemistry images (bottom). Size bars correspond to 50 µm. (*p<0.05 and ***p<0.001 one-way ANOVA followed by Tukey's post hoc test confidence interval 95%, treatment versus solvent, #p<0.05, B20+LY2157299 versus LY2157299, +p<0.05 B20+LY2157299 versus B20).

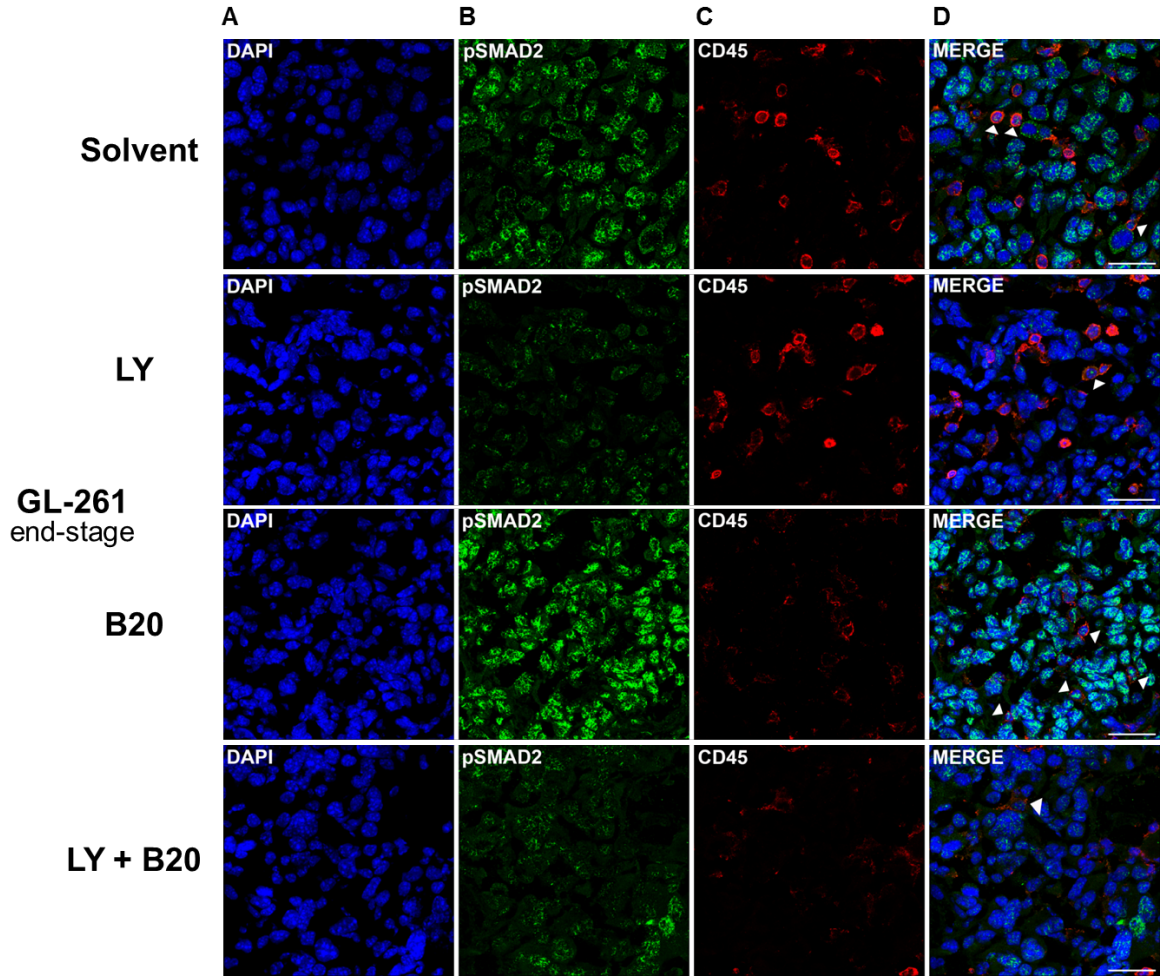

Figure 37. Modulation of pSMAD2 levels and tumor immune cell infiltration in B20 and LY2157299 co-treated GL-261 syngeneic model *in vivo*. Brain sections (end-stage) were examined. Staining of tumor sections was assessed with DAPI (A. blue), pSMAD2 (B. green) and CD45 (C. red). Merged images are shown in (D). CD45+/pSMAD2+ leukocytes are marked by arrow heads. Size bars correspond to 50 µm.

pSMAD2 levels in response to bevacizumab treatment in human glioblastoma

We also analysed human glioblastoma patients who underwent further surgery upon failure of bevacizumab. As groups, neither refractory tumors of 9 non-bevacizumab-treated patients, nor those of 5 patients failing on a bevacizumab-containing regimen,

exhibited an increase or decrease in pSMAD2 levels whereas vessel density was decreased in the latter group (Figure 38,39).

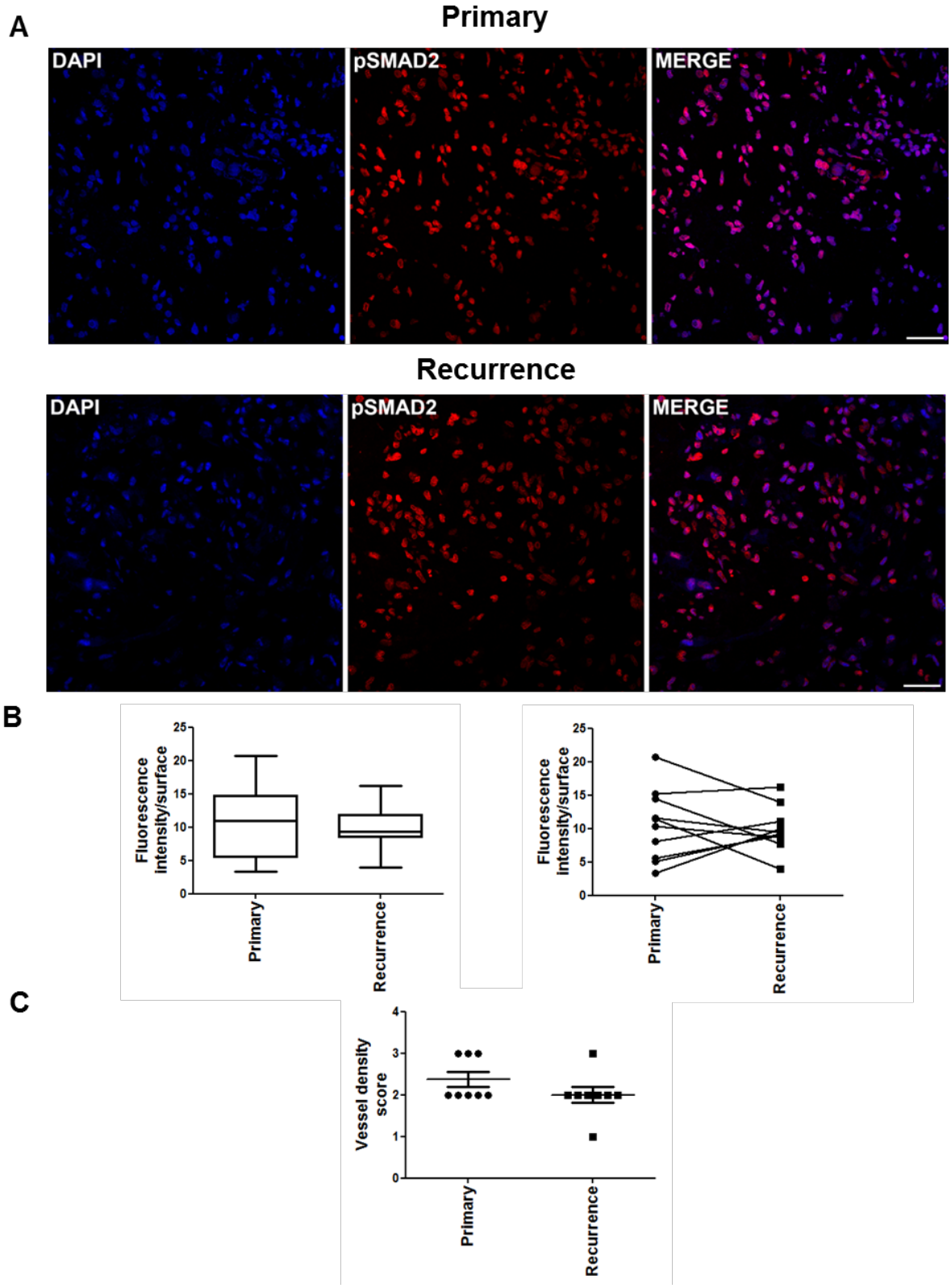

Figure 38. pSMAD2 levels in non-bevacizumab-treated patients. pSMAD2 levels were assessed by immunofluorescence microscopy in primary and recurrent tumor tissue of patients treated with non-bevacizumab regimens (A). Size bars correspond to 20 µM. Quantification of fluorescent images of the cohort is provided in B. (C) Vessel density scores.

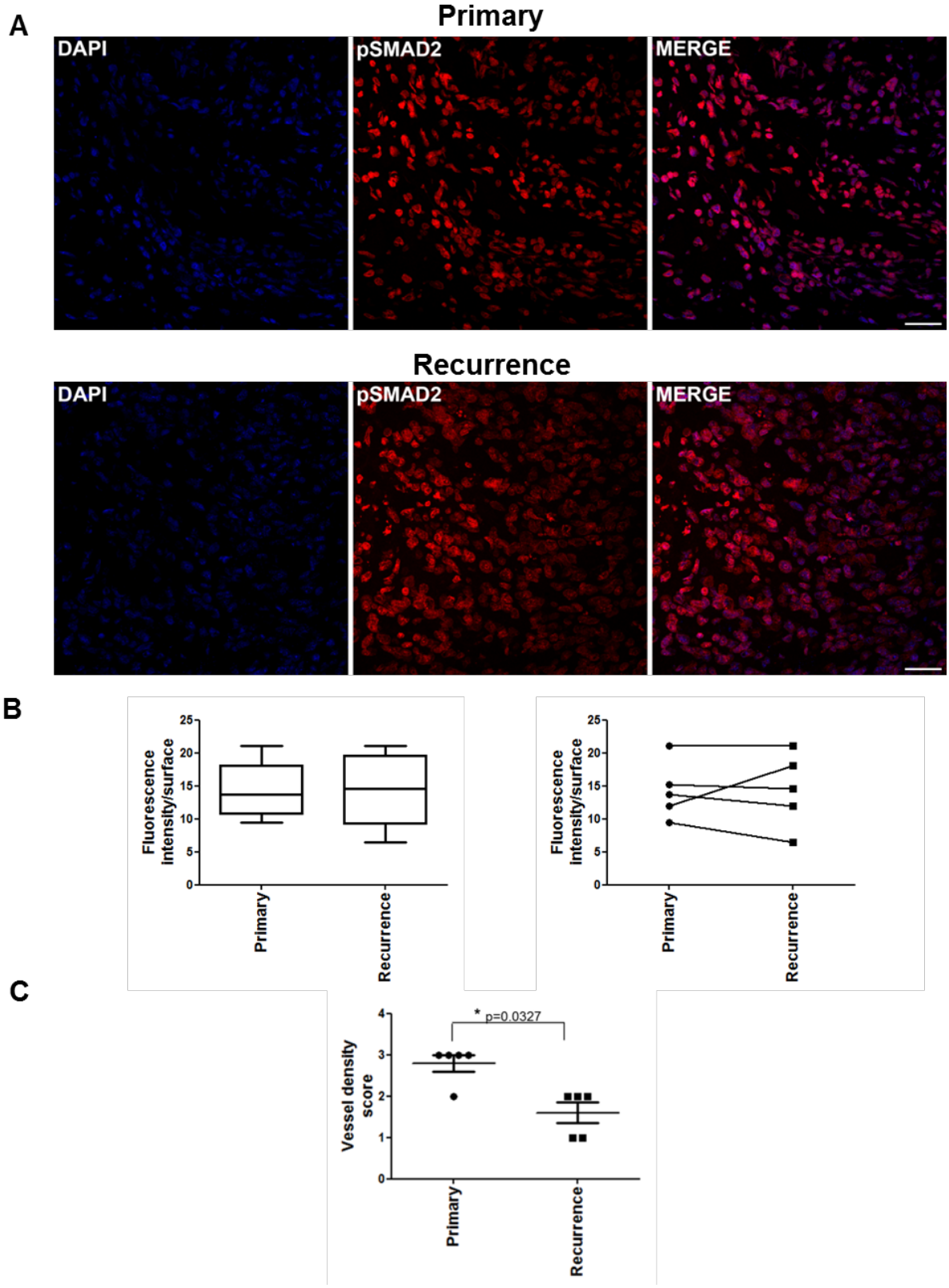

Figure 39. pSMAD2 levels in bevacizumab-treated patients. pSMAD2 levels were assessed by immunofluorescence microscopy in primary and recurrent tumor tissue of patients treated with bevacizumab-containing regimens (A). Size bars correspond to 20 µM. Quantification of fluorescent images of the cohort is provided in B. (C) Vessel density scores. Data are expressed as mean and SEM ($^{*}p<0.05$, paired student t-test, primary versus recurrent).

6.2 Results project 2

Characterization of PD-L1 and PD-L2 basal expression and modulation by TGF-β signalling in mouse glioma cells

PD-L1 was constitutively expressed at mRNA level in all four murine glioma cell lines with highest expression in GL-261 cells. Protein presence on the cell surface was assessed by flow cytometry and showed low, but detectable levels in all cell lines. PD-L2 mRNA was expressed only in SMA-497 cells, yet, this did not translate in protein expression as PD-L2 was not detected on the surface of any cell line (Figure 40A,B). Subsequently, we examined whether TGF-β regulates PD-L1 and PD-L2 expression levels. Neither treatment with a TGFβRI inhibitor (SD-208) nor stimulation with recombinant TGF-β_2 changed the expression of the PD-1 ligands. IFN-γ stimulation was used as positive control for PD-L1 induction, however, it did not affect PD-L2 protein surface expression (Figure 40C,D).

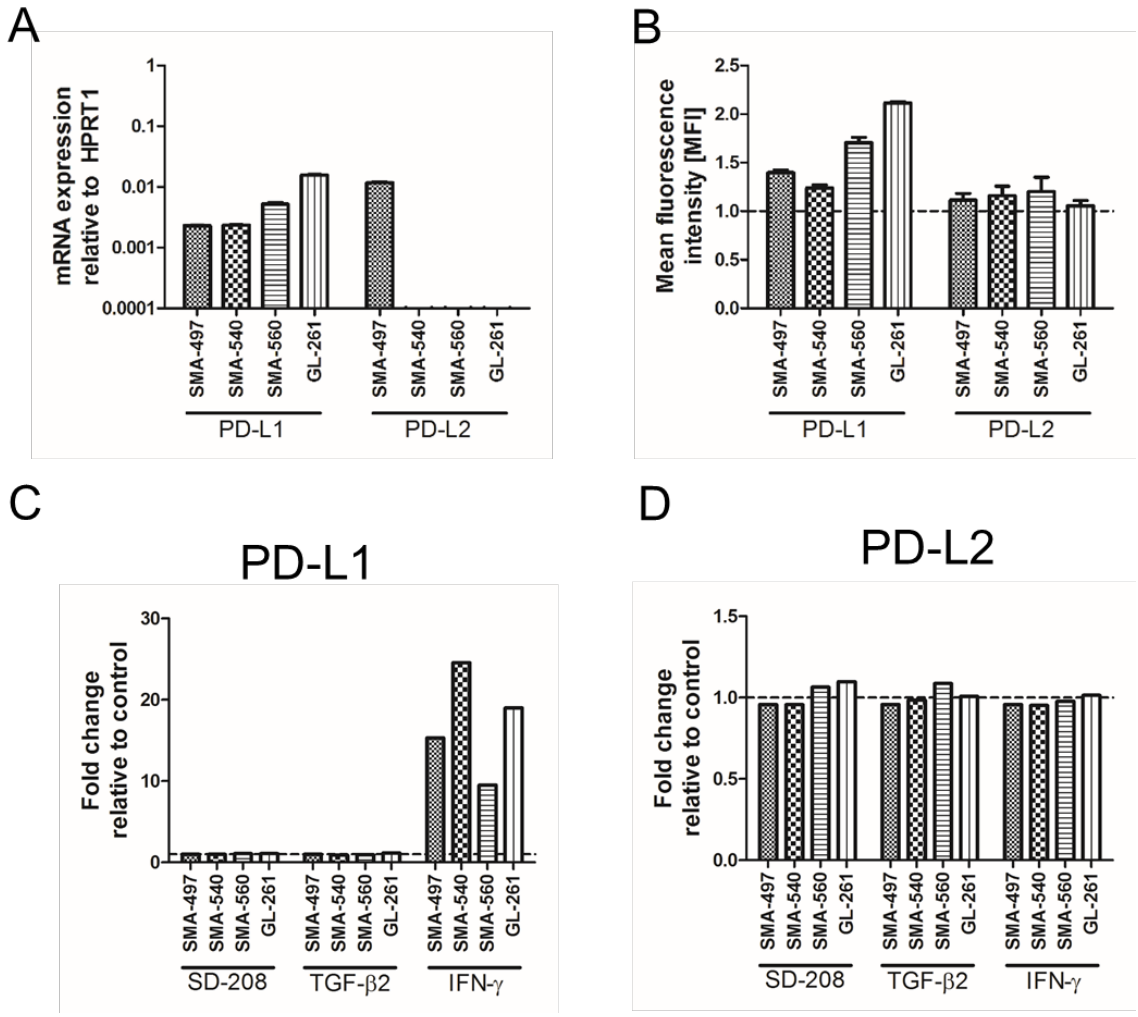

Figure legend 40 on the next page.

Figure 40. Basal and modulated expression of PD-L1 and PD-L2 in mouse glioma cells. A. PD-L1 and PD-L2 mRNA expression was determined by RT-PCR. B. Presence of the protein on the surface was assessed by flow cytometry. Modulation of PD-L1 (C) and PD-L2 (D) protein expression by exposure to SD-208 (1 µM), recombinant TGF-β_2 (2 ng/ml) or IFN-γ (100 U/ml) stimulation was investigated by flow cytometry.

Dual blockade of PD-1 and TGF-β pathways increases cytokine production of $CD4^+$ and $CD8^+$ T cells challenged with syngeneic tumor cells

To investigate whether inhibition of the PD-1 and TGF-β pathway can reverse glioma cell-mediated T cell immunosuppression, we set up an *in vitro* co-culture model. Mouse glioma cells were co-cultured with polyclonally activated syngeneic lymphocytes in the presence or absence of anti-PD1, LY2157299 or a combination thereof (Figure 41A,B). After 4-6 days, floating lymphocytes were harvested to determine intracellular cytokine levels. In a first set of experiments, $CD4^+$ and $CD8^+$ T cell production of IFN-γ and IL-2 was assessed in co-culture systems using SMA-497, SMA-540 or GL-261 cells. Single agent treatment with either anti-PD1 or LY2157299 increased IFN-γ production of both T cell populations with a similar trend in all tested cell lines. Combinatorial treatment resulted in highest IFN-γ production compared to either treatment alone (Figure 42A,B). Differently, IL-2 production was consistently low in SMA-497 and SMA-540 cells and was not affected by any treatment. In the GL-261 model, there was higher basal production of IL-2 compared to SMA cell lines, which was further elicited in $CD4^+$ cells by PD-1 and TGF-β co-targeting (Figure 42A,B).

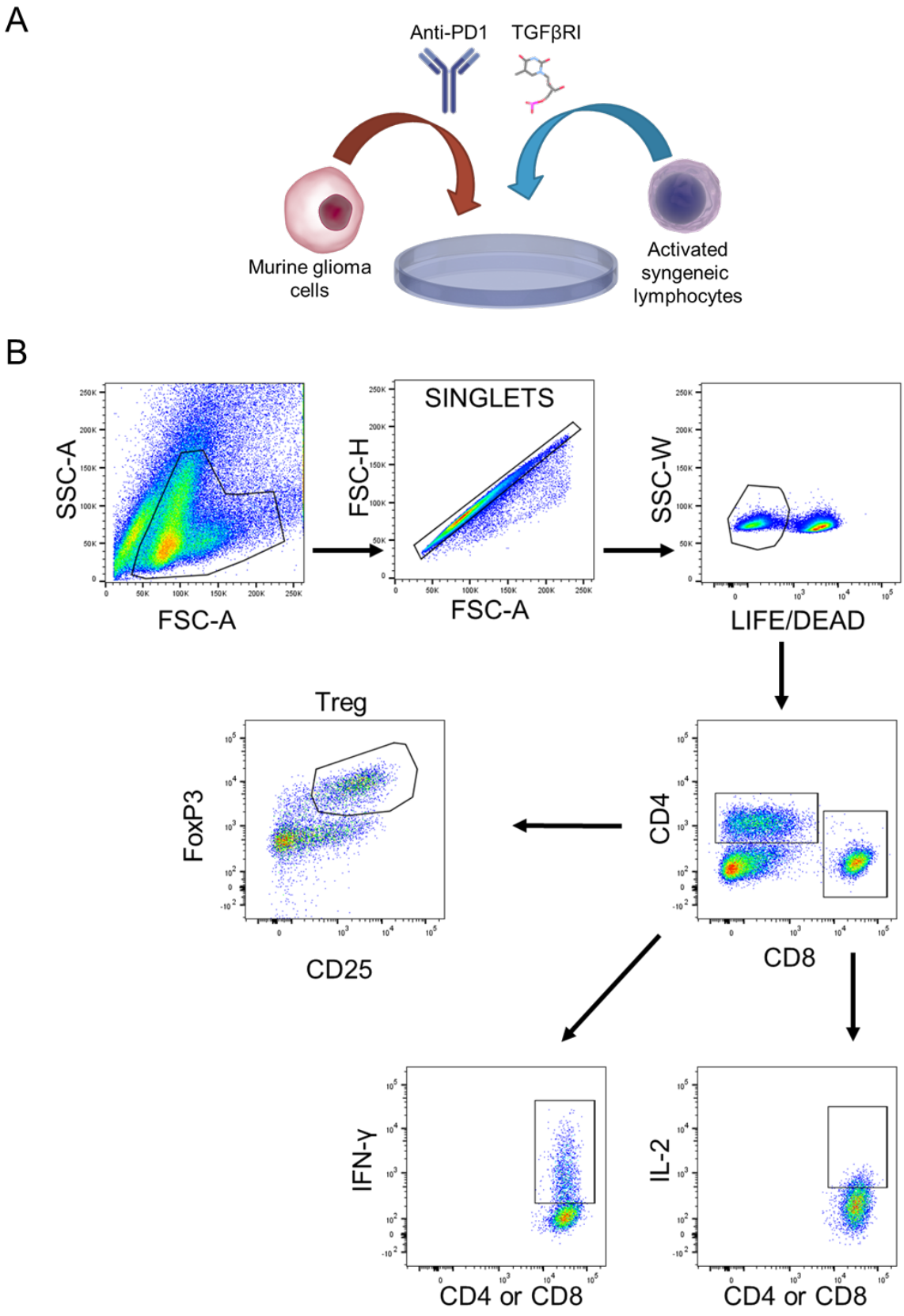

Figure 41. *In vitro* co-culture system and gating strategy. A. Graphic representation of the co-culture model. Actively growing $2x10^5$ tumor cells were co-cultured for 4-6 days with 10^6 syngeneic activated lymphocytes (2 µg/mL concanavalin A) in the absence or presence of anti-PD1 (10 µg/ml), TGFβRI inhibitor (LY2157299, 1 µM) or a combination thereof. B. Gating strategy for downstream analyses.

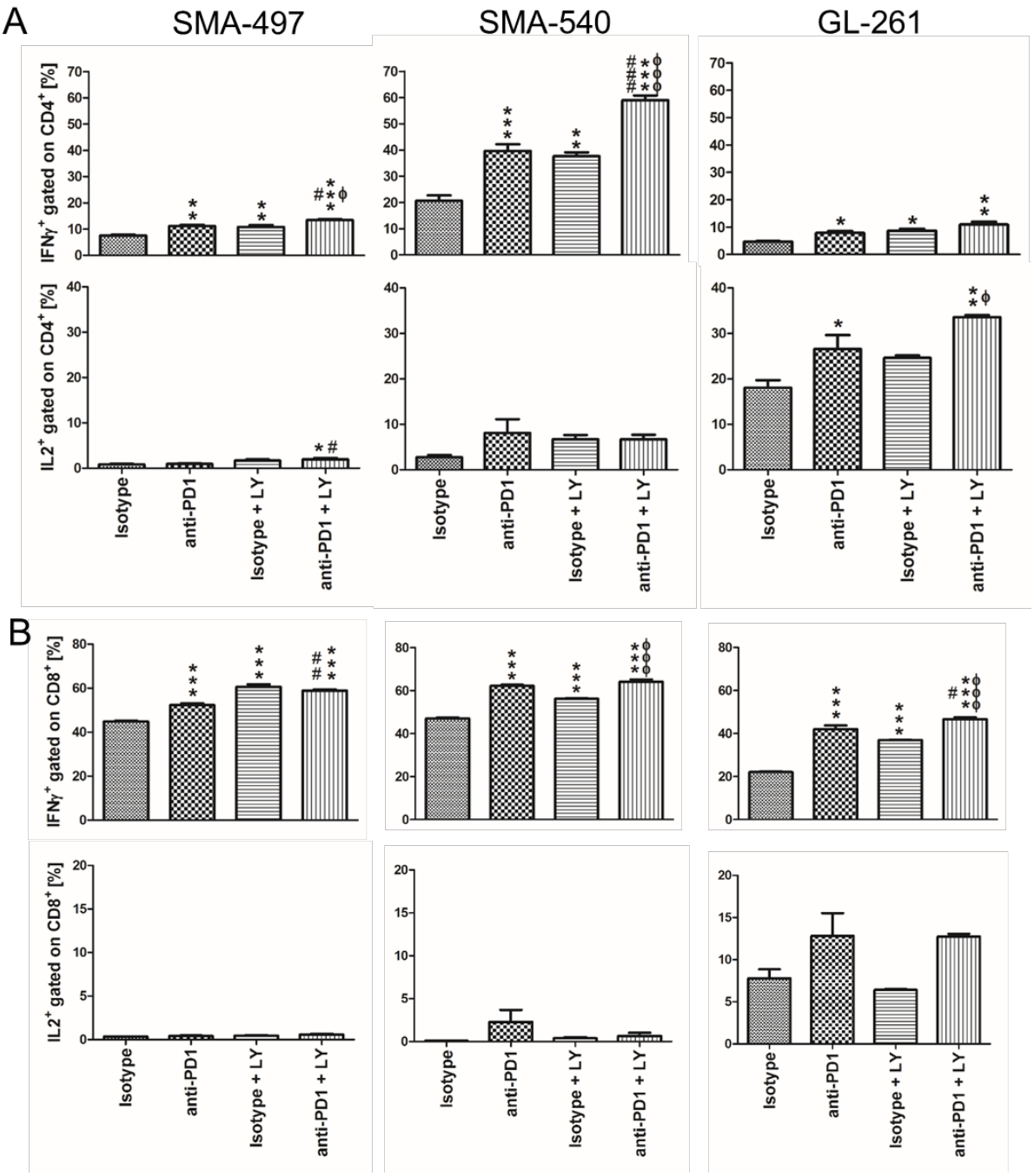

Figure 42. Effects of dual PD-1 and TGF-β pathway blockade on T cell cytokine production. Actively growing $2x10^5$ tumor cells were co-cultured for 4-6 days with 10^6 syngeneic activated lymphocytes (2 µg/mL concanavalin A) in the absence or presence of anti-PD1 (10 µg/ml), TGFβRI inhibitor (LY2157299, 1µM) or a combination thereof. After co-culture, lymphocytes were re-stimulated for 4 h in the presence of ionomycin (500 ng/ml), phorbol-12-myristate-13-acetate (PMA, 50ng/ml) and 1:1000 final concentration of Golgiplug (containing brefeldin A) and Golgistop (containing monensin). Percentage of IFN-γ^+ (top) or IL-2^+ (bottom) cells gated on CD4 (A) or CD8 (B) positive cells after co-culture with the indicated mouse glioma cell line (*P < .05, **P < .01, ***P < 0.001 one-way ANOVA followed by Tukey's post hoc test 95% CI, isotype vs treatment; $^{\#}$P < .05, $^{\#\#}$P < .01, $^{\#\#\#}$P < .001 anti-PD1 vs anti-PD1 + LY; $^{\phi}$P < .05, $^{\phi\phi}$P < .01, $^{\phi\phi\phi}$P < .001, LY vs anti-PD1 + LY).

Effects of dual PD-1 and TGF-β pathway blockade on T cell subsets induction

Using our *in vitro* model system, we further explored whether glioma cells can induce the generation of inhibitory Treg cells. We found in the GL-261 model that around 30% of the $CD4^+$ $CD25^+$ cells expressed the Treg-defining transcription factor FoxP3 (Figure 43A). Conversely, no $CD4^+$ $CD25^+$ $FoxP3^+$ cells were generated during co-culture of SMA-497 and SMA-540 with activated syngeneic lymphocytes. Importantly, Treg cell induction in the GL-261 was dampened by anti-PD1 or anti-TGFβRI, with co-treatment being the most effective (Figure 43A). Furthermore, analysis of T cells after 4-6 days of co-culture with syngeneic tumor cells revealed that anti-PD1 blockade favors either survival or expansion of $CD8^+$ cells compared to $CD4^+$ cells (Figure 43B).

Dual blockade of the PD-1 and TGF-β pathway increases T cell-mediated cytotoxicity against GL-261, but not SMA-497 or SMA-540 cells.

T cells harvested after 4-6 days of co-culture with syngeneic tumor cells were challenged with naïve syngeneic tumor cells in a cell cytotoxicity assay. While T cells isolated from a co-culture with GL-261 cells containing anti-PD1 or anti-TGFβRI alone did not improve killing rates compared to untreated control, combined targeting significantly improved tumor cell lysis (Figure 43C). No differences among the treatment groups were found in the specific lysis of SMA-497 and SMA-540 cells.

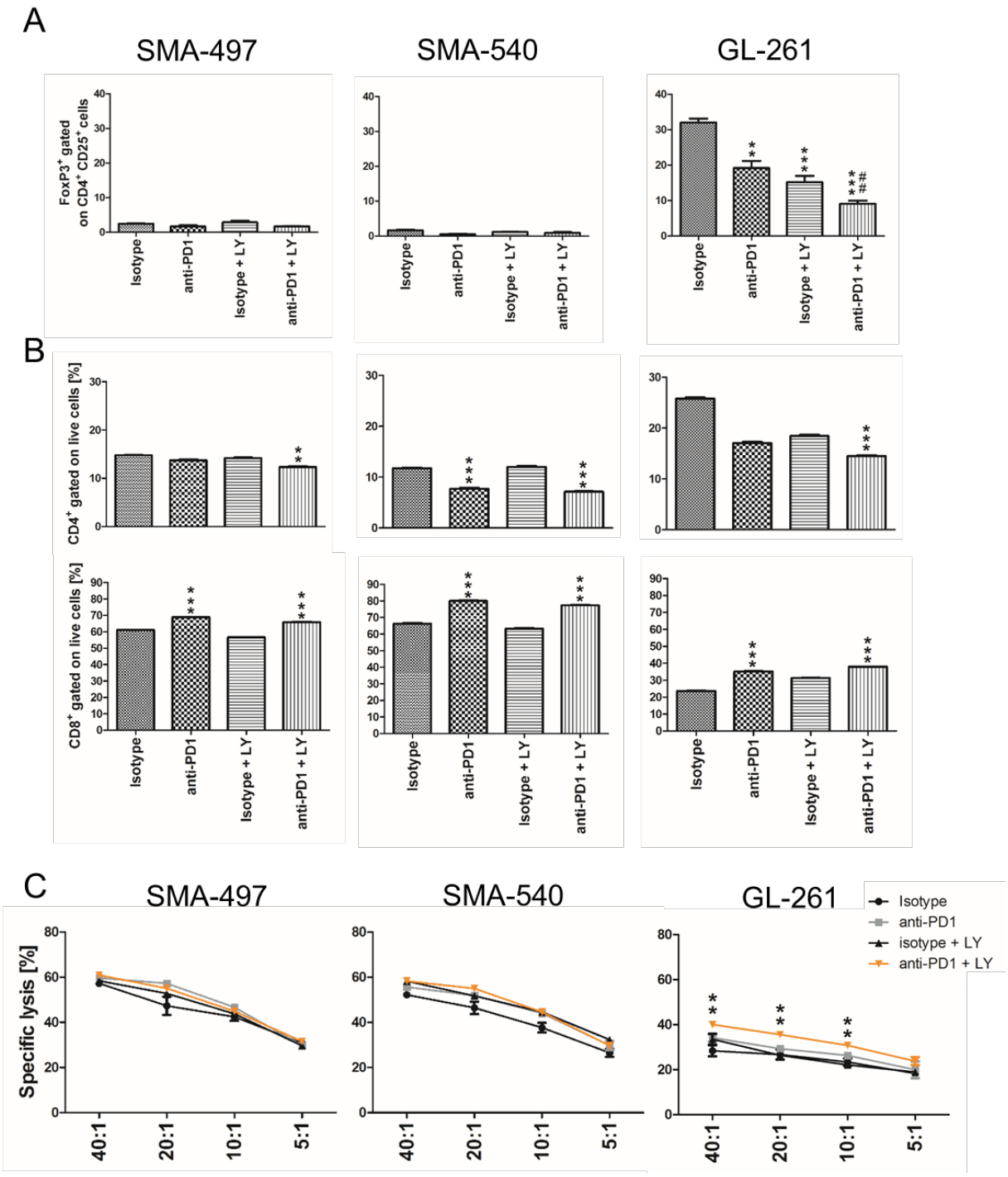

Figure 43. Effects of dual PD-1 and TGF-β pathway blockade on regulatory T cell induction, T cell populations and T cell-mediated cytotoxicity. Actively growing $2x10^5$ tumor cells were co-cultured for 4-6 days with 10^6 syngeneic activated lymphocytes (2 µg/mL concanavalin A) in the absence or presence of anti-PD1 (10 µg/ml), TGFβRI inhibitor (LY2157299, 1 µM) or both. A. Percentage of regulatory T cells defined as $CD4^+$ $CD25^+$ $FoxP3^+$. B. Percentage of $CD4^+$ and $CD8^+$ cells was calculated on the total pool of live cells harvested from the co-culture. C. Lymphocytes isolated after 4-6 days of co-culture were challenged with tumor cells pre-stained with PKH-26 at different effector to target (E:T) ratios as indicated for 4 h. Cell specific lysis is expressed as percentage of dead cells within the PKH-26-positive target cells, corrected for spontaneous background lysis. (**P < .01, ***P < 0.001 one-way ANOVA followed by Tukey's post hoc test 95% CI, isotype vs treatment; $^{\#\#}$P < .01).

7. Discussion

Interactions between human tumors and their specific microenvironment determine growth characteristics and responses to radiotherapy or pharmacotherapy (Hanahan and Weinberg, 2011). This notion is particularly true for glioblastoma, which typically contains major host cell infiltrates that probably support rather than limit tumor growth (Murdoch *et al.*, 2008; Maes *et al.*, 2013; Vom Berg *et al.*, 2013).

In project 1, we focused on two cytokine-dependent signalling pathways attributed a major role in the pathogenesis of glioblastoma, VEGF and TGF-β, using a panel of syngeneic mouse gliomas as model systems (Ahmad *et al.*, 2014).

Responsiveness to VEGF and TGF-β stimulation as assessed by VEGFR and SMAD2 phosphorylation as well as a positive regulation of VEGF by TGF-β, but not vice versa, was confirmed *in vitro* (Figure 11;27-29). Inhibition of neither pathway has prominent effects on glioma cell viability or growth *in vitro* (Figure 16) although growth suppressive properties have been reported for TGF-β_1 in the SMA-560 model (Ashley *et al.*, 1998).

There was differential responsiveness to B20-mediated VEGF inhibition alone. While high expression of VEGF and VEGFR is consistent with responsiveness of SMA-560, the responsiveness of SMA-540 was less well explained, and the expression levels of VEGF in GL-261 did not translate into superior efficacy of B20. The responsiveness of GL-261 despite unaltered proliferation and hypoxia is consistent with direct induction of cell death by VEGF inhibition in some mouse glioma models (Scholz *et al.*, 2015; Pitter *et al.*, 2016). A high constitutive level of hypoxia and failure to reduce blood vessel density in response to B20, consistent with VEGF-independent angiogenesis, were prominent features of the refractory SMA-497 model. Of note, full suppression of angiogenesis was not achieved in any model (Figure 17). Although all SMA lines were derived from one tumor, they exhibited major variation in response to different treatment settings that were tentatively linked to differential transcriptomics specifically among angiogenesis-related gene sets (Figure 21;Tables 2-3).

The TGFβR1 inhibitor LY2157299 was active pharmacodynamically as assessed by a decrease of pSMAD2 levels *in vivo*, although no full suppression was achieved, indicating either insufficient pharmacodynamic properties and target coverage, or ALK-5-independent pathways maintaining pSMAD2 phosphorylation, or both (Figure 23). The two models responsive to LY2157299 *in vivo*, SMA-540 and SMA-560, exhibited increased expression levels of genes of the TGF-β receptor signalling pathway (Figure

25). Similar to anti-angiogenic therapy, also TGF-β antagonism has been linked to vascular normalization and improved drug delivery (Liu *et al.*, 2012). Accordingly, we observed morphological changes related to vascular normalization in tumor vessels upon LY2157299 treatment in all models, consisting of increased vessel wall thickness and decreased vessel diameter (Figure 23). It is tempting to link these uniform changes in blood vessel morphology, induced by LY2157299, to the effects of TGF-β on VEGF and VEGFR expression *in vitro* (Figure 23;28;29). A transcriptional profiling study of human glioblastoma vessels indicated key roles in the process of pathological angiogenesis for *VEGF-A* and *TGF-β_2,* and suggests that TGF-β inhibition may represent a promising option as anti-angiogenic agent (Dieterich *et al.*, 2012). The decrease in pSMAD2 levels in response to hypoxia *in vitro* and to hypoxia in association with B20 treatment *in vivo* in two of three responsive models was surprising (Figure 15;17) since no evidence suggests that the TGF-β pathway is negatively regulated by hypoxia. Interestingly, pSMAD2 levels positively correlated with tumor proliferation assessed by Ki-67 staining in human glioblastoma (Bruna *et al.*, 2007). Accordingly, we also found parallel changes in the levels of both markers as shown by Ki-67 and pSMAD2 stainings upon B20 monotherapy (Figure 17).

VEGFR inhibition *in vitro* did not decrease pSMAD2 levels in any cell line (Figure 27). Yet, the synergistic suppression of pSMAD2 levels by B20 and LY2157299 co-treatment in early-stage tumors may suggest that anti-VEGF therapy leads to a vascular normalization process, thereby improving LY2157299 delivery to the tumor. Importantly, increased pSMAD2 levels in end-stage tumors with B20 treatment alone are consistent with the hypothesis that enhanced TGF-β activity might promote eventual escape from VEGF inhibition at least in the GL-261 model. Immunohistochemical analysis of orthotopic U87MG gliomas had revealed increased TGF-β protein levels upon anti-VEGF treatment, too (Piao *et al.*, 2012a).

Increased levels of CD11b-positive macrophages/microglia have been linked to refractoriness to anti-VEGF treatment (Shojaei *et al.*, 2007) and attributed a role in the VEGF-independent restoration of tumor vessels by vasculogenic, but not angiogenic processes (Kioi *et al.*, 2010). Supporting this concept, we observed that co-targeting VEGF and TGFβR1 decreased the numbers of intratumoral $CD11b^+$ cells and that tumors failed to re-vascularize compared to B20 alone in GL-261 end-stage tumors (Figure 36). Similarly, co-inhibition of VEGF and the Ang-2 pathway provided improved tumor control and reduced numbers of F4/80-positive macrophages in the GL-261

model (Scholz *et al.*, 2015). Possibly, targeting TGF-β alters $CD11b^+$ cell recruitment via interacting with the CXCR4/C-X-C motif chemokine ligand (CXCL)12 axis since VEGFR inhibitors can up-regulate the chemokine CXCR4 in glioblastoma cells by a TGF-β-dependent mechanism (Pham *et al.*, 2015) and since TGF-β up-regulates CXCR4 expression in monocytes, macrophages, T naïve cells and other immune cell populations (Wang *et al.*, 2001; Franitza *et al.*, 2002).

Altogether, according to our analysis in the GL-261 model, the tumor-promoting role of TGF-β would relate more to facilitating angiogenesis or vasculogenesis than to promote a more invasive phenotype even when combined with VEGF antagonists. This is because B20-treated tumors were more invasive early on when pSMAD2 levels were still low and because co-treatment with LY2157299 still suppressed tumor vasculature in end-stage disease (Figure 17;31). Yet, B20-induced hypoxia may ultimately promote lactate dehydrogenase activity (Fack *et al.*, 2015b) which in turn may stimulate TGF-β signalling associated with an angiogenic signalling (Baumann *et al.*, 2009).

Unexpectedly, we observed that mainly tumor cells but not leukocytes exhibited phosphorylated SMAD2 (Figure 37). Previous studies have already indicated that pSMAD2 levels are high in glioblastoma cells, indicating that tumor cells do not have to escape TGF-β signalling at least at the level of SMAD2 phosphorylation (Bruna *et al.*, 2007; Frei *et al.*, 2015). However, pSMAD2 levels in B20-treated GL-261 end-stage tumors increased proportionally in tumor cells and leukocytes. Since the activation of TGF-β signalling in tumors has been linked to immunosuppression (Rich, 2003), increased pSMAD2 levels indicate a TGF-β-induced immunosuppressive tumor micro-milieu during anti-VEGF treatment which might be an important factor of therapy failure. Yet, preliminary studies in paired human glioblastoma samples provided no evidence for enhanced pSMAD2 levels at recurrence, either without or with previous bevacizumab therapy (Figure 38;39). Nevertheless, this finding on human samples has to be viewed with caution, as sample size is small. Moreover, recurrent glioblastoma samples analysed in this small cohort may not necessarily represent the most aggressive tumors, since patients bearing such tumors are rarely re-operated, and thus biopsies are lacking.

Limitations of the project 1 include the challenges in determining volumes of infiltrative rodent gliomas, the restriction to mouse models based on long-term cell lines, and the exploration of co-treatment rather than sequential treatments. Moreover, we did not distinguish B20 or LY2157299 effects on tumor versus host cells and effects of B20 on

VEGFR1 versus VEGFR2 signaling in mouse glioma cells, and the human patient cohort was small.

This study highlights the relevance of hypoxia in the malignant phenotype of glioblastoma and its resistance to therapy. SMA-497 showed the highest constitutive level of hypoxia and was refractory to all therapeutic interventions. GL-261 eventually became hypoxic when escaping combination therapy (Figure 33). We conclude in project 1 that at least for subsets of glioblastomas, co-targeting of VEGF and TGF-β pathways might result in a permanent vascularization deficiency, which results in prolonged tumor control. Ultimately, however, such microenvironment-targeting therapies may only be successful if combined with pharmacological or cell-based therapies that exert relevant tumor cell cytotoxicity, since the major cell biological changes observed in selected models did not translate into major gains in survival.

Findings of project 1 laid the basis to explore a new therapeutic approach in project 2. Recently, so far unseen responses achieved by immune checkpoint blockades in several therapy-refractory tumors, such as non-small cell lung cancer and metastatic melanoma, prompted the investigation of these agents also in glioblastoma (Preusser *et al.*, 2015; Weiss *et al.*, 2015). The clinical efficacy of these agents in glioblastoma is still undetermined, however, experience accumulated in other tumor entities has shown that a significant percentage of patients either never responds or develops refractory tumors. In this regard, substantial work has shown that immune checkpoint blockade efficacy can be improved by targeting of redundant immunosuppressive pathways (Wainwright *et al.*, 2014; Twyman-Saint Victor *et al.*, 2015; Hodi *et al.*, 2016). As already mentioned, the TGF-β pathway has been attributed a central role in orchestrating the immunosuppressive phenotype of glioblastoma (see above). Therefore, we sought to determine whether inhibition of this pathway may improve the efficacy of PD-1 blockade in experimental glioma models. We confirmed the expression of PD-1 ligands by mouse glioma cell lines. PD-L1 was present on the surface of all cell lines, whereas this was not the case for PD-L2 (Figure 40). TGF-β signalling regulated neither basal levels nor induced ligand expression (Figure 40). Dual targeting of the PD-1 and TGF-β pathways elicited T cell responses associated with improved anti-tumor activity in co-culture models. Indeed, $CD4^+$ and $CD8^+$ T cells exhibited increased IFN-γ production during dual blockade compared to controls and either mono-treatment alone in all tested cell lines (Figure 42). IL-2 production was

also increased, yet to a lesser extent (Figure 42). Regulatory T cells are a key cellular components of the glioblastoma micro-environment (section 3.4.2.1). *In vitro*, this cell population was generated only in GL-261-based co-cultures and co-treatment with anti-PD1 and anti-TGFβRI significantly decreased its percentage (Figure 43A). This may be the consequence of the crucial role played by TGF-β in eliciting FoxP3 expression of naïve $CD4^+$ cells and differentiation in regulatory T cells, and the ability of anti-PD1 antibodies to favour T cell-mediated effector responses (Chen *et al.*, 2003; Fu *et al.*, 2004; Pardoll, 2012). Also, treatment with anti-PD1 exerted a population shift favouring the arising of a $CD8^+$ population over $CD4^+$ cells (Figure 43B).

As shown by several reports, T cell-mediated cytotoxicity of tumor cells represents the fundamental last step of anti-tumor immunity (Dunn *et al.*, 2012). We found that combined inhibition of the PD-1 and TGF-β pathway increased lysis of GL-261 cells, but not in other models (Figure 43C). Intriguingly, this model was the only one where regulatory T cells were present and significantly decreased following targeting of PD-1 and TGF-β signalling. It can be speculated that the reduced presence of regulatory T cells in the co-culture system allows for more powerful T cell effector functions against syngeneic tumor cells. Altogether, our findings prompt further investigations of dual PD-1 and TGF-β pathway blockade *in vivo* and these studies are currently ongoing in our laboratory.

8. Bibliography

Abbott NJ, Patabendige AA, Dolman DE, Yusof SR, Begley DJ. Structure and function of the blood-brain barrier. Neurobiol Dis 2010; 37(1): 13-25.

Abbott NJ, Ronnback L, Hansson E. Astrocyte-endothelial interactions at the blood-brain barrier. Nat Rev Neurosci 2006; 7(1): 41-53.

Agarwal S, Manchanda P, Vogelbaum MA, Ohlfest JR, Elmquist WF. Function of the blood-brain barrier and restriction of drug delivery to invasive glioma cells: findings in an orthotopic rat xenograft model of glioma. Drug Metab Dispos 2013; 41(1): 33-9.

Aghi M, Cohen KS, Klein RJ, Scadden DT, Chiocca EA. Tumor stromal-derived factor-1 recruits vascular progenitors to mitotic neovasculature, where microenvironment influences their differentiated phenotypes. Cancer Res 2006; 66(18): 9054-64.

Ahmad M, Frei K, Willscher E, Stefanski A, Kaulich K, Roth P*, et al.* How Stemlike Are Sphere Cultures From Long-term Cancer Cell Lines? Lessons From Mouse Glioma Models. J Neuropath Exp Neur 2014; 73(11): 1062-77.

Akhurst RJ, Hata A. Targeting the TGFbeta signalling pathway in disease. Nat Rev Drug Discov 2012; 11(10): 790-811.

Alvarez JI, Katayama T, Prat A. Glial influence on the blood brain barrier. Glia 2013; 61(12): 1939-58.

Anido J, Saez-Borderias A, Gonzalez-Junca A, Rodon L, Folch G, Carmona MA*, et al.* TGF-beta Receptor Inhibitors Target the CD44(high)/Id1(high) Glioma-Initiating Cell Population in Human Glioblastoma. Cancer Cell 2010; 18(6): 655-68.

Arpaia N, Green JA, Moltedo B, Arvey A, Hemmers S, Yuan SP*, et al.* A Distinct Function of Regulatory T Cells in Tissue Protection. Cell 2015; 162(5): 1078-89.

Ashley DM, Sampson JH, Archer GE, Hale LP, Bigner DD. Local production of TGF beta1 inhibits cerebral edema, enhances TNF-alpha induced apoptosis and improves survival in a murine glioma model. Journal of neuroimmunology 1998; 86(1): 46-52.

Aspelund A, Antila S, Proulx ST, Karlsen TV, Karaman S, Detmar M*, et al.* A dural lymphatic vascular system that drains brain interstitial fluid and macromolecules. J Exp Med 2015; 212(7): 991-9.

Azuma T, Yao S, Zhu G, Flies AS, Flies SJ, Chen L. B7-H1 is a ubiquitous antiapoptotic receptor on cancer cells. Blood 2008; 111(7): 3635-43.

Badie B, Schartner JM. Flow cytometric characterization of tumor-associated macrophages in experimental gliomas. Neurosurgery 2000; 46(4): 957-61; discussion 61-2.

Bao S, Wu Q, Sathornsumetee S, Hao Y, Li Z, Hjelmeland AB*, et al.* Stem cell-like glioma cells promote tumor angiogenesis through vascular endothelial growth factor. Cancer Res 2006; 66(16): 7843-8.

Batchelor TT, Gerstner ER, Emblem KE, Duda DG, Kalpathy-Cramer J, Snuderl M*, et al.* Improved tumor oxygenation and survival in glioblastoma patients who show increased blood perfusion after cediranib and chemoradiation. Proc Natl Acad Sci U S A 2013; 110(47): 19059-64.

Batchelor TT, Reardon DA, de Groot JF, Wick W, Weller M. Antiangiogenic therapy for glioblastoma: current status and future prospects. Clin Cancer Res 2014; 20(22): 5612-9.

Batchelor TT, Sorensen AG, di Tomaso E, Zhang WT, Duda DG, Cohen KS*, et al.* AZD2171, a pan-VEGF receptor tyrosine kinase inhibitor, normalizes tumor vasculature and alleviates edema in glioblastoma patients. Cancer Cell 2007; 11(1): 83-95.

Baumann F, Leukel P, Doerfelt A, Beier CP, Dettmer K, Oefner PJ*, et al.* Lactate promotes glioma migration by TGF-beta2-dependent regulation of matrix metalloproteinase-2. Neuro-oncology 2009; 11(4): 368-80.

Becker CM, Oberoi RK, McFarren SJ, Muldoon DM, Pafundi DH, Pokorny JL*, et al.* Decreased affinity for efflux transporters increases brain penetrance and molecular targeting of a PI3K/mTOR inhibitor in a mouse model of glioblastoma. Neuro Oncol 2015; 17(9): 1210-9.

Beier D, Rohrl S, Pillai DR, Schwarz S, Kunz-Schughart LA, Leukel P*, et al.* Temozolomide preferentially depletes cancer stem cells in glioblastoma. Cancer Res 2008; 68(14): 5706-15.

Bergers G, Hanahan D. Modes of resistance to anti-angiogenic therapy. Nat Rev Cancer 2008; 8(8): 592-603.

Berghoff AS, Kiesel B, Widhalm G, Rajky O, Ricken G, Wohrer A*, et al.* Programmed death ligand 1 expression and tumor-infiltrating lymphocytes in glioblastoma. Neuro Oncol 2015; 17(8): 1064-75.

Bernabeu C, Lopez-Novoa JM, Quintanilla M. The emerging role of TGF-beta superfamily coreceptors in cancer. Biochim Biophys Acta 2009; 1792(10): 954-73.

Binder H, Krohn K, Preibisch S. "Hook"-calibration of GeneChip-microarrays: Chip characteristics and expression measures. Algorithm Mol Biol 2008; 3.

Binder H, Preibisch S. "Hook"-calibration of GeneChip-microarrays: Theory and algorithm. Algorithm Mol Biol 2008; 3.

Binello E, Germano IM. Targeting glioma stem cells: a novel framework for brain tumors. Cancer Sci 2011; 102(11): 1958-66.

Bloch O, Crane CA, Kaur R, Safaee M, Rutkowski MJ, Parsa AT. Gliomas promote immunosuppression through induction of B7-H1 expression in tumor-associated macrophages. Clin Cancer Res 2013; 19(12): 3165-75.

Bogler O, Huang HJ, Kleihues P, Cavenee WK. The p53 gene and its role in human brain tumors. Glia 1995; 15(3): 308-27.

Brandes AA, Carpentier AF, Kesari S, Sepulveda-Sanchez JM, Wheeler HR, Chinot O*, et al.* A Phase II randomized study of galunisertib monotherapy or galunisertib plus lomustine compared with lomustine monotherapy in patients with recurrent glioblastoma. Neuro Oncol 2016; 18(8): 1146-56.

Bruna A, Darken RS, Rojo F, Ocana A, Penuelas S, Arias A*, et al.* High TGFbeta-Smad activity confers poor prognosis in glioma patients and promotes cell proliferation depending on the methylation of the PDGF-B gene. Cancer Cell 2007; 11(2): 147-60.

Bulnes S, Bengoetxea H, Ortuzar N, Argandona EG, Garcia-Blanco A, Rico-Barrio I*, et al.* Angiogenic signalling pathways altered in gliomas: selection mechanisms for more aggressive neoplastic subpopulations with invasive phenotype. J Signal Transduct 2012; 2012: 597915.

Calabrese C, Poppleton H, Kocak M, Hogg TL, Fuller C, Hamner B*, et al.* A perivascular niche for brain tumor stem cells. Cancer Cell 2007; 11(1): 69-82.

Calzascia T, Masson F, Di Berardino-Besson W, Contassot E, Wilmotte R, Aurrand-Lions M*, et al.* Homing phenotypes of tumor-specific CD8 T cells are predetermined at the tumor site by crosspresenting APCs. Immunity 2005; 22(2): 175-84.

Cancer Genome Atlas Research N. Comprehensive genomic characterization defines human glioblastoma genes and core pathways. Nature 2008; 455(7216): 1061-8.

Carmeliet P, Ferreira V, Breier G, Pollefeyt S, Kieckens L, Gertsenstein M*, et al.* Abnormal blood vessel development and lethality in embryos lacking a single VEGF allele. Nature 1996; 380(6573): 435-9.

Carmeliet P, Jain RK. Angiogenesis in cancer and other diseases. Nature 2000; 407(6801): 249-57.

Carmeliet P, Jain RK. Molecular mechanisms and clinical applications of angiogenesis. Nature 2011; 473(7347): 298-307.

Catena R, Larzabal L, Larrayoz M, Molina E, Hermida J, Agorreta J*, et al.* VEGF(1)(2)(1)b and VEGF(1)(6)(5)b are weakly angiogenic isoforms of VEGF-A. Mol Cancer 2010; 9: 320.

Chae SS, Kamoun WS, Farrar CT, Kirkpatrick ND, Niemeyer E, de Graaf AMA*, et al.* Angiopoietin-2 Interferes with Anti-VEGFR2-Induced Vessel Normalization and Survival Benefit in Mice Bearing Gliomas. Clin Cancer Res 2010; 16(14): 3618-27.

Chang CH, Qiu J, O'Sullivan D, Buck MD, Noguchi T, Curtis JD*, et al.* Metabolic Competition in the Tumor Microenvironment Is a Driver of Cancer Progression. Cell 2015; 162(6): 1229-41.

Chemnitz JM, Parry RV, Nichols KE, June CH, Riley JL. SHP-1 and SHP-2 associate with immunoreceptor tyrosine-based switch motif of programmed death 1 upon primary human T cell stimulation, but only receptor ligation prevents T cell activation. J Immunol 2004; 173(2): 945-54.

Chen W, Jin W, Hardegen N, Lei KJ, Li L, Marinos N*, et al.* Conversion of peripheral CD4+CD25- naive T cells to CD4+CD25+ regulatory T cells by TGF-beta induction of transcription factor Foxp3. J Exp Med 2003; 198(12): 1875-86.

Cheng L, Huang Z, Zhou W, Wu Q, Donnola S, Liu JK*, et al.* Glioblastoma stem cells generate vascular pericytes to support vessel function and tumor growth. Cell 2013; 153(1): 139-52.

Chinot OL, Wick W, Mason W, Henriksson R, Saran F, Nishikawa R*, et al.* Bevacizumab plus radiotherapy-temozolomide for newly diagnosed glioblastoma. N Engl J Med 2014; 370(8): 709-22.

Claudio L. Ultrastructural features of the blood-brain barrier in biopsy tissue from Alzheimer's disease patients. Acta Neuropathol 1996; 91(1): 6-14.

Coniglio SJ, Eugenin E, Dobrenis K, Stanley ER, West BL, Symons MH*, et al.* Microglial stimulation of glioblastoma invasion involves epidermal growth factor receptor (EGFR) and colony stimulating factor 1 receptor (CSF-1R) signaling. Mol Med 2012; 18: 519-27.

Corzo CA, Condamine T, Lu L, Cotter MJ, Youn JI, Cheng P*, et al.* HIF-1alpha regulates function and differentiation of myeloid-derived suppressor cells in the tumor microenvironment. J Exp Med 2010; 207(11): 2439-53.

Coulie PG, Van den Eynde BJ, van der Bruggen P, Boon T. Tumour antigens recognized by T lymphocytes: at the core of cancer immunotherapy. Nat Rev Cancer 2014; 14(2): 135-46.

Daneman R, Zhou L, Kebede AA, Barres BA. Pericytes are required for blood-brain barrier integrity during embryogenesis. Nature 2010; 468(7323): 562-6.

Demeule M, Regina A, Jodoin J, Laplante A, Dagenais C, Berthelet F*, et al.* Drug transport to the brain: key roles for the efflux pump P-glycoprotein in the blood-brain barrier. Vascul Pharmacol 2002; 38(6): 339-48.

Dickson MC, Martin JS, Cousins FM, Kulkarni AB, Karlsson S, Akhurst RJ. Defective haematopoiesis and vasculogenesis in transforming growth factor-beta 1 knock out mice. Development 1995; 121(6): 1845-54.

Dieterich LC, Mellberg S, Langenkamp E, Zhang L, Zieba A, Salomaki H*, et al.* Transcriptional profiling of human glioblastoma vessels indicates a key role of VEGF-A and TGFbeta2 in vascular abnormalization. J Pathol 2012; 228(3): 378-90.

Donson AM, Birks DK, Schittone SA, Kleinschmidt-DeMasters BK, Sun DY, Hemenway MF*, et al.* Increased immune gene expression and immune cell infiltration in high-grade astrocytoma distinguish long-term from short-term survivors. J Immunol 2012; 189(4): 1920-7.

Du R, Lu KV, Petritsch C, Liu P, Ganss R, Passegue E*, et al.* HIF1alpha induces the recruitment of bone marrow-derived vascular modulatory cells to regulate tumor angiogenesis and invasion. Cancer Cell 2008a; 13(3): 206-20.

Du R, Petritsch C, Lu K, Liu P, Haller A, Ganss R*, et al.* Matrix metalloproteinase-2 regulates vascular patterning and growth affecting tumor cell survival and invasion in GBM. Neuro Oncol 2008b; 10(3): 254-64.

Dunn GP, Fecci PE, Curry WT. Cancer immunoediting in malignant glioma. Neurosurgery 2012; 71(2): 201-22; discussion 22-3.

Dunn GP, Old LJ, Schreiber RD. The three Es of cancer immunoediting. Annu Rev Immunol 2004; 22: 329-60.

Eisele G, Wischhusen J, Mittelbronn M, Meyermann R, Waldhauer I, Steinle A*, et al.* TGF-beta and metalloproteinases differentially suppress NKG2D ligand surface expression on malignant glioma cells. Brain 2006; 129(Pt 9): 2416-25.

Ekstrand AJ, James CD, Cavenee WK, Seliger B, Pettersson RF, Collins VP. Genes for epidermal growth factor receptor, transforming growth factor alpha, and epidermal growth factor and their expression in human gliomas in vivo. Cancer Res 1991; 51(8): 2164-72.

Ekstrand AJ, Sugawa N, James CD, Collins VP. Amplified and rearranged epidermal growth factor receptor genes in human glioblastomas reveal deletions of sequences encoding portions of the N- and/or C-terminal tails. Proc Natl Acad Sci U S A 1992; 89(10): 4309-13.

El Andaloussi A, Lesniak MS. CD4(+)CD25(+)FoxP3(+) T-cell infiltration and heme oxygenase-1 expression correlate with tumor grade in human gliomas. J Neuro-Oncol 2007; 83(2): 145-52.

Fack F, Espedal H, Keunen O, Golebiewska A, Obad N, Harter PN*, et al.* Bevacizumab treatment induces metabolic adaptation toward anaerobic metabolism in glioblastomas. Acta Neuropathologica 2015a; 129(1): 115-31.

Fack F, Espedal H, Keunen O, Golebiewska A, Obad N, Harter PN*, et al.* Bevacizumab treatment induces metabolic adaptation toward anaerobic metabolism in glioblastomas. Acta Neuropathol 2015b; 129(1): 115-31.

Fecci PE, Sweeney AE, Grossi PM, Nair SK, Learn CA, Mitchell DA*, et al.* Systemic anti-CD25 monoclonal antibody administration safely enhances immunity in murine glioma without eliminating regulatory T cells. Clin Cancer Res 2006; 12(14): 4294-305.

Feldkamp MM, Lau N, Rak J, Kerbel RS, Guha A. Normoxic and hypoxic regulation of vascular endothelial growth factor (VEGF) by astrocytoma cells is mediated by Ras. Int J Cancer 1999; 81(1): 118-24.

Ferrara N, Carver-Moore K, Chen H, Dowd M, Lu L, O'Shea KS*, et al.* Heterozygous embryonic lethality induced by targeted inactivation of the VEGF gene. Nature 1996; 380(6573): 439-42.

Fong GH, Rossant J, Gertsenstein M, Breitman ML. Role of the Flt-1 receptor tyrosine kinase in regulating the assembly of vascular endothelium. Nature 1995; 376(6535): 66-70.

Forstreuter F, Lucius R, Mentlein R. Vascular endothelial growth factor induces chemotaxis and proliferation of microglial cells. J Neuroimmunol 2002; 132(1-2): 93-8.

Franceschini A, Szklarczyk D, Frankild S, Kuhn M, Simonovic M, Roth A*, et al.* STRING v9.1: protein-protein interaction networks, with increased coverage and integration. Nucleic Acids Res 2013; 41(D1): D808-D15.

Franitza S, Kollet O, Brill A, Vaday GG, Petit I, Lapidot T*, et al.* TGF-beta1 enhances SDF-1alpha-induced chemotaxis and homing of naive T cells by up-regulating CXCR4 expression and downstream cytoskeletal effector molecules. European journal of immunology 2002; 32(1): 193-202.

Frei K, Gramatzki D, Tritschler I, Schroeder JJ, Espinoza L, Rushing EJ*, et al.* Transforming growth factor-beta pathway activity in glioblastoma. Oncotarget 2015; 6(8): 5963-77.

Fridlender ZG, Albelda SM. Tumor-associated neutrophils: friend or foe? Carcinogenesis 2012; 33(5): 949-55.

Friese MA, Wischhusen J, Wick W, Weiler M, Eisele G, Steinle A*, et al.* RNA interference targeting transforming growth factor-beta enhances NKG2D-mediated antiglioma immune response, inhibits glioma cell migration and invasiveness, and abrogates tumorigenicity in vivo. Cancer Res 2004; 64(20): 7596-603.

Fu S, Zhang N, Yopp AC, Chen D, Mao M, Chen D*, et al.* TGF-beta induces Foxp3 + T-regulatory cells from CD4 + CD25 - precursors. Am J Transplant 2004; 4(10): 1614-27.

Fukuda S, Kato F, Tozuka Y, Yamaguchi M, Miyamoto Y, Hisatsune T. Two distinct subpopulations of nestin-positive cells in adult mouse dentate gyrus. J Neurosci 2003; 23(28): 9357-66.

Furnari FB, Huang HJ, Cavenee WK. The phosphoinositol phosphatase activity of PTEN mediates a serum-sensitive G1 growth arrest in glioma cells. Cancer Res 1998; 58(22): 5002-8.

Gabrilovich DI, Chen HL, Girgis KR, Cunningham HT, Meny GM, Nadaf S*, et al.* Production of vascular endothelial growth factor by human tumors inhibits the functional maturation of dendritic cells. Nat Med 1996; 2(10): 1096-103.

Gage FH. Mammalian neural stem cells. Science 2000; 287(5457): 1433-8.

Gerstner ER, Duda DG, di Tomaso E, Ryg PA, Loeffler JS, Sorensen AG*, et al.* VEGF inhibitors in the treatment of cerebral edema in patients with brain cancer. Nat Rev Clin Oncol 2009; 6(4): 229-36.

Gilbert MR, Dignam JJ, Armstrong TS, Wefel JS, Blumenthal DT, Vogelbaum MA*, et al.* A randomized trial of bevacizumab for newly diagnosed glioblastoma. N Engl J Med 2014; 370(8): 699-708.

Gilbertson RJ, Rich JN. Making a tumour's bed: glioblastoma stem cells and the vascular niche. Nat Rev Cancer 2007; 7(10): 733-6.

Gong D, Shi W, Yi SJ, Chen H, Groffen J, Heisterkamp N. TGFbeta signaling plays a critical role in promoting alternative macrophage activation. BMC Immunol 2012; 13: 31.

Gorski DH, Beckett MA, Jaskowiak NT, Calvin DP, Mauceri HJ, Salloum RM*, et al.* Blockage of the vascular endothelial growth factor stress response increases the antitumor effects of ionizing radiation. Cancer Res 1999; 59(14): 3374-8.

Grandal MV, Zandi R, Pedersen MW, Willumsen BM, van Deurs B, Poulsen HS. EGFRvIII escapes down-regulation due to impaired internalization and sorting to lysosomes. Carcinogenesis 2007; 28(7): 1408-17.

Haas-Kogan D, Shalev N, Wong M, Mills G, Yount G, Stokoe D. Protein kinase B (PKB/Akt) activity is elevated in glioblastoma cells due to mutation of the tumor suppressor PTEN/MMAC. Curr Biol 1998; 8(21): 1195-8.

Hamerlik P, Lathia JD, Rasmussen R, Wu Q, Bartkova J, Lee M*, et al.* Autocrine VEGF-VEGFR2-Neuropilin-1 signaling promotes glioma stem-like cell viability and tumor growth. J Exp Med 2012; 209(3): 507-20.

Han S, Zhang C, Li Q, Dong J, Liu Y, Huang Y*, et al.* Tumour-infiltrating CD4(+) and CD8(+) lymphocytes as predictors of clinical outcome in glioma. Brit J Cancer 2014; 110(10): 2560-8.

Hanahan D, Weinberg RA. Hallmarks of cancer: the next generation. Cell 2011; 144(5): 646-74.

Happold C, Roth P, Silginer M, Florea AM, Lamszus K, Frei K*, et al.* Interferon-beta induces loss of spherogenicity and overcomes therapy resistance of glioblastoma stem cells. Mol Cancer Ther 2014; 13(4): 948-61.

Hardee ME, Marciscano AE, Medina-Ramirez CM, Zagzag D, Narayana A, Lonning SM*, et al.* Resistance of glioblastoma-initiating cells to radiation mediated by the tumor microenvironment can be abolished by inhibiting transforming growth factor-beta. Cancer Res 2012; 72(16): 4119-29.

Harper SJ, Bates DO. VEGF-A splicing: the key to anti-angiogenic therapeutics? Nat Rev Cancer 2008; 8(11): 880-7.

Hau P, Jachimczak P, Schlaier J, Bogdahn U. TGF-beta2 signaling in high-grade gliomas. Curr Pharm Biotechnol 2011; 12(12): 2150-7.

Heiland DH, Haaker G, Delev D, Mercas B, Masalha W, Heynckes S*, et al.* Comprehensive analysis of PD-L1 expression in glioblastoma multiforme. Oncotarget 2017; [Epub ahead of print].

Heimberger AB, Abou-Ghazal M, Reina-Ortiz C, Yang DS, Sun W, Qiao W*, et al.* Incidence and prognostic impact of FoxP3(+) regulatory T cells in human gliomas. Clin Cancer Res 2008; 14(16): 5166-72.

Hickey WF, Hsu BL, Kimura H. T-lymphocyte entry into the central nervous system. J Neurosci Res 1991; 28(2): 254-60.

Hlobilkova A, Ehrmann J, Knizetova P, Krejci V, Kalita O, Kolar Z. Analysis of VEGF, Flt-1, Flk-1, nestin and MMP-9 in relation to astrocytoma pathogenesis and progression. Neoplasma 2009; 56(4): 284-90.

Hobbs SK, Monsky WL, Yuan F, Roberts WG, Griffith L, Torchilin VP*, et al.* Regulation of transport pathways in tumor vessels: role of tumor type and microenvironment. Proc Natl Acad Sci U S A 1998; 95(8): 4607-12.

Hodi FS, Chesney J, Pavlick AC, Robert C, Grossmann KF, McDermott DF*, et al.* Combined nivolumab and ipilimumab versus ipilimumab alone in patients with advanced melanoma: 2-year overall survival outcomes in a multicentre, randomised, controlled, phase 2 trial. Lancet Oncology 2016; 17(11): 1558-68.

Holash J, Maisonpierre PC, Compton D, Boland P, Alexander CR, Zagzag D*, et al.* Vessel cooption, regression, and growth in tumors mediated by angiopoietins and VEGF. Science 1999; 284(5422): 1994-8.

Hu YL, DeLay M, Jahangiri A, Molinaro AM, Rose SD, Carbonell WS*, et al.* Hypoxia-Induced Autophagy Promotes Tumor Cell Survival and Adaptation to Antiangiogenic Treatment in Glioblastoma. Cancer Research 2012; 72(7): 1773-83.

Huang PH, Xu AM, White FM. Oncogenic EGFR signaling networks in glioma. Sci Signal 2009; 2(87): re6.

Ichimura K, Bolin MB, Goike HM, Schmidt EE, Moshref A, Collins VP. Deregulation of the p14ARF/MDM2/p53 pathway is a prerequisite for human astrocytic gliomas with G1-S transition control gene abnormalities. Cancer Res 2000; 60(2): 417-24.

Ignatova TN, Kukekov VG, Laywell ED, Suslov ON, Vrionis FD, Steindler DA. Human cortical glial tumors contain neural stem-like cells expressing astroglial and neuronal markers in vitro. Glia 2002; 39(3): 193-206.

Ikushima H, Todo T, Ino Y, Takahashi M, Miyazawa K, Miyazono K. Autocrine TGF-beta signaling maintains tumorigenicity of glioma-initiating cells through Sry-related HMG-box factors. Cell Stem Cell 2009; 5(5): 504-14.

Irizarry RA, Hobbs B, Collin F, Beazer-Barclay YD, Antonellis KJ, Scherf U*, et al.* Exploration, normalization, and summaries of high density oligonucleotide array probe level data. Biostatistics 2003; 4(2): 249-64.

Ishida Y, Agata Y, Shibahara K, Honjo T. Induced expression of PD-1, a novel member of the immunoglobulin gene superfamily, upon programmed cell death. EMBO J 1992; 11(11): 3887-95.

Ishihara H, Kubota H, Lindberg RL, Leppert D, Gloor SM, Errede M*, et al.* Endothelial cell barrier impairment induced by glioblastomas and transforming growth factor beta2 involves matrix metalloproteinases and tight junction proteins. J Neuropathol Exp Neurol 2008; 67(5): 435-48.

Jacobs JF, Idema AJ, Bol KF, Grotenhuis JA, de Vries IJ, Wesseling P*, et al.* Prognostic significance and mechanism of Treg infiltration in human brain tumors. J Neuroimmunol 2010; 225(1-2): 195-9.

Jacobs JF, Idema AJ, Bol KF, Nierkens S, Grauer OM, Wesseling P*, et al.* Regulatory T cells and the PD-L1/PD-1 pathway mediate immune suppression in malignant human brain tumors. Neuro Oncol 2009; 11(4): 394-402.

Jain RK. Barriers to drug delivery in solid tumors. Sci Am 1994; 271(1): 58-65.

Jain RK. Normalization of tumor vasculature: an emerging concept in antiangiogenic therapy. Science 2005; 307(5706): 58-62.

Jain RK, di Tomaso E, Duda DG, Loeffler JS, Sorensen AG, Batchelor TT. Angiogenesis in brain tumours. Nat Rev Neurosci 2007a; 8(8): 610-22.

Jain RK, Tong RT, Munn LL. Effect of vascular normalization by antiangiogenic therapy on interstitial hypertension, peritumor edema, and lymphatic metastasis: insights from a mathematical model. Cancer Res 2007b; 67(6): 2729-35.

Jia W, Jackson-Cook C, Graf MR. Tumor-infiltrating, myeloid-derived suppressor cells inhibit T cell activity by nitric oxide production in an intracranial rat glioma + vaccination model. J Neuroimmunol 2010; 223(1-2): 20-30.

Johnson DW, Berg JN, Baldwin MA, Gallione CJ, Marondel I, Yoon SJ*, et al.* Mutations in the activin receptor-like kinase 1 gene in hereditary haemorrhagic telangiectasia type 2. Nat Genet 1996; 13(2): 189-95.

Juliano RL, Ling V. A surface glycoprotein modulating drug permeability in Chinese hamster ovary cell mutants. Biochim Biophys Acta 1976; 455(1): 152-62.

Kaplan DH, Shankaran V, Dighe AS, Stockert E, Aguet M, Old LJ*, et al.* Demonstration of an interferon gamma-dependent tumor surveillance system in immunocompetent mice. Proc Natl Acad Sci U S A 1998; 95(13): 7556-61.

Kargiotis O, Rao JS, Kyritsis AP. Mechanisms of angiogenesis in gliomas. J Neurooncol 2006; 78(3): 281-93.

Keir ME, Butte MJ, Freeman GJ, Sharpe AH. PD-1 and its ligands in tolerance and immunity. Annu Rev Immunol 2008; 26: 677-704.

Kerber M, Reiss Y, Wickersheim A, Jugold M, Kiessling F, Heil M*, et al.* Flt-1 signaling in macrophages promotes glioma growth in vivo. Cancer Res 2008; 68(18): 7342-51.

Keunen O, Johansson M, Oudin A, Sanzey M, Rahim SA, Fack F*, et al.* Anti-VEGF treatment reduces blood supply and increases tumor cell invasion in glioblastoma. Proc Natl Acad Sci U S A 2011; 108(9): 3749-54.

Kim M, Morshead CM. Distinct populations of forebrain neural stem and progenitor cells can be isolated using side-population analysis. J Neurosci 2003; 23(33): 10703-9.

Kinsel LB, Szabo E, Greene GL, Konrath J, Leight GS, Mccarty KS. Immunocytochemical Analysis of Estrogen-Receptors as a Predictor of Prognosis in Breast-Cancer Patients - Comparison with Quantitative Biochemical Methods. Cancer Research 1989; 49(4): 1052-6.

Kioi M, Vogel H, Schultz G, Hoffman RM, Harsh GR, Brown JM. Inhibition of vasculogenesis, but not angiogenesis, prevents the recurrence of glioblastoma after irradiation in mice. J Clin Invest 2010; 120(3): 694-705.

Kita D, Yonekawa Y, Weller M, Ohgaki H. PIK3CA alterations in primary (de novo) and secondary glioblastomas. Acta Neuropathol 2007; 113(3): 295-302.

Knizetova P, Ehrmann J, Hlobilkova A, Vancova I, Kalita O, Kolar Z*, et al.* Autocrine regulation of glioblastoma cell cycle progression, viability and radioresistance through the VEGF-VEGFR2 (KDR) interplay. Cell Cycle 2008; 7(16): 2553-61.

Koch S, Tugues S, Li X, Gualandi L, Claesson-Welsh L. Signal transduction by vascular endothelial growth factor receptors. Biochem J 2011; 437(2): 169-83.

Komohara Y, Ohnishi K, Kuratsu J, Takeya M. Possible involvement of the M2 anti-inflammatory macrophage phenotype in growth of human gliomas. J Pathol 2008; 216(1): 15-24.

Kraus JA, Dabbs DJ, Beriwal S, Bhargava R. Semi-quantitative immunohistochemical assay versus oncotype DX (R) qRT-PCR assay for estrogen and progesterone receptors: an independent quality assurance study. Modern Pathol 2012; 25(6): 869-76.

Krishnan S, Szabo E, Burghardt I, Frei K, Tabatabai G, Weller M. Modulation of cerebral endothelial cell function by TGF-beta in glioblastoma: VEGF-dependent angiogenesis versus endothelial mesenchymal transition. Oncotarget 2015; 6(26): 22480-95.

Lafferty KJ, Cunningham AJ. A new analysis of allogeneic interactions. Aust J Exp Biol Med Sci 1975; 53(1): 27-42.

Lampson LA, Hickey WF. Monoclonal antibody analysis of MHC expression in human brain biopsies: tissue ranging from "histologically normal" to that showing different levels of glial tumor involvement. J Immunol 1986; 136(11): 4054-62.

Latchman YE, Liang SC, Wu Y, Chernova T, Sobel RA, Klemm M*, et al.* PD-L1-deficient mice show that PD-L1 on T cells, antigen-presenting cells, and host tissues negatively regulates T cells. Proc Natl Acad Sci U S A 2004; 101(29): 10691-6.

Lau J, Cheung J, Navarro A, Lianoglou S, Haley B, Totpal K*, et al.* Tumour and host cell PD-L1 is required to mediate suppression of anti-tumour immunity in mice. Nat Commun 2017; 8: 14572.

Leavy O. Distinct role in tissue repair. Nat Rev Immunol 2015; 15(10).

Lee SJ, Jang BC, Lee SW, Yang YI, Suh SI, Park YM*, et al.* Interferon regulatory factor-1 is prerequisite to the constitutive expression and IFN-gamma-induced upregulation of B7-H1 (CD274). FEBS Lett 2006; 580(3): 755-62.

Leung DW, Cachianes G, Kuang WJ, Goeddel DV, Ferrara N. Vascular endothelial growth factor is a secreted angiogenic mitogen. Science 1989; 246(4935): 1306-9.

Li J, Yen C, Liaw D, Podsypanina K, Bose S, Wang SI*, et al.* PTEN, a putative protein tyrosine phosphatase gene mutated in human brain, breast, and prostate cancer. Science 1997; 275(5308): 1943-7.

Libermann TA, Razon N, Bartal AD, Yarden Y, Schlessinger J, Soreq H. Expression of epidermal growth factor receptors in human brain tumors. Cancer Res 1984; 44(2): 753-60.

Liu G, Yuan X, Zeng Z, Tunici P, Ng H, Abdulkadir IR*, et al.* Analysis of gene expression and chemoresistance of CD133+ cancer stem cells in glioblastoma. Mol Cancer 2006; 5: 67.

Liu J, Liao S, Diop-Frimpong B, Chen W, Goel S, Naxerova K*, et al.* TGF-beta blockade improves the distribution and efficacy of therapeutics in breast carcinoma by normalizing the tumor stroma. Proceedings of the National Academy of Sciences of the United States of America 2012; 109(41): 16618-23.

Liu Y, Carlsson R, Ambjorn M, Hasan M, Badn W, Darabi A*, et al.* PD-L1 expression by neurons nearby tumors indicates better prognosis in glioblastoma patients. J Neurosci 2013; 33(35): 14231-45.

Loffler-Wirth H, Kalcher M, Binder H. oposSOM: R-package for high-dimensional portraying of genome-wide expression landscapes on bioconductor. Bioinformatics 2015; 31(19): 3225-7.

Lohr J, Ratliff T, Huppertz A, Ge YZ, Dictus C, Ahmadi R*, et al.* Effector T-Cell Infiltration Positively Impacts Survival of Glioblastoma Patients and Is Impaired by Tumor-Derived TGF-beta. Clin Cancer Res 2011; 17(13): 4296-308.

Lou J, Chofflon M, Juillard C, Donati Y, Mili N, Siegrist CA*, et al.* Brain microvascular endothelial cells and leukocytes derived from patients with multiple sclerosis exhibit increased adhesion capacity. Neuroreport 1997; 8(3): 629-33.

Louis DN, Perry A, Reifenberger G, von Deimling A, Figarella-Branger D, Cavenee WK*, et al.* The 2016 World Health Organization Classification of Tumors of the Central Nervous System: a summary. Acta Neuropathol 2016; 131(6): 803-20.

Louveau A, Smirnov I, Keyes TJ, Eccles JD, Rouhani SJ, Peske JD*, et al.* Structural and functional features of central nervous system lymphatic vessels. Nature 2015; 523(7560): 337-41.

Lowther DE, Goods BA, Lucca LE, Lerner BA, Raddassi K, van Dijk D*, et al.* PD-1 marks dysfunctional regulatory T cells in malignant gliomas. JCI Insight 2016; 1(5).

Lu KV, Chang JP, Parachoniak CA, Pandika MM, Aghi MK, Meyronet D*, et al.* VEGF Inhibits Tumor Cell Invasion and Mesenchymal Transition through a MET/VEGFR2 Complex. Cancer Cell 2012; 22(1): 21-35.

Maes W, Verschuere T, Van Hoylandt A, Boon L, Van Gool S. Depletion of regulatory T cells in a mouse experimental glioma model through anti-CD25 treatment results in the infiltration of non-immunosuppressive myeloid cells in the brain. Clinical & developmental immunology 2013; 2013: 952469.

Maglione D, Guerriero V, Viglietto G, Delli-Bovi P, Persico MG. Isolation of a human placenta cDNA coding for a protein related to the vascular permeability factor. Proc Natl Acad Sci U S A 1991; 88(20): 9267-71.

Malmstrom A, Gronberg BH, Marosi C, Stupp R, Frappaz D, Schultz H*, et al.* Temozolomide versus standard 6-week radiotherapy versus hypofractionated radiotherapy in patients older than 60 years with glioblastoma: the Nordic randomised, phase 3 trial. Lancet Oncol 2012; 13(9): 916-26.

Mantovani A, Sozzani S, Locati M, Allavena P, Sica A. Macrophage polarization: tumor-associated macrophages as a paradigm for polarized M2 mononuclear phagocytes. Trends Immunol 2002; 23(11): 549-55.

Markovic DS, Glass R, Synowitz M, Rooijen N, Kettenmann H. Microglia stimulate the invasiveness of glioma cells by increasing the activity of metalloprotease-2. J Neuropathol Exp Neurol 2005; 64(9): 754-62.

Marvel D, Gabrilovich DI. Myeloid-derived suppressor cells in the tumor microenvironment: expect the unexpected. J Clin Invest 2015; 125(9): 3356-64.

Massague J. TGFbeta in Cancer. Cell 2008; 134(2): 215-30.

Masson F, Calzascia T, Di Berardino-Besson W, de Tribolet N, Dietrich PY, Walker PR. Brain microenvironment promotes the final functional maturation of tumor-specific effector CD8+ T cells. J Immunol 2007; 179(2): 845-53.

McAllister KA, Baldwin MA, Thukkani AK, Gallione CJ, Berg JN, Porteous ME*, et al.* Six novel mutations in the endoglin gene in hereditary hemorrhagic telangiectasia type 1 suggest a dominant-negative effect of receptor function. Hum Mol Genet 1995; 4(10): 1983-5.

Mentlein R, Forstreuter F, Mehdorn HM, Held-Feindt J. Functional significance of vascular endothelial growth factor receptor expression on human glioma cells. J Neurooncol 2004; 67(1-2): 9-18.

Morantz RA, Wood GW, Foster M, Clark M, Gollahon K. Macrophages in experimental and human brain tumors. Part 2: studies of the macrophage content of human brain tumors. J Neurosurg 1979; 50(3): 305-11.

Morimura T, Neuchrist C, Kitz K, Budka H, Scheiner O, Kraft D*, et al.* Monocyte subpopulations in human gliomas: expression of Fc and complement receptors and correlation with tumor proliferation. Acta Neuropathol 1990; 80(3): 287-94.

Muller A, Brandenburg S, Turkowski K, Muller S, Vajkoczy P. Resident microglia, and not peripheral macrophages, are the main source of brain tumor mononuclear cells. Int J Cancer 2015; 137(2): 278-88.

Murdoch C, Muthana M, Coffelt SB, Lewis CE. The role of myeloid cells in the promotion of tumour angiogenesis. Nature reviews Cancer 2008; 8(8): 618-31.

Nagy JA, Dvorak AM, Dvorak HF. VEGF-A and the induction of pathological angiogenesis. Annu Rev Pathol 2007; 2: 251-75.

Nagy JA, Vasile E, Feng D, Sundberg C, Brown LF, Manseau EJ*, et al.* VEGF-A induces angiogenesis, arteriogenesis, lymphangiogenesis, and vascular malformations. Cold Spring Harb Symp Quant Biol 2002; 67: 227-37.

Nakamura M, Watanabe T, Klangby U, Asker C, Wiman K, Yonekawa Y*, et al.* p14ARF deletion and methylation in genetic pathways to glioblastomas. Brain Pathol 2001; 11(2): 159-68.

Nduom EK, Wei J, Yaghi NK, Huang N, Kong LY, Gabrusiewicz K*, et al.* PD-L1 expression and prognostic impact in glioblastoma. Neuro Oncol 2016; 18(2): 195-205.

Nishie A, Ono M, Shono T, Fukushi J, Otsubo M, Onoue H*, et al.* Macrophage infiltration and heme oxygenase-1 expression correlate with angiogenesis in human gliomas. Clin Cancer Res 1999; 5(5): 1107-13.

Nishimura H, Nose M, Hiai H, Minato N, Honjo T. Development of lupus-like autoimmune diseases by disruption of the PD-1 gene encoding an ITIM motif-carrying immunoreceptor. Immunity 1999; 11(2): 141-51.

Nishimura H, Okazaki T, Tanaka Y, Nakatani K, Hara M, Matsumori A*, et al.* Autoimmune dilated cardiomyopathy in PD-1 receptor-deficient mice. Science 2001; 291(5502): 319-22.

Noman MZ, Desantis G, Janji B, Hasmim M, Karray S, Dessen P*, et al.* PD-L1 is a novel direct target of HIF-1alpha, and its blockade under hypoxia enhanced MDSC-mediated T cell activation. J Exp Med 2014; 211(5): 781-90.

Nurieva R, Thomas S, Nguyen T, Martin-Orozco N, Wang Y, Kaja MK*, et al.* T-cell tolerance or function is determined by combinatorial costimulatory signals. EMBO J 2006; 25(11): 2623-33.

Obermeier B, Daneman R, Ransohoff RM. Development, maintenance and disruption of the blood-brain barrier. Nat Med 2013; 19(12): 1584-96.

Ohgaki H, Kleihues P. Genetic alterations and signaling pathways in the evolution of gliomas. Cancer Sci 2009; 100(12): 2235-41.

Olson JJ, Nayak L, Ormond DR, Wen PY, Kalkanis SN, Ryken TC*, et al.* The role of targeted therapies in the management of progressive glioblastoma : a systematic review and evidence-based clinical practice guideline. J Neurooncol 2014; 118(3): 557-99.

Ostrom QT, Gittleman H, Fulop J, Liu M, Blanda R, Kromer C*, et al.* CBTRUS Statistical Report: Primary Brain and Central Nervous System Tumors Diagnosed in the United States in 2008-2012. Neuro Oncol 2015; 17 Suppl 4: iv1-iv62.

Padera TP, Stoll BR, Tooredman JB, Capen D, di Tomaso E, Jain RK. Pathology: cancer cells compress intratumour vessels. Nature 2004; 427(6976): 695.

Paez-Ribes M, Allen E, Hudock J, Takeda T, Okuyama H, Vinals F*, et al.* Antiangiogenic therapy elicits malignant progression of tumors to increased local invasion and distant metastasis. Cancer Cell 2009; 15(3): 220-31.

Pardoll DM. The blockade of immune checkpoints in cancer immunotherapy. Nat Rev Cancer 2012; 12(4): 252-64.

Pardridge WM. The blood-brain barrier: bottleneck in brain drug development. NeuroRx 2005; 2(1): 3-14.

Parney IF, Waldron JS, Parsa AT. Flow cytometry and in vitro analysis of human glioma-associated macrophages. Laboratory investigation. J Neurosurg 2009; 110(3): 572-82.

Parsa AT, Waldron JS, Panner A, Crane CA, Parney IF, Barry JJ*, et al.* Loss of tumor suppressor PTEN function increases B7-H1 expression and immunoresistance in glioma. Nat Med 2007; 13(1): 84-8.

Penuelas S, Anido J, Prieto-Sanchez RM, Folch G, Barba I, Cuartas I*, et al.* TGF-beta increases glioma-initiating cell self-renewal through the induction of LIF in human glioblastoma. Cancer Cell 2009; 15(4): 315-27.

Peranzoni E, Zilio S, Marigo I, Dolcetti L, Zanovello P, Mandruzzato S*, et al.* Myeloid-derived suppressor cell heterogeneity and subset definition. Curr Opin Immunol 2010; 22(2): 238-44.

Perry JR, Laperriere N, O'Callaghan CJ, Brandes AA, Menten J, Phillips C*, et al.* Short-Course Radiation plus Temozolomide in Elderly Patients with Glioblastoma. N Engl J Med 2017; 376(11): 1027-37.

Pham K, Luo D, Siemann DW, Law BK, Reynolds BA, Hothi P*, et al.* VEGFR inhibitors upregulate CXCR4 in VEGF receptor-expressing glioblastoma in a TGFbetaR signaling-dependent manner. Cancer Lett 2015; 360(1): 60-7.

Piao Y, Liang J, Holmes L, Zurita AJ, Henry V, Heymach JV*, et al.* Glioblastoma resistance to anti-VEGF therapy is associated with myeloid cell infiltration, stem cell accumulation, and a mesenchymal phenotype. Neuro-oncology 2012a; 14(11): 1379-92.

Piao YJ, Liang J, Holmes L, Zurita AJ, Henry V, Heymach JV*, et al.* Glioblastoma resistance to anti-VEGF therapy is associated with myeloid cell infiltration, stem cell accumulation, and a mesenchymal phenotype. Neuro-Oncology 2012b; 14(11): 1379-92.

Pickup M, Novitskiy S, Moses HL. The roles of TGFbeta in the tumour microenvironment. Nat Rev Cancer 2013; 13(11): 788-99.

Pitter KL, Tamagno I, Alikhanyan K, Hosni-Ahmed A, Pattwell SS, Donnola S*, et al.* Corticosteroids compromise survival in glioblastoma. Brain 2016; 139(Pt 5): 1458-71.

Plate KH, Mennel HD. Vascular morphology and angiogenesis in glial tumors. Exp Toxicol Pathol 1995; 47(2-3): 89-94.

Platten M, Wick W, Weller M. Malignant glioma biology: role for TGF-beta in growth, motility, angiogenesis, and immune escape. Microsc Res Tech 2001; 52(4): 401-10.

Polfliet MM, Zwijnenburg PJ, van Furth AM, van der Poll T, Dopp EA, Renardel de Lavalette C*, et al.* Meningeal and perivascular macrophages of the central nervous system play a protective role during bacterial meningitis. J Immunol 2001; 167(8): 4644-50.

Preusser M, Lim M, Hafler DA, Reardon DA, Sampson JH. Prospects of immune checkpoint modulators in the treatment of glioblastoma. Nat Rev Neurol 2015; 11(9): 504-14.

Pyonteck SM, Akkari L, Schuhmacher AJ, Bowman RL, Sevenich L, Quail DF*, et al.* CSF-1R inhibition alters macrophage polarization and blocks glioma progression. Nat Med 2013; 19(10): 1264-72.

Raychaudhuri B, Rayman P, Huang P, Grabowski M, Hambardzumyan D, Finke JH*, et al.* Myeloid derived suppressor cell infiltration of murine and human gliomas is associated with reduction of tumor infiltrating lymphocytes. J Neurooncol 2015; 122(2): 293-301.

Reardon DA, Gokhale PC, Klein SR, Ligon KL, Rodig SJ, Ramkissoon SH*, et al.* Glioblastoma Eradication Following Immune Checkpoint Blockade in an Orthotopic, Immunocompetent Model. Cancer Immunol Res 2016; 4(2): 124-35.

Reifenberger G, Liu L, Ichimura K, Schmidt EE, Collins VP. Amplification and overexpression of the MDM2 gene in a subset of human malignant gliomas without p53 mutations. Cancer Res 1993; 53(12): 2736-9.

Reifenberger G, Weber RG, Riehmer V, Kaulich K, Willscher E, Wirth H*, et al.* Molecular characterization of long-term survivors of glioblastoma using genome- and transcriptome-wide profiling. Int J Cancer 2014; 135(8): 1822-31.

Riabov V, Gudima A, Wang N, Mickley A, Orekhov A, Kzhyshkowska J. Role of tumor associated macrophages in tumor angiogenesis and lymphangiogenesis. Front Physiol 2014; 5: 75.

Ricci-Vitiani L, Pallini R, Biffoni M, Todaro M, Invernici G, Cenci T*, et al.* Tumour vascularization via endothelial differentiation of glioblastoma stem-like cells. Nature 2010; 468(7325): 824-8.

Rich JN. The role of transforming growth factor-beta in primary brain tumors. Frontiers in bioscience : a journal and virtual library 2003; 8: e245-60.

Rich JN. The Implications of the Cancer Stem Cell Hypothesis for Neuro-Oncology and Neurology. Future Neurol 2008; 3(3): 265-73.

Rizvi NA, Mazieres J, Planchard D, Stinchcombe TE, Dy GK, Antonia SJ*, et al.* Activity and safety of nivolumab, an anti-PD-1 immune checkpoint inhibitor, for patients with advanced, refractory squamous non-small-cell lung cancer (CheckMate 063): a phase 2, single-arm trial. Lancet Oncol 2015; 16(3): 257-65.

Robson DK. Pathology & Genetics. Tumours of the Nervous System. World Health Organisation Classification of Tumours. P. Kleihues and k. Cavenee (eds). IARC Press, Lyon, 2000. No. of pages: 314. ISBN: 92 832 2409 4. The Journal of Pathology 2001; 193(2): 276-.

Roth P, Aulwurm S, Gekel I, Beier D, Sperry RG, Mittelbronn M*, et al.* Regeneration and tolerance factor: a novel mediator of glioblastoma-associated immunosuppression. Cancer Res 2006; 66(7): 3852-8.

Roth P, Junker M, Tritschler I, Mittelbronn M, Dombrowski Y, Breit SN*, et al.* GDF-15 contributes to proliferation and immune escape of malignant gliomas. Clin Cancer Res 2010; 16(15): 3851-9.

Roth P, Silginer M, Goodman SL, Hasenbach K, Thies S, Maurer G*, et al.* Integrin control of the transforming growth factor-beta pathway in glioblastoma. Brain 2013; 136(Pt 2): 564-76.

Sakaguchi S. Naturally arising CD4+ regulatory t cells for immunologic self-tolerance and negative control of immune responses. Annu Rev Immunol 2004; 22: 531-62.

Sampson JH, Schmittling RJ, Archer GE, Congdon KL, Nair SK, Reap EA*, et al.* A Pilot Study of IL-2R alpha Blockade during Lymphopenia Depletes Regulatory T-cells and Correlates with Enhanced Immunity in Patients with Glioblastoma. Plos One 2012; 7(2).

Sanford LP, Ormsby I, Gittenberger-de Groot AC, Sariola H, Friedman R, Boivin GP*, et al.* TGFbeta2 knockout mice have multiple developmental defects that are non-overlapping with other TGFbeta knockout phenotypes. Development 1997; 124(13): 2659-70.

Santarelli JG, Udani V, Yung YC, Cheshier S, Wagers A, Brekken RA*, et al.* Incorporation of bone marrow-derived Flk-1-expressing CD34+ cells in the endothelium of tumor vessels in the mouse brain. Neurosurgery 2006; 59(2): 374-82; discussion -82.

Schmidt KF, Ziu M, Schmidt NO, Vaghasia P, Cargioli TG, Doshi S*, et al.* Volume reconstruction techniques improve the correlation between histological and in vivo tumor volume measurements in mouse models of human gliomas. J Neuro-Oncol 2004; 68(3): 207-15.

Scholz A, Harter PN, Cremer S, Yalcin BH, Gurnik S, Yamaji M*, et al.* Endothelial cell-derived angiopoietin-2 is a therapeutic target in treatment-naive and bevacizumab-resistant glioblastoma. EMBO Mol Med 2015; 8(1): 39-57.

Schwyzer M, Fontana A. Partial purification and biochemical characterization of a T cell suppressor factor produced by human glioblastoma cells. J Immunol 1985; 134(2): 1003-9.

Senger DR, Galli SJ, Dvorak AM, Perruzzi CA, Harvey VS, Dvorak HF. Tumor cells secrete a vascular permeability factor that promotes accumulation of ascites fluid. Science 1983; 219(4587): 983-5.

Serrano M, Hannon GJ, Beach D. A new regulatory motif in cell-cycle control causing specific inhibition of cyclin D/CDK4. Nature 1993; 366(6456): 704-7.

Serrats J, Schiltz JC, Garcia-Bueno B, van Rooijen N, Reyes TM, Sawchenko PE. Dual roles for perivascular macrophages in immune-to-brain signaling. Neuron 2010; 65(1): 94-106.

Seystahl K, Papachristodoulou A, Burghardt I, Schneider H, Hasenbach K, Janicot M*, et al.* Biological role and therapeutic targeting of TGF-beta3 in glioblastoma. Mol Cancer Ther 2017.

Seystahl K, Tritschler I, Szabo E, Tabatabai G, Weller M. Differential regulation of TGF-beta-induced, ALK-5-mediated VEGF release by SMAD2/3 versus SMAD1/5/8 signaling in glioblastoma. Neuro-Oncology 2015; 17(2): 254-65.

Shackleton M, Quintana E, Fearon ER, Morrison SJ. Heterogeneity in cancer: cancer stem cells versus clonal evolution. Cell 2009; 138(5): 822-9.

Shalaby F, Rossant J, Yamaguchi TP, Gertsenstein M, Wu XF, Breitman ML*, et al.* Failure of blood-island formation and vasculogenesis in Flk-1-deficient mice. Nature 1995; 376(6535): 62-6.

Sheppard KA, Fitz LJ, Lee JM, Benander C, George JA, Wooters J*, et al.* PD-1 inhibits T-cell receptor induced phosphorylation of the ZAP70/CD3zeta signalosome and downstream signaling to PKCtheta. FEBS Lett 2004; 574(1-3): 37-41.

Shojaei F, Wu X, Malik AK, Zhong C, Baldwin ME, Schanz S*, et al.* Tumor refractoriness to anti-VEGF treatment is mediated by CD11b+Gr1+ myeloid cells. Nature biotechnology 2007; 25(8): 911-20.

Singh SK, Clarke ID, Terasaki M, Bonn VE, Hawkins C, Squire J*, et al.* Identification of a cancer stem cell in human brain tumors. Cancer Res 2003; 63(18): 5821-8.

Singh SK, Hawkins C, Clarke ID, Squire JA, Bayani J, Hide T*, et al.* Identification of human brain tumour initiating cells. Nature 2004; 432(7015): 396-401.

Sippel TR, White J, Nag K, Tsvankin V, Klaassen M, Kleinschmidt-DeMasters BK*, et al.* Neutrophil degranulation and immunosuppression in patients with GBM: restoration of cellular immune function by targeting arginase I. Clin Cancer Res 2011; 17(22): 6992-7002.

Sitohy B, Nagy JA, Dvorak HF. Anti-VEGF/VEGFR therapy for cancer: reassessing the target. Cancer Res 2012; 72(8): 1909-14.

Soda Y, Myskiw C, Rommel A, Verma IM. Mechanisms of neovascularization and resistance to anti-angiogenic therapies in glioblastoma multiforme. J Mol Med 2013; 91(4): 439-48.

Street SE, Cretney E, Smyth MJ. Perforin and interferon-gamma activities independently control tumor initiation, growth, and metastasis. Blood 2001; 97(1): 192-7.

Stupp R, Mason WP, van den Bent MJ, Weller M, Fisher B, Taphoorn MJ*, et al.* Radiotherapy plus concomitant and adjuvant temozolomide for glioblastoma. N Engl J Med 2005; 352(10): 987-96.

Szabo E, Schneider H, Seystahl K, Rushing EJ, Herting F, Weidner KM*, et al.* Autocrine VEGFR1 and VEGFR2 signaling promotes survival in human glioblastoma models in vitro and in vivo. Neuro Oncol 2016; 18(9): 1242-52.

Tammela T, Enholm B, Alitalo K, Paavonen K. The biology of vascular endothelial growth factors. Cardiovasc Res 2005; 65(3): 550-63.

Thang NNT, Derouazi M, Philippin G, Arcidiaco S, Di Berardino-Besson W, Masson F*, et al.* Immune Infiltration of Spontaneous Mouse Astrocytomas Is Dominated by Immunosuppressive Cells from Early Stages of Tumor Development. Cancer Research 2010; 70(12): 4829-39.

Thomas AA, Fisher JL, Rahme GJ, Hampton TH, Baron U, Olek S*, et al.* Regulatory T cells are not a strong predictor of survival for patients with glioblastoma. Neuro-Oncology 2015; 17(6): 801-9.

Thomas DA, Massague J. TGF-beta directly targets cytotoxic T cell functions during tumor evasion of immune surveillance. Cancer Cell 2005; 8(5): 369-80.

Tivol EA, Borriello F, Schweitzer AN, Lynch WP, Bluestone JA, Sharpe AH. Loss of CTLA-4 leads to massive lymphoproliferation and fatal multiorgan tissue destruction, revealing a critical negative regulatory role of CTLA-4. Immunity 1995; 3(5): 541-7.

Tseng D, Vasquez-Medrano DA, Brown JM. Targeting SDF-1/CXCR4 to inhibit tumour vasculature for treatment of glioblastomas. Brit J Cancer 2011; 104(12): 1805-9.

Tumeh PC, Harview CL, Yearley JH, Shintaku IP, Taylor EJ, Robert L*, et al.* PD-1 blockade induces responses by inhibiting adaptive immune resistance. Nature 2014; 515(7528): 568-71.

Twyman-Saint Victor C, Rech AJ, Maity A, Rengan R, Pauken KE, Stelekati E*, et al.* Radiation and dual checkpoint blockade activate non-redundant immune mechanisms in cancer. Nature 2015; 520(7547): 373-+.

Ueda R, Fujita M, Zhu X, Sasaki K, Kastenhuber ER, Kohanbash G*, et al.* Systemic inhibition of transforming growth factor-beta in glioma-bearing mice improves the therapeutic efficacy of glioma-associated antigen peptide vaccines. Clin Cancer Res 2009; 15(21): 6551-9.

Uhl M, Aulwurm S, Wischhusen J, Weiler M, Ma JY, Almirez R*, et al.* SD-208, a novel transforming growth factor beta receptor I kinase inhibitor, inhibits growth and invasiveness and enhances immunogenicity of murine and human glioma cells in vitro and in vivo. Cancer Res 2004; 64(21): 7954-61.

van Tellingen O, Yetkin-Arik B, de Gooijer MC, Wesseling P, Wurdinger T, de Vries HE. Overcoming the blood-brain tumor barrier for effective glioblastoma treatment. Drug Resist Updat 2015; 19: 1-12.

Venere M, Hamerlik P, Wu Q, Rasmussen RD, Song LA, Vasanji A*, et al.* Therapeutic targeting of constitutive PARP activation compromises stem cell phenotype and survival of glioblastoma-initiating cells. Cell Death Differ 2014; 21(2): 258-69.

Verhaak RG, Hoadley KA, Purdom E, Wang V, Qi Y, Wilkerson MD*, et al.* Integrated genomic analysis identifies clinically relevant subtypes of glioblastoma characterized by abnormalities in PDGFRA, IDH1, EGFR, and NF1. Cancer Cell 2010; 17(1): 98-110.

Vitucci M, Hayes DN, Miller CR. Gene expression profiling of gliomas: merging genomic and histopathological classification for personalised therapy. Br J Cancer 2011; 104(4): 545-53.

Vom Berg J, Vrohlings M, Haller S, Haimovici A, Kulig P, Sledzinska A*, et al.* Intratumoral IL-12 combined with CTLA-4 blockade elicits T cell-mediated glioma rejection. The Journal of experimental medicine 2013; 210(13): 2803-11.

Voron T, Colussi O, Marcheteau E, Pernot S, Nizard M, Pointet AL*, et al.* VEGF-A modulates expression of inhibitory checkpoints on CD8+ T cells in tumors. J Exp Med 2015; 212(2): 139-48.

Wainwright DA, Chang AL, Dey M, Balyasnikova IV, Kim CK, Tobias A*, et al.* Durable therapeutic efficacy utilizing combinatorial blockade against IDO, CTLA-4, and PD-L1 in mice with brain tumors. Clin Cancer Res 2014; 20(20): 5290-301.

Wainwright DA, Dey M, Chang A, Lesniak MS. Targeting Tregs in Malignant Brain Cancer: Overcoming IDO. Front Immunol 2013; 4: 116.

Wainwright DA, Sengupta S, Han Y, Lesniak MS. Thymus-derived rather than tumor-induced regulatory T cells predominate in brain tumors. Neuro Oncol 2011; 13(12): 1308-23.

Wakefield LM, Hill CS. Beyond TGFbeta: roles of other TGFbeta superfamily members in cancer. Nat Rev Cancer 2013; 13(5): 328-41.

Wang J, Guan E, Roderiquez G, Calvert V, Alvarez R, Norcross MA. Role of tyrosine phosphorylation in ligand-independent sequestration of CXCR4 in human primary monocytes-macrophages. The Journal of biological chemistry 2001; 276(52): 49236-43.

Wang L, Shi J, van Ginkel FW, Lan L, Niemeyer G, Martin DR*, et al.* Neural stem/progenitor cells modulate immune responses by suppressing T lymphocytes with nitric oxide and prostaglandin E2. Exp Neurol 2009; 216(1): 177-83.

Wang R, Chadalavada K, Wilshire J, Kowalik U, Hovinga KE, Geber A*, et al.* Glioblastoma stem-like cells give rise to tumour endothelium. Nature 2010; 468(7325): 829-33.

Waterhouse P, Penninger JM, Timms E, Wakeham A, Shahinian A, Lee KP*, et al.* Lymphoproliferative disorders with early lethality in mice deficient in Ctla-4. Science 1995; 270(5238): 985-8.

Weiss T, Weller M, Roth P. Immunotherapy for glioblastoma: concepts and challenges. Curr Opin Neurol 2015; 28(6): 639-46.

Weller M, van den Bent M, Hopkins K. EANO guideline for the diagnosis and treatment of anaplastic gliomas and glioblastoma (vol 15, pg e395, 2014). Lancet Oncology 2014; 15(13): E587-E.

Weller M, Wick W, Aldape K, Brada M, Berger M, Pfister SM*, et al.* Glioma. Nat Rev Dis Primers 2015; 1: 15017.

Wesolowska A, Kwiatkowska A, Slomnicki L, Dembinski M, Master A, Sliwa M*, et al.* Microglia-derived TGF-beta as an important regulator of glioblastoma invasion--an inhibition of TGF-beta-dependent effects by shRNA against human TGF-beta type II receptor. Oncogene 2008; 27(7): 918-30.

Wick A, Dorner N, Schafer N, Hofer S, Heiland S, Schemmer D*, et al.* Bevacizumab Does Not Increase the Risk of Remote Relapse in Malignant Glioma. Ann Neurol 2011; 69(3): 586-92.

Wick W, Cloughesy TF, Nishikawa R, Mason W, Saran F, Henriksson R*, et al.* Tumor response based on adapted Macdonald criteria and assessment of pseudoprogression (PsPD) in the phase III AV Aglio trial of bevacizumab (Bv) plus temozolomide (T) plus radiotherapy (RT) in newly diagnosed glioblastoma (GBM). Journal of Clinical Oncology 2013; 31(15).

Wick W, Platten M, Meisner C, Felsberg J, Tabatabai G, Simon M*, et al.* Temozolomide chemotherapy alone versus radiotherapy alone for malignant astrocytoma in the elderly: the NOA-08 randomised, phase 3 trial. Lancet Oncol 2012; 13(7): 707-15.

Wick W, Platten M, Weller M. Glioma cell invasion: regulation of metalloproteinase activity by TGF-beta. J Neurooncol 2001; 53(2): 177-85.

Wick W, Puduvalli VK, Chamberlain MC, van den Bent MJ, Carpentier AF, Cher LM*, et al.* Phase III study of enzastaurin compared with lomustine in the treatment of recurrent intracranial glioblastoma. J Clin Oncol 2010; 28(7): 1168-74.

Wilmotte R, Burkhardt K, Kindler V, Belkouch MC, Dussex G, Tribolet N*, et al.* B7-homolog 1 expression by human glioma: a new mechanism of immune evasion. Neuroreport 2005; 16(10): 1081-5.

Wintterle S, Schreiner B, Mitsdoerffer M, Schneider D, Chen L, Meyermann R*, et al.* Expression of the B7-related molecule B7-H1 by glioma cells: a potential mechanism of immune paralysis. Cancer Res 2003; 63(21): 7462-7.

Wirth H, Loffler M, von Bergen M, Binder H. Expression cartography of human tissues using self organizing maps. Bmc Bioinformatics 2011; 12.

Wirth H, von Bergen M, Binder H. Mining SOM expression portraits: feature selection and integrating concepts of molecular function. Biodata Min 2012; 5.

Wolburg H, Lippoldt A. Tight junctions of the blood-brain barrier: development, composition and regulation. Vascul Pharmacol 2002; 38(6): 323-37.

Wolchok JD, Kluger H, Callahan MK, Postow MA, Rizvi NA, Lesokhin AM*, et al.* Nivolumab plus ipilimumab in advanced melanoma. N Engl J Med 2013; 369(2): 122-33.

Wong AJ, Ruppert JM, Bigner SH, Grzeschik CH, Humphrey PA, Bigner DS*, et al.* Structural alterations of the epidermal growth factor receptor gene in human gliomas. Proc Natl Acad Sci U S A 1992; 89(7): 2965-9.

Woods SA, McGlade CJ, Guha A. Phosphatidylinositol 3'-kinase and MAPK/ERK kinase 1/2 differentially regulate expression of vascular endothelial growth factor in human malignant astrocytoma cells. Neuro Oncol 2002; 4(4): 242-52.

Xiao Y, Yu S, Zhu B, Bedoret D, Bu X, Francisco LM*, et al.* RGMb is a novel binding partner for PD-L2 and its engagement with PD-L2 promotes respiratory tolerance. J Exp Med 2014; 211(5): 943-59.

Yano S, Shinohara H, Herbst RS, Kuniyasu H, Bucana CD, Ellis LM*, et al.* Expression of vascular endothelial growth factor is necessary but not sufficient for production and growth of brain metastasis. Cancer Res 2000; 60(17): 4959-67.

Yuan F, Salehi HA, Boucher Y, Vasthare US, Tuma RF, Jain RK. Vascular permeability and microcirculation of gliomas and mammary carcinomas transplanted in rat and mouse cranial windows. Cancer Res 1994; 54(17): 4564-8.

Zeng J, See AP, Phallen J, Jackson CM, Belcaid Z, Ruzevick J*, et al.* Anti-PD-1 blockade and stereotactic radiation produce long-term survival in mice with intracranial gliomas. Int J Radiat Oncol Biol Phys 2013; 86(2): 343-9.

9. Curriculum Vitae

Personal Information

Name: Davide
Surname: Mangani
Address: Elisabethenstrasse 6, Zurich 8004, Switzerland
Phone: +41 789769324
Nationality: Italian
e-mail: davide.mangani@usz.com ; davide.mangani@gmail.com
OrcID: orcid.org/0000-0001-5297-0234

Education and Training

January 2014 – today, Switzerland, Zurich, Laboratory for Molecular Neuro-Oncology, University of Zurich (UZH), Cancer Biology PhD (en route)
PhD thesis title: Targeting the vascular and immunosuppressive networks in glioblastoma

September 2011 – July 2013, Italy, Naples, University of Naples "Federico II", Medical Biotechnologies MSc
MSc Thesis title: MIR-221/222 target the DNA Methyltransferase MGMT in glioma cells and regulate therapy response and DNA damage.
Final Grade: 110/110 *summa cum laude*

September 2008 – September 2011, Italy, Naples, University of Naples "Federico II", Health Biotechnologies BSc
BSc Thesis title: Utilizzo della tecnica RFLP per valutare l'arricchimento di molecole di RNA selezionate mediante tecnologia SELEX.
Enrichment evaluation by RFLP technique of RNA molecules selected via SELEX technology.
Final Grade: 110/110 *summa cum laude*

September 2003- July 2008
5-years Scientific Diploma, Liceo "G.Mercalli".
Final Grade: 100/100

Research Experience and descriptions

January 2014- Today (expected PhD defense June 2017)
PhD candidate at the laboratory for Molecular Neuro-Oncology, University of Zurich
Supervisor: Prof. Michael Weller
Targeting the vascular and immunosuppressive networks in glioblastoma
Main focus of the research activity: investigation of new therapeutic strategies targeting the tumor vascular network or fostering the immune-mediated recognition and destruction of malignant tumor cells.

September 2012- December 2013

Graduate training at the Department of Molecular Medicine and Medical Biotechnologies,
University of Naples "Federico II".
Supervisor: Prof. Gerolama Condorelli.
MIR-221/222 target the DNA Methyltransferase MGMT in glioma cells and regulate therapy response and DNA damage.
Main focus of the research activity**:** MicroRNA-mediated modulation of the therapeutic response to temozolomide (TMZ) and molecular pathways involved in DNA damage-response in glioblastoma (GBM).

July 2011 – September 2011
Summer Internship at “Sbarro Health Research Organization” as visiting student.
Supervisor: Prof. Antonio Giordano
Study of emerging molecular networks in Burkitt’s lymphoma.

July 2010 – September 2010
Summer Internship at “Sbarro Health Research Organization” as visiting student.
Supervisor: Dr. Flavio Rizzolio
Evaluation of Pin1 protein role in lung cancer pathogenesis through multistep HBEC cell systems.

February 2010 – September 2012
Undergraduate training at the Department of “Cellular and Molecular Biology and Pathology L.Califano”, University of Naples "Federico II".
Supervisor: Prof. Gerolama Condorelli.
Study of molecular pathways involved in carcinogenesis; apoptosis, autophagy and stemness.

July 2009 – September 2009
Summer Internship at “Sbarro Health Research Organization” as visiting student.
Supervisor: Dr. Flavio Rizzolio
Evaluation of molecular and anti-proliferative effects caused by Pin1 protein inhibition in glioma cell lines.

Conferences, Achievements and Prizes

Oral presentation at the “7th Cancer Network Zurich Retreat” held in Emmetten (Switzerland) from 26th to 28th of March 2017.

Poster presentation at the “Midwinter Conference, Advances in Immunbiology” held in Seefeld (Austria) from the 21st to the 25th of January 2017

Awarded with a scholarship from the Life Science Zurich Graduate School (LSZGS) to present a poster at the AACR international meeting “Tumor Immunology and Immunotherapy” held in Boston (MA, USA) from 20th to 23rd of October 2016.

Poster presentation at the Brupbacher international meeting “Breakthroughs in Cancer Research and Therapy” held from 28th to 30th of January 2015 in Zurich.

Honor degree Medical Biotechnologies MSc, year 2013, Italy, Naples, University of Naples “Federico II”

Awarded with a three-month research internship as visiting student (Jul ’11 – Sep ’11) at the Sbarro Institute for Cancer Research and Molecular Medicine and Center of Biotechnology, College of Science and Technology, Temple University (Philadelphia, PA, USA).

Awarded with a three-month research internship as visiting student (Jul ’10 – Sep ’10) at the Sbarro Institute for Cancer Research and Molecular Medicine and Center of Biotechnology, College of Science and Technology, Temple University (Philadelphia, PA, USA).

Awarded with a three-month research internship as visiting student (Jul ’09 – Sep ’09) at the Sbarro Institute for Cancer Research and Molecular Medicine and Center of Biotechnology, College of Science and Technology, Temple University (Philadelphia, PA, USA).

10. Publication list

1) **Mangani D.**, Weller M., Seyed Sadr E., Willscher E,. Seystahl K., Reifenberger G., Tabatabai G., Binder H., Schneider H. (2016) Limited role for transforming growth factor-β pathway activation-mediated escape from VEGF inhibition in murine glioma models. *Neuro Oncol.* 2016 Dec;18(12):1610-1621.

2) **Mangani D.,** Roth P., Weller M. (2016) The network of immunosuppressive pathways in glioblastoma. *Biochem Pharmacol.* 2016 Dec 22. pii: S0006-2952(16)30491-9. doi: 10.1016/j.bcp.2016.12.011. [Epub ahead of print] Review.

3) Quintavalle C.,* **Mangani D**.,* Roscigno G., Romano G., Diaz-Lagares A, et al. (2013) miR-221/222 Target the DNA Methyltransferase MGMT in Glioma Cells. *PLoS ONE* 8(9): e74466. doi:10.1371/journal.pone.0074466

4) **Mangani D.,** Roberti A., Rizzolio F., Giordano A. (2013) Emerging molecular networks in Burkitt's lymphoma. *J Cell Biochem.* 114(1):35-8, 2012.

* These authors contributed equally to this work

11. Declaration

I hereby certify that the PhD thesis above has been written by me following the regulations of UZH-MNF. Published work from others has been duly cited. Any other contributions to the work have been acknowledged appropriately. Guidance in the project's conception and linguistic expressions are acknowledged to my thesis supervisors. The material presented here has not been used for any other degree or diploma.

Zürich, 01.05.2017	Davide Mangani
Place, date	Signature